



**HAL**  
open science

# Contribution to the enhancement of the efficiency of IP-over-WDM networks by evaluating and attaining the limits of multilayer network planning

Maksym Nikolayev

► **To cite this version:**

Maksym Nikolayev. Contribution to the enhancement of the efficiency of IP-over-WDM networks by evaluating and attaining the limits of multilayer network planning. Networking and Internet Architecture [cs.NI]. Institut National des Télécommunications, 2014. English. NNT : 2014TELE0022 . tel-01186232

**HAL Id: tel-01186232**

**<https://theses.hal.science/tel-01186232>**

Submitted on 24 Aug 2015

**HAL** is a multi-disciplinary open access archive for the deposit and dissemination of scientific research documents, whether they are published or not. The documents may come from teaching and research institutions in France or abroad, or from public or private research centers.

L'archive ouverte pluridisciplinaire **HAL**, est destinée au dépôt et à la diffusion de documents scientifiques de niveau recherche, publiés ou non, émanant des établissements d'enseignement et de recherche français ou étrangers, des laboratoires publics ou privés.



**THESE DE DOCTORAT CONJOINT TELECOM SUDPARIS et L'UNIVERSITE  
PIERRE ET MARIE CURIE**

**Spécialité : Electronique et Télécommunications**

**Ecole doctorale : Informatique, Télécommunications et Electronique de Paris**

**Présentée par**

**Maksym NIKOLAYEV**

**Pour obtenir le grade de  
DOCTEUR DE TELECOM SUDPARIS**

**Contribution à l'amélioration de l'efficacité des réseaux IP sur WDM en  
évaluant et en dépassant les limites du dimensionnement multicouche**

**Soutenance le 29 Septembre 2014**

**devant le jury composé de :**

**Directeur de thèse : Catherine LEPERS, Professeur, Telecom-SudParis, France**

**Encadrant de thèse : Annalisa MOREA, Ingénieur de Recherche, Alcatel-Lucent Bell Labs, France**

**Rapporteurs : Joanna TOMASIK, Professeur, SUPELEC, France**

**Bernard COUSIN, Professeur, Université de Rennes 1, France**

**Examineurs : Esther LE ROUZIC, Ingénieur de Recherche, Orange Labs Lannion, France**

**Cédric WARE, Maître de Conférences, Télécom-ParisTech, France**

**Stefano SECCI, Maître de Conférences, UPMC, France**



# Abstract

The traffic passing through backbone networks grows by nearly 25% each year. To bring the costs under control, the different network layers of the backbone network should work together to include more and more parameters into the cost optimization. This is called “multilayer network planning”. We study the multilayer network planning of static networks composed of two circuit switched layers (typically IP/MPLS-over-WDM).

We propose a theory explaining the behavior of algorithms responsible for aggregation and routing in both layers. This theory allows comparing multilayer planning algorithms between them and explaining their performance.

We then describe the impact of the optical reach constraint in WDM networks on the results of a multilayer planning algorithm.

# Contents

<b>ABSTRACT .....</b>	<b>3</b>
<b>CONTENTS .....</b>	<b>4</b>
<b>ABBREVIATIONS .....</b>	<b>8</b>
<b>NOTATIONS .....</b>	<b>9</b>
<b>INTRODUCTION .....</b>	<b>10</b>
<b>CHAPTER 1: STATE OF THE ART ON MULTILAYER NETWORK PLANNING.....</b>	<b>12</b>
<b>I. CORE AND METROPOLITAN NETWORKS .....</b>	<b>12</b>
<i>A. Segmentation of the networks .....</i>	<i>12</i>
<i>B. Network layers and protocol stack.....</i>	<i>14</i>
<i>C. Evolution of node architecture .....</i>	<i>15</i>
1) Opaque networks.....	15
2) Transparent networks.....	15
3) Hybrid networks.....	16
<b>II. NETWORK PLANNING OF IP-OVER-WDM NETWORKS .....</b>	<b>18</b>
<i>A. Cost functions .....</i>	<i>18</i>
<i>B. Constraints.....</i>	<i>19</i>
<i>C. Pre-multilayer network planning.....</i>	<i>20</i>
1) Opaque network planning .....	20
2) Overlay network planning.....	21
<i>D. Multilayer network planning .....</i>	<i>21</i>
<i>E. Additional parameters for multilayer network planning .....</i>	<i>23</i>

1) Better accounting for constraints.....	23
2) Better accounting for costs .....	23
3) Dissymmetric topologies .....	24
<i>F. Technological evolutions that impact the multilayer planning process .....</i>	<i>24</i>
1) Extra layers .....	24
2) Resiliency .....	25
3) Mixed Line Rate (MLR) optical layer and elastic transponders.....	25
4) Evolution towards dynamic and elastic optical layers .....	26
III. CONCLUSION.....	26

## **CHAPTER 2: THE CHARACTERISTIC FUNCTION OF ROUTING AND GROOMING**

<b>METHODS .....</b>	<b>27</b>
I. STATE OF THE ART AND PROBLEMATIC .....	27
II. INSPIRATION .....	29
III. HYPOTHESES .....	30
<i>A. Network topologies.....</i>	<i>30</i>
<i>B. Node architecture.....</i>	<i>30</i>
<i>C. Traffic matrices .....</i>	<i>31</i>
IV. HOW TO OBTAIN THE CHARACTERISTIC FUNCTION OF A RG METHOD .....	32
<i>A. Overlay network planning.....</i>	<i>32</i>
<i>B. Opaque network planning.....</i>	<i>33</i>
1) Analytical explanation .....	34
2) Simulation results for four network topologies .....	35
<i>C. Multilayer network planning.....</i>	<i>37</i>
1) Stair function of multilayer RG when density=1 .....	37
2) Stair function of multilayer RG when density<1 .....	39
3) Analytical explanation .....	40
4) Comparative study of performances of heuristics and MILP formulation using the characteristic function .....	43
5) Characteristic function of a multilayer RG heuristic for large networks.....	44
V. EXTRAPOLATING A STAIR FUNCTION TO REALISTIC TRAFFIC MATRICES .....	51
<i>A. Traffic hypotheses.....</i>	<i>51</i>

B. <i>Explanation and first results</i> .....	51
C. <i>Domain of validity of the estimation by correlation</i> .....	54
D. <i>Generalization</i> .....	56
1) <i>Analytical form of estimator for a given type of PDF of traffic demands</i> .....	56
2) <i>Linearity of the estimator for traffic distributions with high standard deviation</i> ....	58
E. <i>Links with existing literature</i> .....	61
VI. <b>ENHANCING MULTILAYER RG HEURISTICS USING THE STAIR FUNCTION</b> .....	62
A. <i>Enhancement of our heuristic through the characteristic function</i> .....	62
1) <i>From V1 to V2</i> .....	62
2) <i>From V2 to V3</i> .....	64
B. <i>Study of two Alcatel-Lucent Bell Labs tools</i> .....	64
1) <i>Study of Tool A</i> .....	65
2) <i>Study of Tool B</i> .....	68
VII. <b>CONCLUSION</b> .....	70

### **CHAPTER 3: IMPACT OF THE OPTICAL REACH ON MULTILAYER PLANNING**

<b>OF IP-OVER-WDM NETWORKS</b> .....	<b>72</b>
I. <b>INTRODUCTION</b> .....	72
A. <i>Importance of the optical reach</i> .....	72
B. <i>Optical reach constraint in multilayer network planning</i> .....	73
II. <b>NETWORK MODEL</b> .....	74
A. <i>Node architecture</i> .....	74
B. <i>Cost model</i> .....	75
III. <b>PLANNING METHODS</b> .....	76
A. <i>Heuristic</i> .....	76
B. <i>MILP formulations</i> .....	76
IV. <b>SIMULATION HYPOTHESES</b> .....	77
A. <i>Traffic assumptions</i> .....	77
B. <i>Implementation of the planning methods</i> .....	77
C. <i>Studied topologies</i> .....	77
D. <i>Cost assumptions</i> .....	78
V. <b>SIMULATIONS &amp; RESULTS</b> .....	79

A. <i>Network planning under optical reach constraint</i> .....	79
B. <i>Impact of the traffic granularity on the network planning</i> .....	81
1) Impact of the granularity and the optical reach on the total network cost .....	81
2) Impact of the granularity and the optical reach on the optical connection length ..	85
3) Impact of the granularity and the optical reach on the distribution of optical connections .....	86
4) Cost gains of taking into account the optical reach in the planning algorithm .....	89
5) Simple estimation of the required optical reach.....	90
6) Validation with realistic case study .....	91
VI. CONCLUSION.....	93
<b>CONCLUSION AND PERSPECTIVES .....</b>	<b>95</b>
I. CONCLUSION .....	95
II. PERSPECTIVES.....	96
<b>APPENDIXES.....</b>	<b>97</b>
I. APPENDIX 1: MILP FORMULATION .....	97
A. <i>Objective function</i> .....	98
B. <i>Constraints</i> .....	98
II. APPENDIX 2: HEURISTIC FORMULATION .....	100
III. APPENDIX 3 : IMPACT OF THE DENSITY.....	102
<b>BIBLIOGRAPHY .....</b>	<b>104</b>
<b>SUMMARY IN FRENCH / RÉSUMÉ EN FRANÇAIS .....</b>	<b>111</b>
I. INTRODUCTION.....	111
II. FONCTION CARACTERISTIQUE .....	113
III. IMPACT DE LA PORTEE OPTIQUE SUR LE DIMENSIONNEMENT DE RESEAUX IP-SUR-WDM	115
IV. CONCLUSION.....	115

# Abbreviations

**ADSL** - Asymmetric Digital Subscriber Line  
**CapEx** - Capital Expenditure  
**CPU** - Central Processing Unit  
**DWDM** - Dense Wavelength Division Multiplexing  
**EDFA** - Erbium-Doped Fiber Amplifier  
**EXC** - Electric Cross-Connect  
**Gb/s** - Gigabits per second  
**GRWA** - Grooming Routing and Wavelength Assignment  
**IETF** - Internet Engineering Task Force  
**IP** - Internet Protocol  
**IT** - Information Technology  
**ITU** - International Telecommunication Union  
**MILP** - Mixed Integer Linear Programming  
**MLR** - Mixed Line Rate  
**OAM** - Operations Administration and Management  
**ODU** - Optical Data Unit  
**OpEx** - Operational Expenditure  
**OTN** - Optical Transport Network protocol  
**OXC** - Optical Cross-Connect  
**PON** - Passive Optical Network  
**PDF** - Probability Distribution Function  
**RG** - Routing and Grooming  
**RP** - Router Port  
**SDH** - Synchronous Digital Hierarchy  
**SONET** - Synchronous Optical NETWORK  
**TDM** - Time Division Multiplexing  
**TSP** - Transponder  
**WDM** - Wavelength Division Multiplexing

# Notations

$\lceil x \rceil$  - ceiling function, i.e. the smallest integer superior or equal to  $x$

**1SP-MILP** - our MILP formulation for multilayer network planning routing each demand on its shortest path

**anySP-MILP** - our MILP formulation for multilayer network planning routing each demand on any path in the topology

$C$  - total number of unidirectional optical connections needed to transport all the traffic demands of a traffic matrix via a given a network topology

$\delta$  - connectivity of a topology

**erf** - "error function"

$g$  - traffic granularity

$L$  - number of links of a network topology

$M$  - number of client traffic demands in a traffic matrix

$N$  - number of nodes of a network topology

$\mathbb{N}$  - the set of natural numbers

$\mathbb{N}^*$  - the set of non-zero natural numbers

# Introduction

Over the past 10 years we have witnessed a traffic rate growth of about 60% per year [1] on to a point where it was estimated that IT technologies consume circa 6% of the world's electricity [2]. Due to the emergence of services such as of ultra-high definition video, 3D multimedia and multimedia-supported social networks we can say that the exponential growth of traffic in telecommunication networks will keep growing. Another reason for growth is the "thin client" paradigm consisting in the reduction of consumption and complexity of client terminals and migration of machine resources (CPU, memory...) into distant servers. As the terminals represent the largest part of the overall IT energy consumption, this allows for an overall energy economy [3]. In the telecommunication networks, the access is historically the most power consuming segment. However with the replacement of power consuming technologies such as ADSL by PON access, the transport networks represent a growing share of the power consumption [4]. The cost of networks also grows faster than the revenues of the telecommunication operators, which puts their current business model into jeopardy [5]. The consumption and the costs of the transport networks sore. It is therefore urgent to make efforts to increase their overall efficiency.

Beyond the fact that we expect different network devices to cost and consume less, the whole paradigm behind network planning and network administration is called into question. Major hypotheses on which current networks are based, lead to overheads and margins. These hypotheses, elaborated to facilitate the planning and the administration of networks, are to be reconsidered. For example, too much transport capacity remains unused because of the mismatch between the capacity and the optical reach of the WDM connections and the transported traffic. Also, too many resources are deployed to fit dynamically changing client traffic into static optical connections. And finally too much over-provisioning occurs so as to protect the traffic against equipment failures. This is why new network paradigms are coming. The mixed line rate networks and the elastic networks allow adapting the capacity and the optical reach to match client traffic. The Software Defined Networks allow dynamically allocating and de-allocating resources. All these changes will inevitably lead to a major transformation of the network planning and network administration software tools.

The contemporary planning tools are predominantly implementing algorithms solving multilayer resource allocation. Our studies confirm findings of other teams about savings provided by these planning algorithms as compared to legacy planning methods (opaque and overlay network planning). The essential mechanism of multilayer planning tools is the routing and planning mechanism. Undoubtedly, it is going to be found in the planning software of the future. Yet we have found that the routing and grooming mechanism was

studied only with empirical approaches. Therefore no theoretical or numerical model could explain nor predict the behavior of a routing and grooming algorithm. This is why the first part of this manuscript concerns the study of the routing and grooming process alone.

Among the constraints that apply to the results of multilayer planning, we single out the optical reach constraint for two reasons. Firstly, in the current technologies there is a push towards higher bitrates in the optical equipment, in conformity with the Shannon limit this shortens the transmission distance [6]. Therefore this constraint cannot be ignored in any short-term network scenario. Secondly, in the short-term, in mixed line rate (MLR) and elastic networks the interdependence between optical layer costs, optical reach, and transport capacity is essential to the multilayer planning process. For these reasons in the second part of the manuscript we present the influence of the optical reach and the costs of the optical layer on the results of multilayer network planning.

The manuscript is organized as follows:

In Chapter 1 we introduce the segmentation of the network and the properties of metropolitan and core networks. We also present the evolution of architectures and protocols found in these networks. Then we describe network planning paradigms that follow this evolution. The state of the art in multilayer network planning is detailed and the routing and grooming process is identified as the essential mechanism of multilayer network planning.

In Chapter 2 we establish the objectives of our theoretical and numerical work on routing and grooming process. We present “the characteristic function” which is a numerical function allowing to characterize the accuracy of a routing and grooming method. We argue that it allows understanding of the routing and grooming process as well as the ability to easily predict the results of multilayer network planning over a wide range of traffic scenarios. Finally we show how in practice “the characteristic function” can be used to compare algorithms between them and with theoretical bounds, and finally to propose most impactful algorithmic modifications.

In Chapter 3 we discuss the influence of the optical reach on the cost of the devices in the optical layer. We show how the optical reach impacts the total network cost in multilayer network planning and as well as the set of optical connections established during network planning. We demonstrate and explain the added value of including the optical reach and the cost of regenerators during the routing and grooming process. We highlight the cases where the impact and the benefits of this inclusion are the highest. To maximize the cost saving we argue that the choice of the equipment defining the optical reach should not be done before processing the inputs of the network planning scenario. Finally, we present a method of selection of optical equipment defining the optical reach.

In the last section of this manuscript we draw a conclusion and present the perspectives offered by our work.

# Chapter 1: State of the art on multilayer network planning

## I. CORE AND METROPOLITAN NETWORKS

### *A. Segmentation of the networks*

Telecommunication networks are separated into three segments (Figure 1):

- Access networks that collect the data flows from users,
- Metropolitan (or metro) networks that transport data at a local level and aggregate all the flows with a non-local destination and direct them to the edge router, which is the interface with the core network.
- Core networks that transport data at the scale of a country or a continent.

Metropolitan and core networks are called transport networks. Transport networks cover distances going from less than 10 km (for small metropolitan networks) up to thousands of kilometers (core networks covering entire continents). Metropolitan networks have distances that are in general one order of magnitude below those of core networks. The total quantity of traffic transport networks have to carry increases exponentially. It grew at a rate of 60% per year in the 2000's [1][1] and is expected to continue growing by more than 20% per year in the current decade [7]. The technology that allows transmitting this information between the different nodes of the network is wavelength division multiplexing (WDM) using optical signals transported through optical fiber. In WDM systems, an optical fiber can simultaneously carry several optical signals occupying disjoint channels in the spectral domain. This sharing of the optical fiber by different optical signals is allowed by the deployment of optical devices called WDM multiplexers. Today all of the core networks and most of the metropolitan networks use this transport technology.

As the client traffic is a flow of data frames received from edge routers, the nodes are composed at least of a router capable of treating and switching the data frames and a WDM node that treats the optical signal, as shown in Figure 1. Transport networks are made of 2 to more than 100 nodes, linked by pieces of optical fiber called links. The number of nodes in the topology is growing with time because operators interconnect more and more towns. The set of nodes and links is called the topology of the network. For resiliency's sake each node is connected to the network with at least two links.

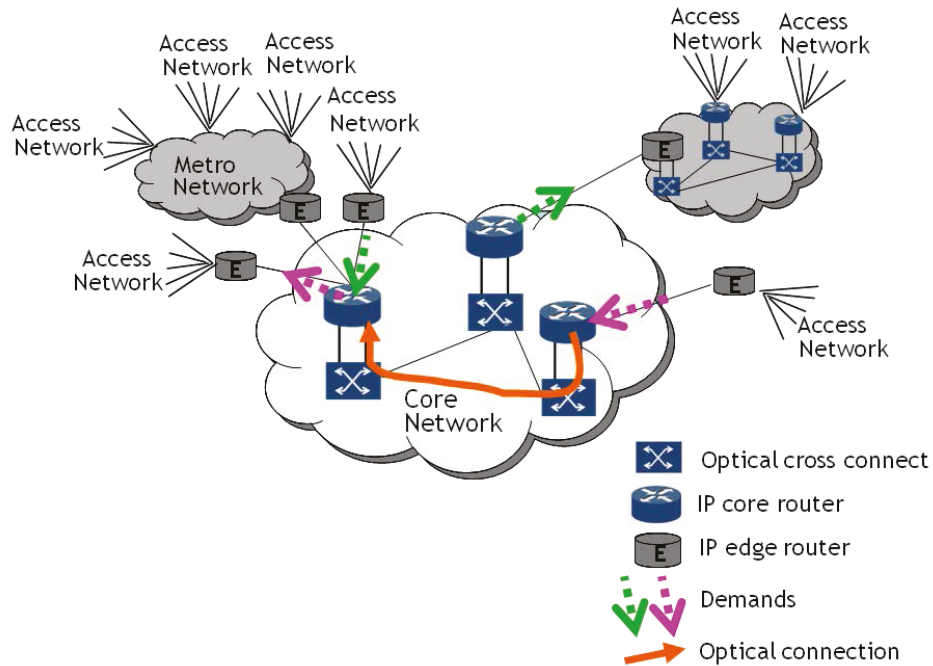


Figure 1: Segmentation of telecommunication networks, with one client traffic demand transported over the core network.

In transport networks, the flows of client traffic that are received from edge routers are in fact flows of data frames from a great number of users multiplexed in the time domain (TDM). Because of this multiplexing over a large number of random communications, the resulting flows vary little in time. Due to a greater scale, this is generally the case for core networks, and to a lesser extent for metropolitan networks, in which the traffic is more variable. Nonetheless, in general, in core and metropolitan networks client traffic flows are approximated to have a constant capacity. We consider that all the flows that need to be transported from one source to one destination to be aggregated in one flow called *client traffic demands*. Their capacity is in practice set to the maximum capacity of the flow (in Gb/s). Client traffic demands are received by the core routers (as shown on Figure 1) and are transported between nodes using *optical connections* which also have a constant capacity, source node and destination node. Client traffic demands are generally considered as being bidirectional (same capacity exchanged from source to destination node and from destination node to source node)[8]; therefore the optical connections are made bidirectional, but this state of affairs may soon change [8]. Client traffic demands generally have capacities lower than those of optical connections.

## B. Network layers and protocol stack

Traditionally the network is cut up into layers, in transport networks there is a functional separation between the electronic (or IP) layer and the optical (or WDM) layer. The IP layer primarily routes the client traffic demands in the IP layer and aggregates them into optical connections, this function is called *grooming*. The WDM layer transports optical connections between nodes by assigning them a WDM channel in the optical spectrum, these functions are called *optical routing* and *wavelength assignment*.

To implement all the functions of a transport network, a few protocol stacks were available at any moment in history and the stack implemented in transport network nodes has evolved a lot during the past 20 years. We sum up the evolution and the diversity of the protocol stack in Figure 2. Today the trend is towards a convergence of all data protocols to the IP protocol which is communicating through an OTN interface with WDM or OTN equipment.

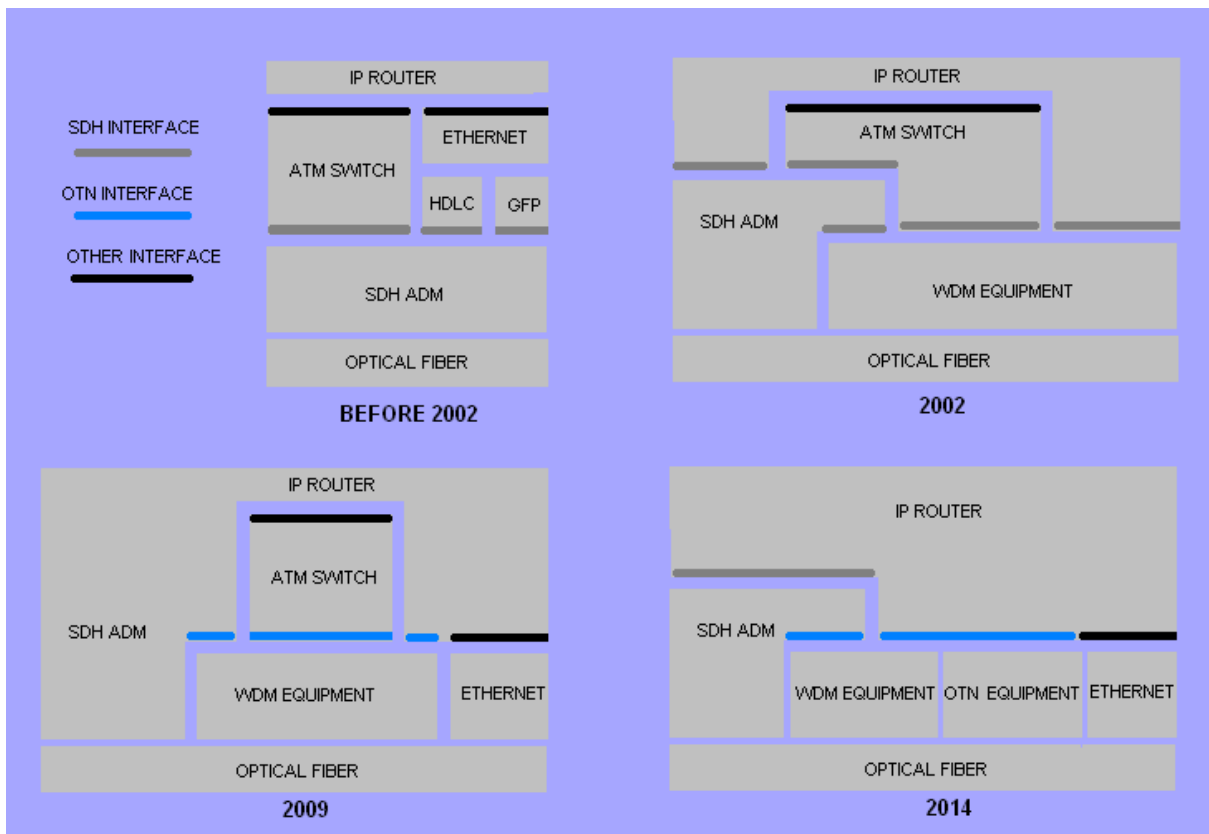


Figure 2: Evolution of the protocol stack in transport networks (approximate dates).

## C. Evolution of node architecture

The evolution of the protocol stack accompanied the evolution of the optical node architecture.

### 1) Opaque networks

Historically the WDM layer was *opaque* meaning that it ensured simply an interconnection between adjacent nodes. Optoelectronic conversions, conversions from an optical signal to an electric signal, were performed at the ends of every link: the optical signal was received by an optoelectronic device called a transponder (TSP) connected to router ports (RP), the packets it transported were then processed entirely in the electronic layer (supervision, demultiplexing, switching, aggregation into a new optical connection...). If the client traffic demand reached its destination node it left the transport network. Otherwise the packets were multiplexed and aggregated with other client traffic demands and reentered the optical layer through a transponder; this functionality is called regrooming (or reaggregation).

The functioning of opaque nodes is shown in Figure 3.

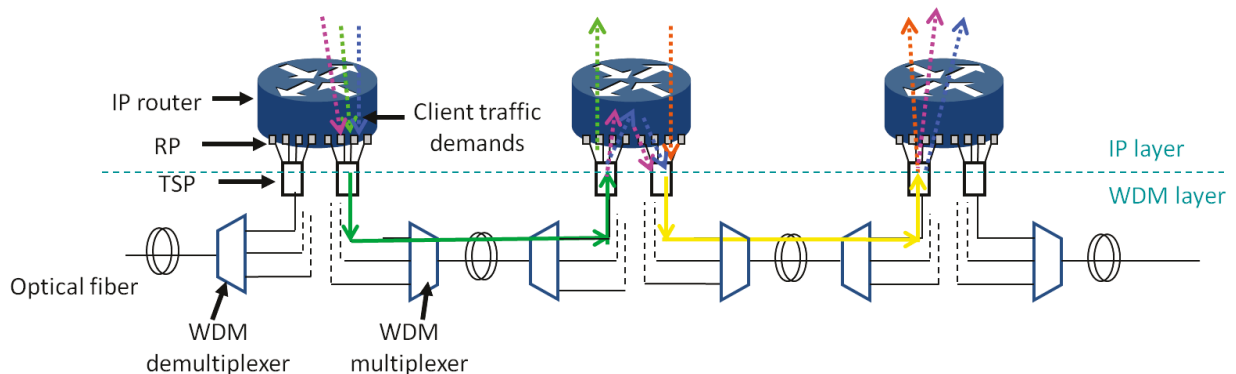


Figure 3: Three opaque nodes transporting four traffic demands. RP=router port, TSP=transponder.

In opaque networks, optoelectronic conversions are done at every intermediate node using many transponders and router resources. For this reason alternative node architectures allowing economies were invented.

### 2) Transparent networks

In the 2000's, optical cross connects (OXC) were deployed in the optical part of the nodes [9], [10]. OXCs are all-optic switching matrices allowing some of optical signals to pass through the optical part of the node without any optoelectronic conversion. The deployment of these switching technologies combined with the gradual increase of the distance over which optical signals could be transmitted shifted the paradigm to transparent optical networks. In this paradigm each traffic demand is extracted from the WDM layer only at its destination node. As no electronic treatment takes place in the nodes on the signal's path, from the IP layer point of view, each demand is transported directly from its source node to its destination node. This paradigm is also called overlay network and is standardized by the IETF [11].

The functioning of an overlay network is shown in Figure 4. For each of the four traffic demands (dotted arrows), one pair of transponders and one optical connection

(continuous arrows) is deployed. For the longer (red and the blue continuous arrows) optical channels no optoelectronic treatment is needed in the intermediate node.

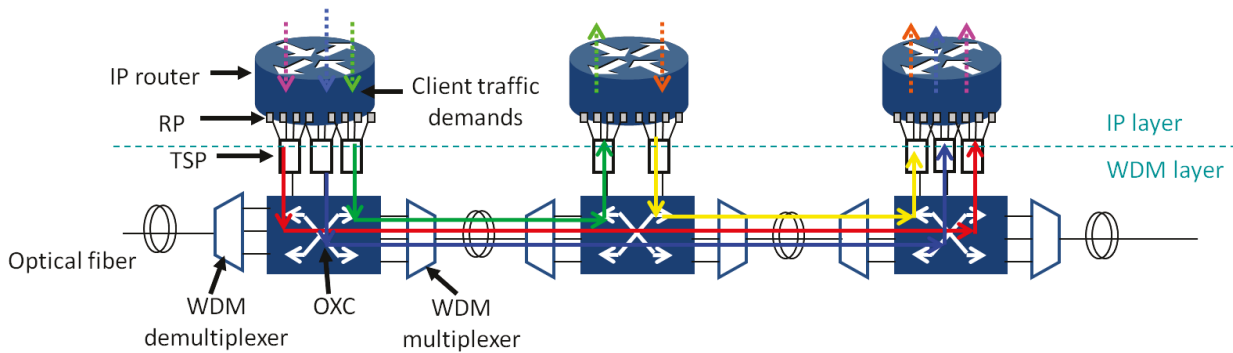


Figure 4: Three transparent nodes transporting four traffic demands. RP=router port, TSP=transponder, OXC=optical cross-connect.

### 3) Hybrid networks

The shortcoming of the overlay network paradigm is that if a client traffic demand has a very small capacity, for example 200 Mb/s, it is still assigned a pair of transponders and an optical connection which has capacities of up to 100 Gb/s today. This means that the devices can be used at only 0.2% of their capacity. This is why the hybrid (sometime abusively called translucent) network paradigm appeared. The idea is, for any traffic demand, to allow optical bypass as well as optoelectronic conversions in any node of the topology [12] - [14].

The main operations possible in a hybrid node are shown in Figure 5.

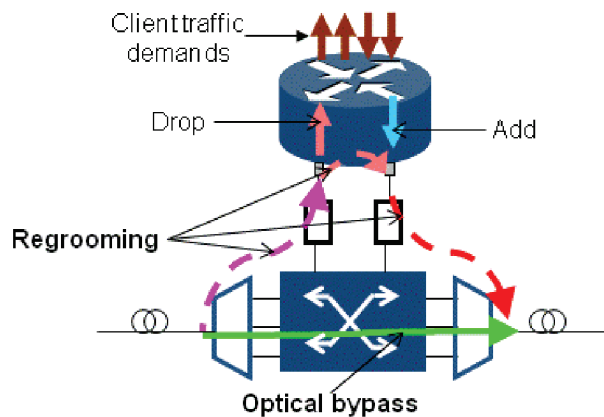


Figure 5: Operations possible in a hybrid IP-over-WDM node.

An optical signal arriving in a hybrid node can

- be optically switched towards another optical fiber connected to the node. It is not treated in any way and in particular does not undergo any optoelectronic conversions. It optically bypasses the electronic node (Continuous green arrow in the figure)

- be optically switched towards a transponder and converted into an electrical signal (purple dashed arrow). The signal is treated so as to detect and correct errors. The data frames multiplexed by TDM (Time Division Multiplexing) are demultiplexed and treated depending on their destination. Those frames whose destination node is the current node are "dropped" (large pink arrow). They constitute the client traffic demands that

have arrived to destination. The client traffic demands entering the network at that node (large blue arrow) can be "added" to the remaining data frames. All these data frames will be aggregated together, assigned a channel in the spectral domain and sent to the corresponding transponder (red dashed arrow). This is regrooming (or reaggregation).

Transponders are usually linked to only one router port; transponders that can multiplex/demultiplex data incoming to/from several (2 to 10) router ports are called muxponders. Only nodes using transponders are studied in this work. Therefore, each hybrid node has the architecture depicted in Figure 6.

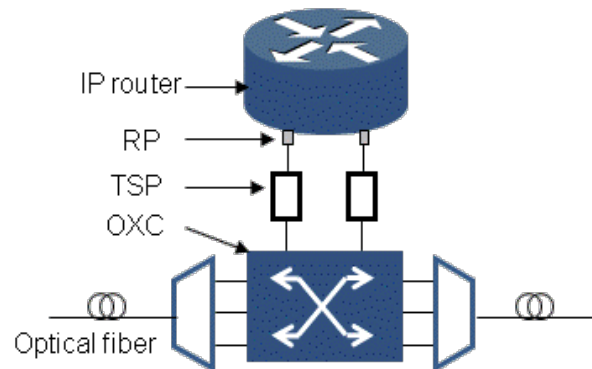


Figure 6: Hybrid IP-over-WDM node used in our work.

We have explained how hybrid networks allow much more possibilities as compared to prior network paradigms. This allows minimizing the resources needed to transport all the client traffic, but it also makes the network planning much more complex as we will see in the following section.

## II. NETWORK PLANNING OF IP-OVER-WDM NETWORKS

When a network needs to be deployed or changed, different pieces of equipment must be placed and properly configured in different links and nodes so as to transport all the traffic demands while minimizing a certain cost function. This process is called *network planning*.

### A. *Cost functions*

A cost function used for network planning is a combination of network parameters that are most important to the network manager. Existing cost functions can be classified into two families:

- Network throughput: given a limited number of resources (optical spectrum in each link and/or limited number of devices), network planning has to maximize the amount of client traffic that can be transported without being blocked at any bottleneck [15].

- Network cost: given the existing and/or the forecasted client traffic demands, deploy the resources so as to minimize the total cost of the network. Typically the cost is the capital expenditure (CapEx), the operational expenditure (OpEx), or energy consumption.

In our work we use cost functions aiming to minimize the network cost. Historically, CapEx cost functions, the cost that the owner of the network has to pay for the deployment, were predominant. Indeed, the cost of ownership, or OpEx, was regarded as less important because it appeared when the network was already bringing money. The balance started to shift in circa 2009 when the energy consumption of network (a part of the OpEx) started to become costly and progressing at enormous rates [3], [16]-[18]. Indeed in 2007 at the Nature Photonics Technology conference, it was stated that “by 2020, Telecoms would move from switching Terabits to Petabits, but based on today’s technology a 100 Pb/s IP router would consume 10 Megawatts and require a nuclear power station to supply it with electricity”. This is why the energy consumption has become a cost function as common as the CapEx in scientific literature. In our work we did not choose between CapEx or energy consumption, our results can be applied to both. Also, the devices that consume the most energy happen to be those who cost the most [19]-[23]. This is why the term “cost” is applicable to both of these cost functions.

A transport network is composed of nodes and links. The devices in the optical links are mainly the optical amplifiers. These amplifiers do not constitute an important part of the network cost; also their quantity depends little on the network planning. The major part of the network cost and consumption is concentrated in the nodes. The most detailed planning tools take into account all the components [20]-[23]. When a less detailed approach is taken, it is considered that devices that cost most are the IP routers, the OXCs, the regenerators and the transponders. The approximate cost of the OXC and the router is generally considered to be proportional to the number of ports it has. Therefore, in the rest of our work we will seek to minimize the linear combination of the number of router ports, OXC ports, transponders and regenerators multiplied by their individual cost, as it is currently done in the vast majority of the literature on the subject.

## B. Constraints

The devices found in the links and the nodes have their technological and physical limitations, generating constraints that the results of network planning are subject to. Here we study the most important of these constraints:

-The limited number of optical channels per physical link. To achieve an optical fiber transmission, signals need to be amplified every 50 to 100 km. Thanks to EDFA (erbium-doped fiber amplifier) technology, this can be performed for signals whose wavelength is in the 191.56 THz-195.942 THz C-Band (Common Band). The DWDM standard of the ITU-T [24][24] divides the optical spectrum into fixed 12.5 GHz frequency slots (a channel can be made up of one or several adjacent slots). It means that there are at most 350 slots per fiber. In a heavy traffic network, a physical link may be saturated, i.e. all its frequency slots are occupied. It may also happen that an optical connection, passing through several optical links, cannot be established using the same frequency slots from source to destination due to high occupation of those links. This problem is called spectrum contention. Wavelength converter devices can be used to change the optical wavelength between two adjacent links avoiding spectrum contention problem [25][25]. This constraint is called the spectrum continuity problem.

-The limited propagation distance of the optical transmission. An optical signal is degraded during its propagation via great distances of fiber and optical cross-connects. These degradations are called physical impairments and consist of optical signal deformations due to physical phenomena that apply to optical propagation. If the transmission distance is too long, physical impairments induce such an important signal degradation that the optical receiver is not able to transpose it to electric data without an excessive bit error rate (BER): the receiver maximum sensitivity has been reached. To determine whether an optical connection is feasible at a given BER threshold, the signal propagation equations, namely the Nonlinear Schrödinger Equation [26] have to be solved along its path: this leads to heavy computations. In practice, when a network with a WDM layer is planned, a software module is used to determine if the optical connection is feasible or not. This module is an estimator for the solution of the Nonlinear Schrödinger Equation called “physical impairment estimator” [27]. We use a simplified physical estimator called the *optical reach*, which is a scalar equal to the maximal distance an optical signal can travel while ensuring at the reception a BER lower than a given threshold. Also, a scalar “length” is attributed to each physical link. An optical connection passing through several links is considered feasible if the sum of the lengths of these links is lower than the optical reach. This approximation does not affect the generality of our results and it has been demonstrated in [27] that the optical reach models well the impact of physical impairments on the choice of optical connections. If an optical connection longer than the optical reach must be established, one or several regenerators (additional optoelectronic equipment) can be placed in intermediate nodes in order to retime, reshape, and reamplify the optical signal [27], [28].

-The limited capacity of electronic nodes. The routers of each node are limited by the number of packets they can switch per second; moreover the number of slots for router ports is limited. These limitations are specific to the router implementation.

-The indivisibility of certain flows of client traffic. Indeed, the main protocols ensuring the interface between the IP and the WDM layer (SDH, SONET, OTN) implement the “virtual concatenation”, i.e. the possibility to send data frames belonging to one flow of client traffic over two different routes in the IP and/or the WDM layer. It is not always implemented because of the need of buffers capable of storing data frames that arrive earlier than the other parts of the flow. The absence of virtual concatenation is an additional constraint on the network planning.

-The limited number of regenerators/wavelength converters that can be deployed in the WDM node. This limitation depends on the architecture of the OXC.

-The limited number of transporters that can be connected to one OXC in the WDM node, this limitation depends on the architecture of the OXC.

-The delay that is needed for a client traffic demand to cross the network is an emerging concern for network operators who face an increase of live video data. We expect this constraint to be more present in future research [29], [30].

-The obligation to route all the traffic between two nodes in the topology over a given path, commonly the shortest path for a given length metric [31]. This constraint is useful to facilitate the operations, administration and management (OAM) of the network. Indeed in any moment it is easier to find out which links are used by which client traffic demands.

-The bidirectionality of the optical connections is also a constraint on the network planning tool. Indeed the hypothesis of bidirectional client traffic demands is widespread, and bidirectional optical connections facilitate the OAM. Therefore, today transponders are bidirectional. But this status quo may soon be challenged [8][8].

The routines that minimize the cost function while complying with the constraints are the network planning routines; which are separated into two categories: pre-multilayer and multilayer.

## C. Pre-multilayer network planning

### 1) Opaque network planning

As mentioned in I.C.1), first core networks were composed of opaque nodes, where no optical bypass is possible. The first studies on this subject known to us have been published in 1998 [32]. In opaque network planning, in general, each client traffic demand follows the path that minimizes the number of links it transits through, so as to occupy the less router processing time and transponder capacity as possible. Also, among two routing paths having the same number of links, the one composed of links with the shortest length are chosen to avoid physical impairments.

This is the general case, but sometimes it is more advantageous to use available capacity in transponders that have already been deployed for other client traffic demands or to unload links that are almost full to their maximum capacity, but these are exceptions. Therefore in our work we suppose that each demand is routed on its shortest path [31] using link length as the metric.

## 2) *Overlay network planning*

In overlay networks, for each node pair that exchanges a client traffic demand, the transponders (one or more pairs) needed to transport the aggregated capacity are placed in the source and the destination node. The grooming is trivial in overlay network planning; the routing and the wavelength assignment is where the main difficulty is. Indeed, the lengths of the optical connections are much longer than in opaque networks, where they are made of only one link. In transparent networks the connections can be longer than the optical reach and regenerators have to be placed in intermediate nodes. To avoid the deployment of expensive regenerators, the routing tends to follow the shortest path in terms of link length. But, when a network is heavily loaded with client traffic, some links have no more available optical spectrum, they become bottlenecks and may cause blockage of some of the traffic demands. To avoid the blockage, some of the demands have to be routed over paths where more spectrum is available and wavelength converters can be set up to shift the frequency of the spectrum slots originally allocated to the demand to avoid spectrum contention. Many works have been carried out on the topic of routing, wavelength assignment and regenerator placement [23], [27], [28], [33]-[39]. The routing, grooming and wavelength assignment in the overlay network paradigm is trivial unless the risk of blockage appears, then the routing, wavelength assignment and regenerator placement problem becomes a lot more complex.

We note that, in overlay network planning the IP layer decides of the optical connections to establish without information on the optical links. No exchange of information between the two layers is needed. This is in fact the segmentation of the network planning problem into two separate problems. The grooming and the routing in the IP layer are solved first. Then the routing in the optical layer and the wavelength assignment take place.

## D. *Multilayer network planning*

In overlay network planning tools, the network planning is broken up into two separate problems. This simplifies the resolution, but as in reality the two problems are correlated and not independent, this approach is necessarily suboptimal. As we have seen in section I.C.3), hybrid nodes offer much more possibilities for the regrooming of client traffic demands which allows saving optical equipment by enabling the sharing of optical connections between client traffic demands. First study of network planning for hybrid networks known to us concerns circular topologies [40], it has been published in 2000. Starting from the following year studies concerning mesh topologies were published, e.g. in [41].

In Figure 7 we examine the transport over a hybrid network of three bidirectional client traffic demands:  $i \leftrightarrow j$ ,  $j \leftrightarrow k$ , and  $i \leftrightarrow k$ .

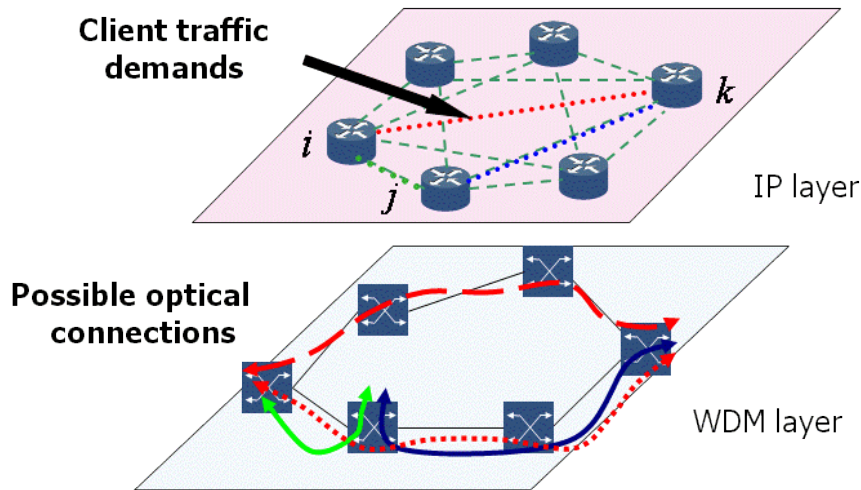


Figure 7: Illustration of the multilayer network planning problem on the example of 3 client traffic demands in a circular topology.

Let us suppose that for each of the demands  $i \leftrightarrow j$  and  $j \leftrightarrow k$  it has been decided to establish an end-to-end optical connection (continuous blue and green arrows). For  $i \leftrightarrow k$  it is also possible to establish an end-to-end optical connection, if the shortest path is chosen it corresponds to the dotted red arrow. For different reasons (for example to leave free spectrum on the shortest path), we can establish the other possible end-to-end connection (red dashed arrow). If these two long connections are longer than the optical reach or if the aim is to save costs, we can regroom the client traffic from the demand  $i \leftrightarrow k$  in node  $j$  with the traffic on the already established optical connections. If there is enough free capacity, this demand can be transported without any additional resource allocation. This kind of decision has to be taken for every client traffic demand. Once all the client traffic demands have been processed, each demand will be routed in the IP layer, it will be groomed with other demands into optical connections, each optical connection will be routed in the optical layer using spectral slots that will be assigned to it on every link it passes through.

This problem is known as the routing, grooming and wavelength assignment (GRWA) problem.

Solving the GRWA problem is called *multilayer network planning* because it requires exchanges of information between the WDM layer and the IP layer to be executed. Indeed, unlike in overlay network planning, information about the WDM layer is required to decide on the grooming and the routing in the IP layer. To the very least this information includes:

- the topology of the WDM layer, so as to know which client traffic demands can have the same path in the WDM layer and share an optical connection by grooming them together.

- the costs of different devices, so as to know which expenses are entailed by each planning decision on the total cost of the network.

Many other types of information can be shared in order to minimize the cost of the network as we explain in section E below.

In meshed network topologies solving the GRWA problem can be extremely complex and it has been proven that the routing and grooming (RG) problem alone is NP-complete [42]. This means that it cannot be solved in polynomial time. Exact resolutions of the

GRWA problem exist, by modeling it as a system of linear equations; this formulation is done using Mixed Integer Linear Programming (MILP). Solving a MILP formulation allows obtaining the absolute minimum of the cost function. These problems are computationally heavy and can be solved only for topologies with 4 to 20 nodes with computation time amounting from hours or days as evidenced by publications [13]-[15], [19], [25], [30], [42]-[51]. This is why heuristics are developed for actual network planning tools as well as for research purposes [12], [14], [25], [30], [42]-[45], [48], [51]-[56]. MILP formulations are thus used usually to validate the performance of the heuristics on the example of a topology with only a few nodes [25], [30], [42]-[45], [48], [51].

In multilayer network planning, as in overlay network planning, wavelength assignment influences the result of network planning only when bottlenecks appear in the optical links, which is not the general case. Therefore the routing and grooming (RG) problem is an acceptable approximation for multilayer planning. In spite of the importance of this mechanism we did not find in the literature any work establishing a theoretical framework to study it. It has been done for the routing and spectrum assignment in [57]. For the RG problem only empiric numerical studies exist [12].

Heuristics allow bringing down the computational time needed to solve the RG problem, thus additional information can be added to the problem in order to refine the results of GRWA and provide a more holistic approach to network planning.

## *E. Additional parameters for multilayer network planning*

The GRWA problem has thus far been presented at a high level. We have explained in the previous chapters that some of the assumptions on the constraints and the costs are approximations. Many studies have been published taking into account more detailed and realistic costs and constraints. By including them in the GRWA process it is proven that cost savings are achieved. A non-exhaustive list of such approaches is presented here.

### *1) Better accounting for constraints*

In section II.B, we have presented various constraints that apply to the results of network planning. Including constraints into the planning process complicates the problem but it ensures that the final results comply with the constraints which avoids their discovery later during the deployment. For example, taking into account the feasibility of optical connections allows placing regenerators during the GRWA process. According to our results presented in Chapter 3 and existing publications [58] this allows cost savings. Similarly, accounting for the limited spectrum in the fiber links allows minimizing the number of wavelength converters or the number of blocked client traffic demands appearing because of capacity bottlenecks.

### *2) Better accounting for costs*

In section A, we have discussed the cost functions that the network planning process can optimize. We have come to a total network cost that is a weighted sum of the number of IP ports, OXC ports, regenerators and transponders. The costs' details are much more complex. The nodes are composed of racks holding a great variety of devices [23], also the cost of operating equipment may vary from one node to another [29], and finally the energy consumption of different devices can be dependent on the quantity of

traffic they process [30], [59]. Considering all these aspects of the pricing has been proven to yield cost savings.

### 3) *Dissymmetric topologies*

It is frequent in operational networks that the nodes have very different architecture, indeed it is possible to have nodes consisting of only an IP router (linked directly router-port-to-router-port to their neighbors), or at the opposite of only a WDM node (no traffic added or dropped at this node). These topologies are called dissymmetrical (or sparse) and the planning tools should be adapted so as to use at best the “incomplete nodes” [53], [60].

Additional parameters allow refining the quality of the solution and allow minimizing the network cost. But there is also research on the RG algorithms that take the approach of adopting a more holistic version of network optimization by adding more aspects (and therefore more variables) to the problem.

## F. *Technological evolutions that impact the multilayer planning process*

### 1) *Extra layers*

Some node architectures propose to add an additional layer to the network by adding switching capacities lower or higher than the capacity of WDM connections. This results in an additional switching layer under the WDM layer (wavebands and superchannels) or between the IP and the WDM layer (TDM switching).

#### -TDM switching

Researchers and equipment vendors study a possibility to have an intermediate layer capable of switching TDM flows with capacities under that of WDM. The corresponding node architecture is presented in Figure 8. The electric cross-connect (EXC) allows to switch and groom TDM flows without having to process each packet in the IP layer, which is much more energy efficient. The disadvantage is that additional pieces of equipment need to be acquired and powered. Network planning studies have to be carried out to evaluate the cost gains. MILP formulations [46] are intractable even for 4 node topologies, therefore only heuristics can be used [61], [62] and few studies using heuristics are available in the literature.

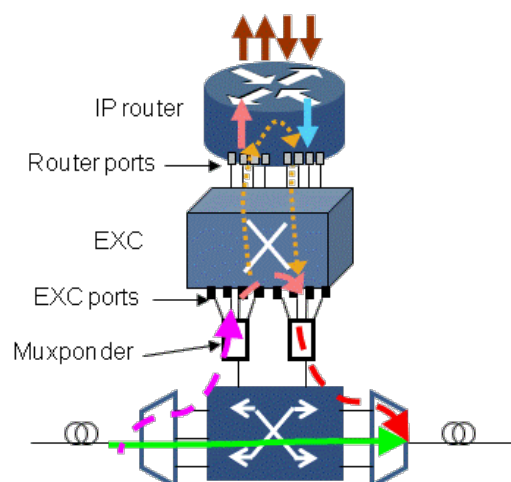


Figure 8: Hybrid IP-over-EXC-over-WDM node. EXC=electric cross-connect.

### -Wavebands and superchannels

Another approach is to switch circuits with a capacity above those proposed by OTN and WDM. By grouping optical connections together either into wavebands or into superchannels, the main gains are to be found in the simplification of the OXC. Waveband advocates propose to add additional switching equipment to manipulate groups of optical connection having adjacent optical spectrum [63], [64]; similarly, superchannel advocates propose to switch large portions of the optical spectrum, but no additional equipment is needed, superchannels can be switched using state-of-the art OXCs. In addition, superchannels allow more spectrum-efficient solutions due to the reduction of margins called guard-bands between adjacent optical signals [65]-[67]. Superchannels are expected to appear in WDM products in the next years.

To carry out multilayer planning of networks with three layers, new heuristics have to be proposed. As a first approximation, the problem can be split into two successive independent two-layer subproblems. But for better performances more research is still needed.

## 2) *Resiliency*

Historically, in core networks, it is a common practice to double or even triple each network resource to avoid service interruption in case of break-downs. Finding ways to lower the proportion of thus unused equipment is a vast field of study. Its results may impact multilayer network planning. For instance, the reconfigurability of network nodes allows protecting some of the client traffic demands by leaving free additional optical paths in the network to reestablish connections in case of localized breakdowns [48], [68]. The planning process of IP-over-WDM networks with restoration is in fact a sequence of planning of the network where one or several resources are emulated as being out of order.

## 3) *Mixed Line Rate (MLR) optical layer and elastic transponders*

With the fast changes of generations of transponders during the past years, many networks contain transponders of heterogeneous capacities; they are called Mixed Line Rate (MLR). Previously each type of transponders was treated separately; network planning for each capacity was done separately with its specific optical reach. Multilayer MLR network planning takes into account all the possibilities of each transponder to adopt a more holistic view of the network planning [54]-[56], [69]. It is also proposed to deploy transponders capable of changing both their capacity and reach according to the needs of the network. Such transponders are called *elastic*.

Network planning with MLR or an elastic optical layer is much more complex than the normal GRWA problem. Indeed not only the placement of resources needs to be decided but also the capacity, the optical reach and the cost of the equipment must be chosen. We have not proposed a MLR heuristic, we rather concentrated on the rigorous study of the RG process and the influence of the reach and the cost of the transponders on its results. Our results can be used as a starting point for a better comprehension of the planning of MLR networks.

#### 4) *Evolution towards dynamic and elastic optical layers*

The most radical change coming in the core networks is a shift towards a more dynamic optical layer. Indeed, as we mentioned in section I.A, the common hypothesis that applies to the core networks, and by extension to metro networks, is that the variability of client traffic demands is limited. But this assumption is not true, especially for metropolitan networks. Since the scientific community seeks to increase the energy efficiency of transport networks, this hypothesis was questioned. Turning off network devices when they are not needed is considered as one of the main ways to save energy [4], [13], [23], [49], [50], [70]-[75]. A more dynamic network can also allow protecting optical connection without doubling equipment and with minimal information loss [76], [77].

If combined with new *elastic transponders* capable of changing their capacity (and therefore their optical reach) dynamically, *dynamic elastic optical networks* are obtained.

In the dynamic paradigm, the network provisions or releases resources to client traffic demands on their arrival or departure, respectively. Such a behavior will obviously produce network configurations that will be much less cost effective than results of static network planning for the same client traffic demands. This is why periodical reoptimizations are still expected to take place. These reoptimizations will be very similar to static network planning of today's networks.

### III. CONCLUSION

We have presented the transport networks and the network planning methods. We have explained the RG process, which is the essential mechanism of multilayer network planning. Four types of technological evolution we presented in this chapter, extend the range of possible solutions for network planning tools. For each of them we explained how the RG mechanism remains central to these evolutions of the multilayer planning problem. As there is no theoretical or numerical framework enabling a good understanding of this process we decided to research it. Our work in this direction is presented in Chapter 2.

Among the constraints that impact network planning we have distinguished the optical reach constraint as being of great importance. We have explained that we expect it to become even more important in the future because of the decrease of the optical reach with the increase of capacity of transponders. We have also highlighted the importance of a greater understanding of the impact of this constraint on multilayer network planning for future mixed line rate and elastic optical networks. Our work concerning this constraint is presented in Chapter 3.

# Chapter 2: The characteristic function of routing and grooming methods

A numerical model for estimating the results of multilayer network planning.

## I. STATE OF THE ART AND PROBLEMATIC

Network planning tools may serve in different conditions each requiring a specific compromise between computation time and cost savings. For example a long and detailed network planning is made just before deploying a network. More reactivity is necessary to respond to a tender offer where many options (costs, technologies, design margins...) need to be explored in a few hours. In dynamic networks, which are yet to come with the development of SDN (Software Defined Networks), it is needed to allocate resources on the arrival of new demands, and, periodically, reoptimizations of the virtual topology take place. For each time constraint, a heuristic algorithm maximizing cost savings needs to be found. To quantify cost savings of a network planning algorithm, two approaches are generally available:

-When a **RG** heuristic is presented, its results are compared to those of the corresponding MILP formulation, on a small topology (3 to 20 nodes) for one given traffic matrix [25], [30], [42]-[45], [48], [51]. Sometimes all the demands of the traffic matrix are multiplied by a variable to study various traffic loads. The advantage of this approach is the possibility to estimate the gap between the cost of a solution provided by the heuristic and the cost of the the optimal solution provided by the MILP approach. However one cannot deduce whether the size of gap in terms of costs will decrease or increase for different traffic matrices or larger topologies.

-In industrial studies, a few heuristics are usually proposed, their performances are compared in some *representative scenario* (topology and traffic matrix that represent a typical case study). Such an approach allows comparing heuristics in operational conditions, but cannot estimate the gap in terms of cost with the optimal solution. Hence no clue is given on whether it is possible to obtain lower network costs by enhancing the heuristic .

In addition, the shortcomings we identify for both approaches are that they do not:

- give indications about how to improve the heuristic to yield cost savings,
- insure that the result of a comparison between heuristics, or between a heuristic and the MILP formulation, apply to other traffic matrices
- allow estimating the quantity of equipment to be deployed to transport another traffic matrix.

To cope with these issues, we introduce the “characteristic function” which fulfills 3 objectives:

Objective 1: compare all the RG methods on a common basis and understand easily the cost difference of the solutions they yield.

Objective 2: introduce a representative scenario, so that the results obtained for this scenario may be generalized to more generic traffic matrices.

Objective 3: obtain for a given RG heuristic and topology an estimation of the cost for simple traffic matrices.

This chapter is organized as follows. First we mention the literature sources that inspired us and the hypotheses we use in our studies. Then we explain what a characteristic function is, how it is obtained and how it can be used to fulfill Objective 1. Then we show that the characteristic function also fulfills Objectives 2 and 3 via extrapolation of characteristic function to realistic traffic matrices. Finally we show how the application of characteristic function helps to enhance two existing network planning tools.

## II. INSPIRATION

An analytical model of the routing and wavelength assignment process has been presented in [57], it allows creating a framework where the results of WDM layer planning can be understood and compared to theoretical limits. As multilayer network planning has become the main network planning paradigm, we found an analytical model is also needed in this domain. An analytical model can be developed from a numerical model, that is why we worked in this direction.

We have found similar motivations to our objectives in [12]. The authors searched for a numerical model of RG process for a two-layered network. They chose to plan for 10 Gb/s transponders and traffic matrices with a discrete statistical distribution of traffic demands. The traffic demands were composed of 50% 155.52 Mb/s demands, 20% 622 Mb/s demands, and 30% 2.5 Gb/s demands. The curves linking the number of transponders to the traffic load are shown in Figure 9.

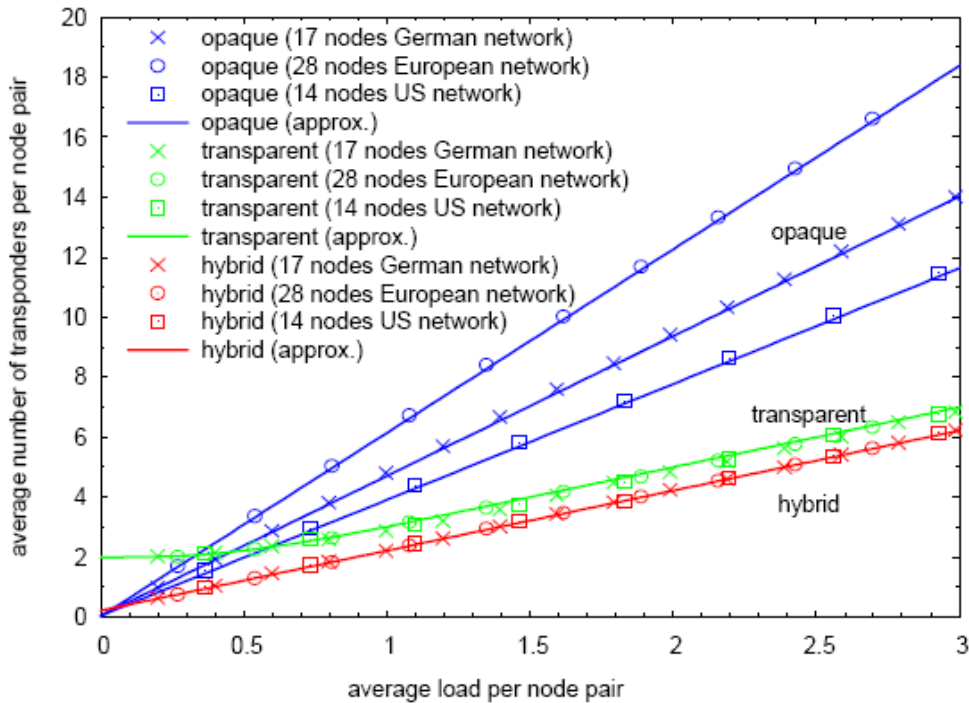


Figure 9: Approximation vs. simulation results for the number of required 10 Gb/s transponders in different network scenarios from [10]. “Transparent” corresponds to overlay RG and “hybrid” corresponds to multilayer RG.

What they call “transparent” corresponds to the overlay RG and “hybrid” corresponds to the multilayer RG. We see that these dependencies are linear for the overlay, opaque and multilayer planning. The authors could not extract from the equations of these curves the parameters linked to the topology, to the planning algorithm, and the statistical distribution of traffic matrix. Thus the obtained results lacked generality. We show that much more general and useful conclusion can be drawn by using very specific traffic hypotheses.

### III. HYPOTHESES

#### A. Network topologies

In this study we use four topologies called National 1, National 2, Continental 1 and Continental 2. They are shown in Figure 10 and their main characteristics are summarized in Table 1.

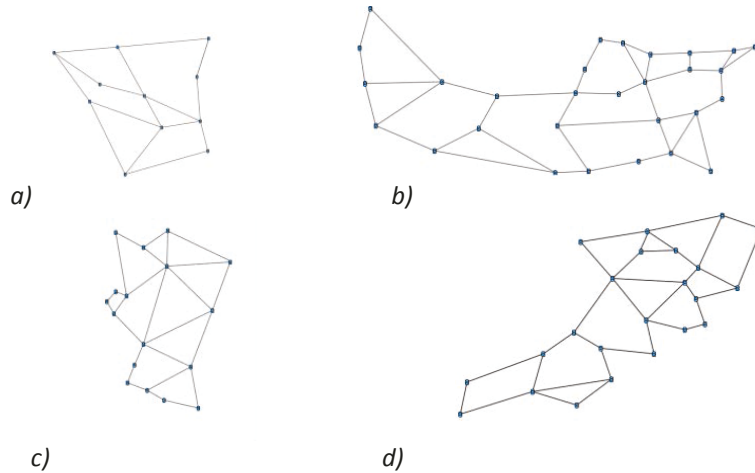


Figure 10: Studied network topologies. a) National 1 b) Continental 1 c) National 2 d) Continental 2

From now on we denote  $N$  the number of nodes in the studied topology,  $L$  the number of links,  $\delta$  the connectivity, defined as  $\delta = 2L/N$ .

Table 1: The characteristics of the studied topologies

	National 1	National 2	Continental 1	Continental 2
Nodes $N$	11	17	29	23
Links $L$	16	26	41	37

#### B. Node architecture

We aim to study the RG process alone. For this reason we remove all the constraints that network planning tools integrate (introduced in Chapter 1 section II.B). Even if we are aware of the fact that these constraints are essential, the aim here is to let the RG algorithm look into the vast scope of all the possible solutions (without being limited by constraints) to see whether it can find the optimal solution. It is after the evaluation of algorithm, during its implementation, that its developer has to limit the scope of possible solutions to those that conform to specific constraints of the network. This allows us to judge algorithms in the most general case, in agreement with Objective 1. It is for this reason that we shall omit all the constraints presented in Chapter 1 section II.B.

In this study we suppose that all the nodes have the IP-over-WDM architecture described in Chapter 1 section I.C.3). The part of network cost that depends on the RG process is the number of router ports, the number of transponders and the number of

OXC ports. The cost and the energy consumption of OXC ports are typically negligible as compared to the rest of the equipment [20], [23]. Each transponder is connected to the router by one router port. The number of router ports is therefore equal to the number of transponders, which is the double of the number of optical connections established by the algorithm. Denoted  $C$  hereafter, the number of optical connections is our cost metric in sections IV to VI.

### C. Traffic matrices

We define the *homogeneous traffic matrices* as uniform traffic matrices where the same amount of traffic is requested by each pair of communicating nodes. In other words, to construct a traffic matrix, the source and the destination of each traffic demand are chosen randomly and the capacity of this demand is a constant associated to the traffic matrix. The capacity of traffic demands is quantified in gigabits per second (Gb/s). For the sake of generality, we normalize the capacity of traffic demands by the transponder capacity (also in Gb/s), and the obtained dimensionless parameter is called *traffic granularity*, noted by  $g$ . A homogeneous traffic matrix can be represented as a *connection matrix* containing only zeroes and unities (determining whether a client traffic demand exists between each pair of nodes), multiplied by the traffic granularity. For any homogeneous matrix we call *density* the proportion of non-zero elements. We denote  $M$  the number of non-zero traffic demands.

For more clarity we represent in Figure 11 an example of a homogeneous traffic matrix for a eleven-node topology with  $g=0.4$  and  $M=48$ .

		Source node index										
		1	2	3	4	5	6	7	8	9	10	11
Destination node index	1	0	0	0,4	0	0	0,4	0	0	0,4	0	0,4
	2	0	0	0	0,4	0,4	0	0,4	0,4	0	0	0,4
	3	0,4	0	0	0	0,4	0	0,4	0,4	0,4	0	0
	4	0	0,4	0	0	0	0	0,4	0	0	0	0,4
	5	0	0,4	0,4	0	0	0,4	0	0	0,4	0	0
	6	0,4	0	0	0	0,4	0	0	0,4	0	0	0
	7	0	0,4	0,4	0,4	0	0	0	0,4	0,4	0	0,4
	8	0	0,4	0,4	0	0	0,4	0,4	0	0	0	0,4
	9	0,4	0	0,4	0	0,4	0	0,4	0	0	0,4	0,4
	10	0	0	0	0	0	0	0	0	0,4	0	0
	11	0,4	0,4	0	0,4	0	0	0,4	0,4	0,4	0	0

Figure 11: Example of a homogeneous traffic matrix for a eleven-node topology with  $g=0.4$  and  $M=48$

We note that in any traffic matrix the diagonal contains only zeros because there is no sense of considering a demand from a node to itself.

With our notations we can write:  $M = \text{density} \times N \times (N-1)$ . For Figure 11 we have  $N=11$ ,  $M=48$  and  $\text{density}=0.44$ .

From our experience we observe that in core networks, as the traffic load grows every year, the density is tending towards 1. This is why we find this case to be the most important to study when qualifying RG methods. Nevertheless in section IV.C.5) we study the impact of density on the results of the RG process.

To trace the characteristic function of an RG method we plot  $C/M$  as a function of  $g$ . In the following we study first the overlay and opaque RG methods and then multilayer RG methods.

## IV. HOW TO OBTAIN THE CHARACTERISTIC FUNCTION OF A RG METHOD

### A. Overlay network planning

As explained earlier in Chapter 1 section II.C.2), in overlay network planning, for each client traffic demand we provision an integer number of optical connections between its source and destination nodes for carrying the required capacity.

In Figure 12 we plot the number of optical connections  $C$  obtained after overlay network planning, divided by  $M$ , as a function of  $g$ . The graph has been obtained using National 1 topology and 40 homogeneous traffic matrices with a density of 1.

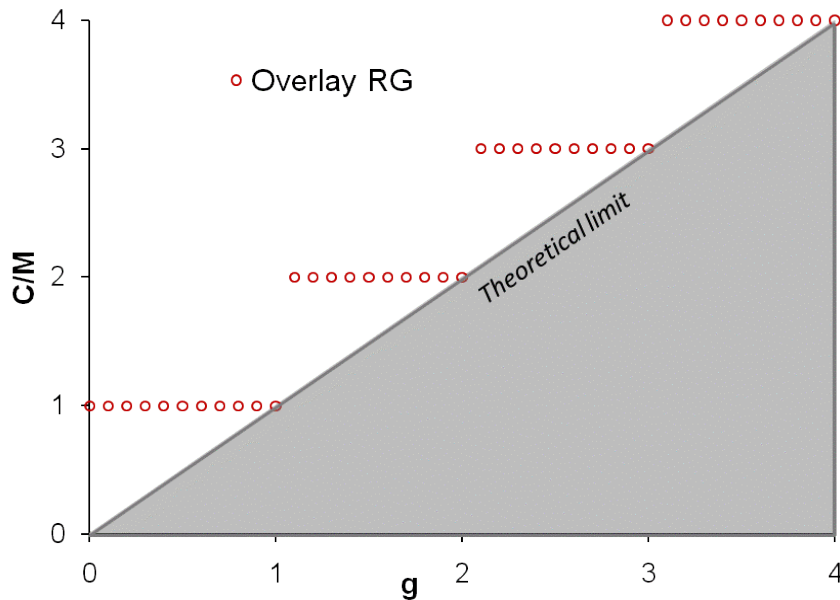


Figure 12: Characteristic function of the overlay routing and grooming (RG) method for National 1 topology and density=1

When  $g$  is lower than 1, the capacity of each of the traffic demands is lower than the transponder capacity, one optical connection is sufficient to transport each of the traffic demands, i.e.  $C = M$ . When  $1 < g \leq 2$ , two optical connections are required to transport each traffic demand, i.e.  $C = 2M$ . And so on. And this is independent of the topology and traffic density.

The data points of Figure 12 can be interpolated by a cyclically additive function with a period equal to 1. This function is the *characteristic function* of the overlay network planning method.

We represented in Figure 12 the theoretical limit of  $C/M$ , representing the minimal number of required optical connections, which occurs when the total capacity of optical connections equals the sum of the client traffic demands in the traffic matrix. Whatever the traffic matrix, the network planning cannot require fewer optical connections ( $C$ ) than this theoretical limit, as confirmed in [12]. When this limit is reached, each optical connection is perfectly filled with client traffic. A planning attains this limit only when

demand capacity is a multiple of the transponder capacity for every client traffic demand. Indeed, as we can see in Figure 12, the theoretical limit is achieved for integer values of  $g$ .

We note that the gap between the characteristic function of overlay network planning and the theoretical limit is large, especially for values of  $g$  much smaller than 1. This is due to the fact that even if the traffic demand has a small capacity in overlay network planning, it cannot be groomed with other demands having different sources or destinations.

## B. Opaque network planning

As explained in Chapter 1 section II.C.1), this network planning method corresponds to the case where each client traffic demand is routed over its shortest path on the physical topology and at every intermediate node each optical connection is terminated and its contents regroomed. It is the planning method that has to be used if optical bypass is impossible, which is the case in some legacy networks.

Figure 13 shows the characteristic function of an opaque network. Results are obtained using National 1 topology for which we generated 200 homogeneous traffic matrices with a density of 1.

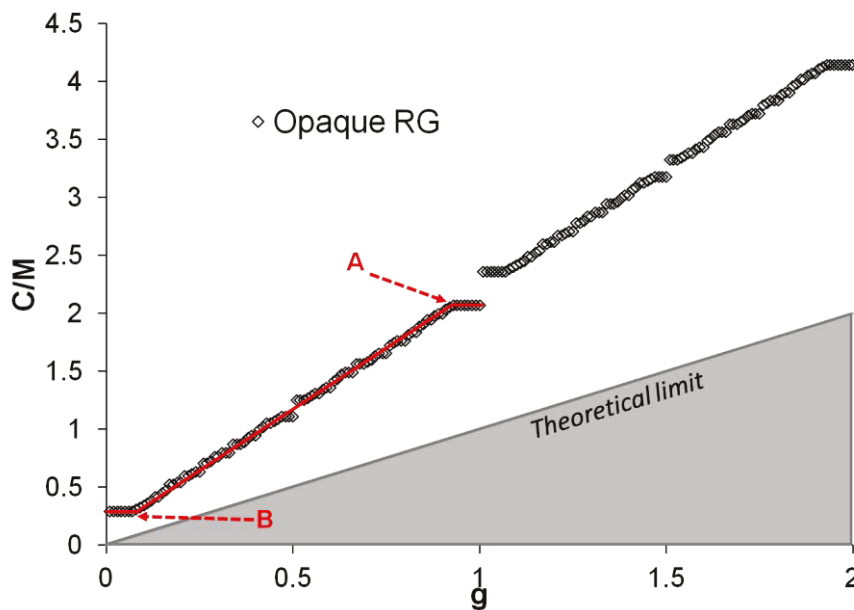


Figure 13: Characteristic function of the opaque routing and grooming (RG) method for National 1 topology and density=1

As shown in Figure 13, the data points obtained after planning can be interpolated by a cyclically additive function with period of  $g=1$ . This characteristic function can be approximated as an infinitely repeating pattern composed of 3 lines, called “stair function”, in red. To quantify the relevance of this approximation we introduce DELTA the mean L1-distance between the stair function and the data points. In our work we arbitrarily fix the upper limit of DELTA under which we accept the stair function approximation to DELTA=0.035. Above this value we found that, visually, the data points deviate from the stair function to the point where other approximations are more relevant. For the case represented in Figure 13, we obtain DELTA= 0.012.

The 3 lines composing the pattern are delimited by two point A and B. If we manage to obtain the coordinates of the points A and B we will have described the stair function. If

their value can be obtained analytically, the equation pattern can be foreseen without any simulation.

### 1) Analytical explanation

To achieve an analytical explanation of the characteristic function for the opaque case, the following notations should be introduced:

$X(l)$  – for a given link  $l$  of the topology, it is the number of unidirectional traffic demands whose routing path contains  $l$

$L(i)$  – number of links belonging to exactly  $i$  routing paths, i.e. number of links whose  $X(l) = i$

$i_{max}$  – maximal value of  $i$  for which  $L(i) \neq 0$

$\overline{hops}$  – mean number of links (hops) per routing path.

We note that by definition of  $L(i)$ :

$$\sum_{i=0}^{\infty} L(i) = L \quad (1)$$

and

$$\sum_{i=0}^{\infty} iL(i) = \sum_{l=0}^L X(l) = \overline{hops} \times M$$

To obtain the number of optical connections needed on a given link  $l$  we need to find the lowest integer number of optical connections capable of transporting the total capacity of traffic on this link which can be written as  $\lceil g \cdot X(l) \rceil$ . If we sum this over all  $L$  links, we obtain the total number of optical connections needed in the network:

$$C = \sum_{l=0}^L \lceil g \cdot X(l) \rceil$$

Now we rewrite this equation using the variable  $L(i)$  defined above:

Given  $i \in \mathbb{N}^*$  we investigate the links whose  $X(l) = i$ :

Let the demands having granularity  $g$  be already routed by the network. Let us replan the network for demands with  $g + \varepsilon$  granularity. If  $\lceil g \cdot i \rceil < \lceil (g + \varepsilon) \cdot i \rceil$  then on links where  $X(l) = i$ , an additional connection is needed, therefore  $C$  increases by  $L(i)$ . This happens when  $g \approx \frac{k}{i}$  with  $k \in \mathbb{N}$ . This occurs  $i$  times between 0 and 1 adding  $L(i)$  connections to  $C$ . Therefore the stair function is a sum of  $i_{max}$  functions of the form  $f_i(g) = L(i) \sum_{k=0}^i \mathbb{1}_{\lceil \frac{k}{i}, 1 \rceil}(g) = L(i) \lceil g \cdot i \rceil$ , where  $\mathbb{1}_{\lceil \frac{k}{i}, 1 \rceil}$  is a function worth 1 on  $\lceil \frac{k}{i}, 1 \rceil$  and 0 everywhere else.

$$C = \sum_{i=0}^{\infty} \lceil g \cdot i \rceil L(i)$$

By definition of  $i_{max}$ :

$$C = \sum_{i=0}^{i_{max}} \lceil g \cdot i \rceil L(i)$$

$C$  is a sum of  $i_{max}$  ceiling functions  $f_i(g)$ . The greater the value of  $i_{max}$ , the closer their sum is to a linear function.

Now that we have established the exact analytical expression for  $C$ , let us study the behavior of  $C$  when  $g \rightarrow 0^+$ ,  $g \rightarrow 1^-$  and  $g > 1$ .

When  $g = \varepsilon \rightarrow 0^+$

Any link  $l$  carries  $\varepsilon \times X(l)$  normalized traffic capacity. It is a very small quantity but four transponders (two for each direction) are still needed for each link, except those links whose  $X(l) = 0$ . There are  $L(0)$  links for which  $X(l) = 0$ . When  $g = \varepsilon$  we thus need  $2(L - L(0))$  pairs of transponders. If density=1 then every link of the topology is part of at least one shortest path, and therefore  $L(0) = 0$ . If we increase  $g$ , the value of  $C = 2(L - L(0))$  stays constant until point A is reached, where one of the  $f_i(g)$  functions increases. As the functions  $f_i(g)$  are cyclically additive with a period of  $1/i$ , the one that increases first is the one corresponding to  $i_{max}$  :  $f_{i_{MAX}}(g) = L(i_{MAX}) \sum_{k=0}^{i_{MAX}} \mathbb{1}_{\lfloor \frac{k}{i_{MAX}i'} \rfloor} (g)$ . Therefore, the coordinates of point B are  $(1/i_{max} ; 2(L - L(0))/M)$ .

When  $g \rightarrow 1^-$

$$C = \sum_{l=0}^L [g \cdot X(l)] \rightarrow \sum_{l=0}^L X(l)$$

But  $\sum_{l=0}^L X(l) = \overline{hops} \times M$  therefore  $C$  normalized by the number of traffic demands is  $\overline{hops}$  thus the ordinate of point A is  $\overline{hops}$ .

If the value of  $g$  decreases, according to  $C = \sum_{i=0}^{i_{max}} f_i(g)$  the value of  $C$  will be constant until the value of one of the  $f_i(g)$  function will decrease, the first is, once again, the one corresponding to  $i_{max}$ . It decreases when  $g = 1 - 1/i_{max}$ . Thus the abscissa of point A is  $1 - 1/i_{max}$ .

When  $g > 1$  :

All the optical connections created while  $g \rightarrow 1^-$  are established and are completely filled. The choice of the optical connections needed to route the remaining traffic is not influenced by the existence of completely filled connections (we remind that we do not consider blockage). Therefore, the pattern composed of the three straight lines is reproduced to the infinity and the explanations provided for  $g < 1$  apply here too as confirmed by Figure 13 for values of  $g$  greater than 1.

## 2) Simulation results for four network topologies

We plot  $C/M$  as a function of  $g$  for all the topologies using opaque and overlay routing and grooming methods to obtain their stair functions. As we have seen above, these functions are cyclically additive with period of  $g = 1$ . Therefore we study only  $0 < g < 1$ .

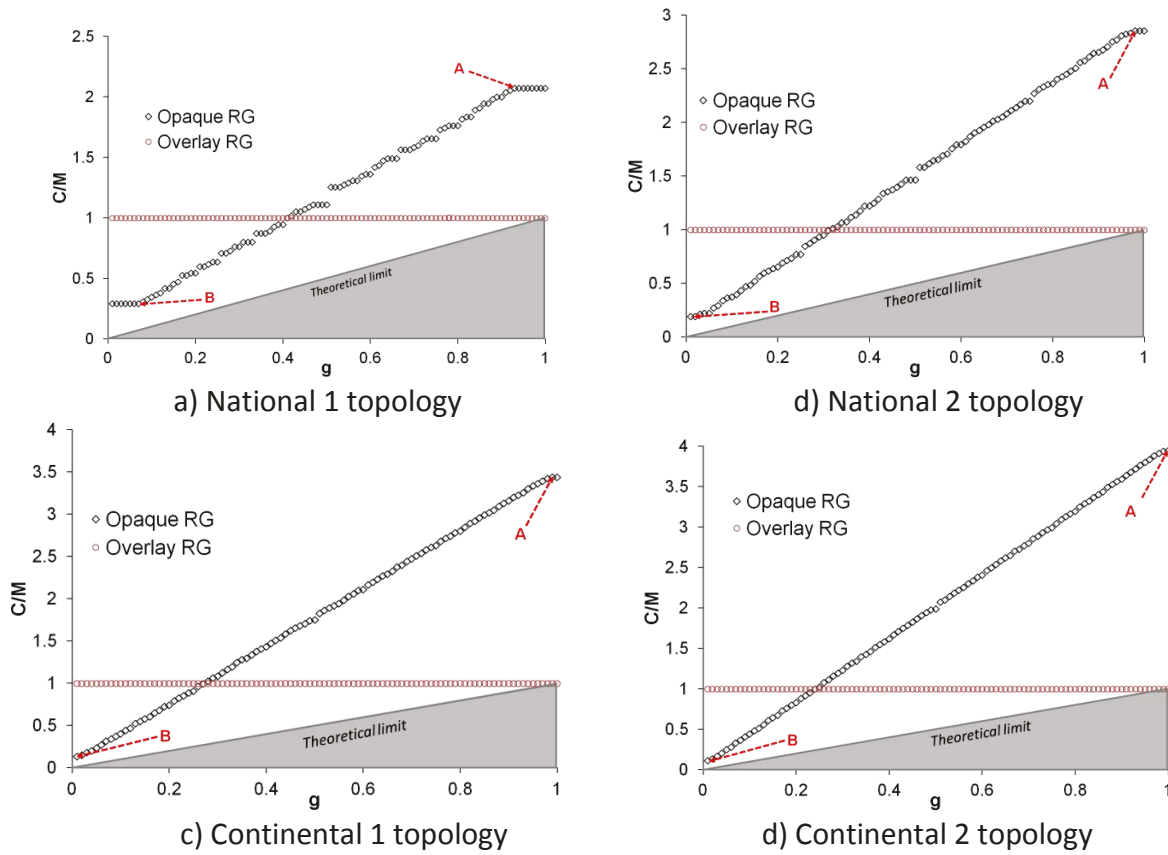


Figure 14: Stair function of the opaque routing and grooming (RG) method for all four topologies and density=1

Let us verify whether the analytical model exposed above allows predicting the coordinates of points A and B. Indeed, the analytical model predicts that that  $x_A$  matches  $1-1/i_{max}$ ,  $y_A$  matches  $\overline{hops}$ ,  $x_B$  matches  $1/i_{max}$ ,  $y_B$  matches  $2L/M$ .

Table2: Validation of the analytical model through the examination of the coordinates of points A and B for the 4 topologies

	National 1	National 2	Continental 1	Continental 2
$x_A$	0.92	0.98	1.00	0.99
$1-1/i_{max}$	0.923	0.975	0.992	0.987
$y_A$	2.06	2.85	3.43	3.94
$\overline{hops}$	2.07	2.85	3.43	3.94
$x_B$	0.07	0.02	0.01	0.01
$1/i_{max}$	0.0769	0.0250	0.00775	0.0130
$y_B$	0.291	0.191	0.101	0.146
$2L/M$	0.291	0.191	0.101	0.146

In Table 2, we put the coordinates of points A and B for every topology obtained from the graphs in Figure 14. We observe that for opaque RG, the analytical model allows predicting exactly the coordinates of A and B, and therefore the entire stair function corresponding to the topology. The only needed values are  $i_{max}$  and  $\overline{hops}$ , both can be obtained by simply applying shortest path routing to the topology.

In addition, we confirm that as predicted by the analytical model, the stair function tends towards a linear function with the growing  $i_{max}$ .

Finally, in Figure 14 we also observe that opaque RG is less expensive than overlay RG for  $g$  below a value varying between 0.24 and 0.41, depending on the topology. Indeed, when traffic demands are small, systematically regrooming them makes sense to better fill the optical connections. For larger traffic demands capacities, opaque routing and grooming requires more optical connections than overlay network planning, where each demand bypasses every intermediate node. An efficient multilayer RG algorithm should make the best mix between optical bypass and regrooming. This is what is done in multilayer network planning.

### C. Multilayer network planning

A multilayer RG algorithm finds, for each traffic demand, the best balance between optical bypass (to avoid electronic treatment in intermediate nodes) and intermediate grooming (to ensure a good filling of optical connections). The solutions studied during multilayer RG planning encompass those available to overlay RG or opaque RG. The scope of possible solutions explored by multilayer RG algorithms is much vaster, but if implemented correctly, they can provide solutions that are necessarily more advantageous than those provided by overlay RG or opaque RG.

#### 1) Stair function of multilayer RG when density=1

As explained earlier in Chapter 1 section D, the resolution of MILP formulations gives the minimal solution of the multilayer RG problem. We tried solving two MILP formulations detailed in Appendix 1, for the simplest of the studied topologies, National 1, using homogeneous matrices with density=1. 1SP-MILP is the formulation that has the constraint of routing every demand on its shortest path (using link length (in km) as the metric); anySP-MILP does not have this constraint any demand can be routed via any link, this allows finding a more economical solution, but needs much more computation to study all the additional possibilities. To solve MILP formulations we use CPLEX 12.1 software [78]. Both implementations are run using a workstation equipped with 8x2 GHz processors and 16 GB of RAM. Unfortunately using our machines (cf. Chapter 3 section IV.B) we were unable to make anySP-MILP converge for matrixes with density=1. Figure 15 represents solely the data points of 1SP-MILP represented with open circles; 50 values of  $g$  ranging from 0 to 1 were studied.

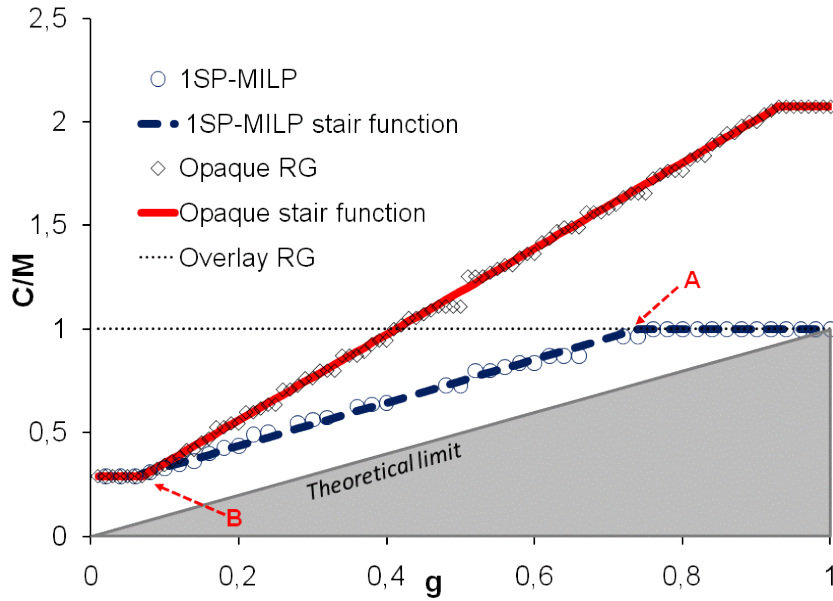


Figure 15: Stair functions of the 1SP-MILP formulation, opaque RG and overlay RG obtained for National 1 topology and traffic matrices with density=1.

In Figure 15, we observe that the data points of the 1SP-MILP can be interpolated with a stair function just like in the opaque RG. Just like for the opaque RG, DELTA describes the quality of interpolation; points A and B may also be defined. Here DELTA=0.009 for 1SP-MILP, which is much lower than the 0.035 limit fixed earlier and validates the stair function as a relevant interpolation of this characteristic function. The coordinates of A are (.06, .29), those of B are (.74, 1).

We also observe that the MILP formulation yields solutions that require less optical connections than opaque and overlay methods for any  $g$ . For lower granularities 1SP-MILP requires as much connections as opaque RG and for high granularities as much optical connections as overlay RG. This observation is explained in the analytical explanation that follows.

We have been unable to make anySP-MILP converge when using traffic matrices with a density of 1. For this scenario the number of created variables is too high to be solved by our machines. A way to decrease the number of variables in the MILP formulation is to consider traffic matrices with a density lower than one (less traffic demands) as it is done in the following section.

## 2) Stair function of multilayer RG when density<1

When lowering the density to 0.6 anySP-MILP converges. We succeeded in obtaining data points for both MILP formulations as shown in Figure 16. For each MILP formulation and each value of  $g$ , a new connection matrix (cf. III.C) is drawn and the RG process is launched.

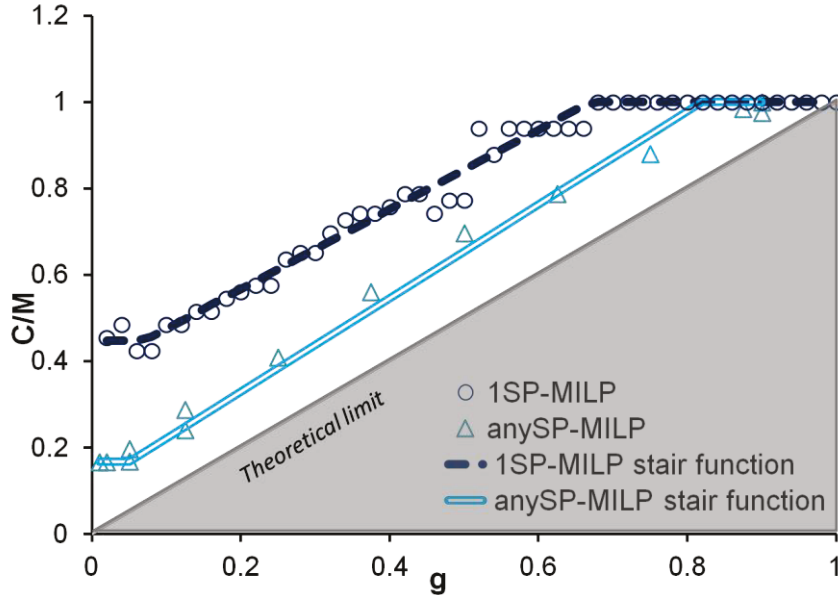


Figure 16: Stair function of 2 multilayer RG MILP formulations. National 1 topology. Density=0.6

The DELTA corresponding to the stair function approximation for 1SP-MILP is 0.024. Indeed we can see in Figure 16 that for 1SP-MILP the data points are more scattered as compared to Figure 15. This is due to the fact that from one data point to another the connection matrix changes. The optical connections established by the RG routine depend on the connection matrices. The lower the density of traffic matrices, the less two different connection matrices are correlated, and, therefore, the more differences can be between the number of optical connections for a given value of  $g$ .

We also observe that for every value of  $g$  anySP-MILP allocates fewer connections than 1SP-MILP. As explained in Appendix 1, while 1SP-MILP is constrained to route each client demand over the shortest path between source and destination nodes, anySP-MILP does not have this constraint. AnySP-MILP has therefore more grooming and routing combinations. This increases the computation time but results in fewer optical connections than 1SP-MILP.

Finally, DELTA for the stair function approximation of the anySP-MILP characteristic function is 0.019, which is under the 0.035 limit and therefore validates the stair function as an acceptable approximation in this case. Nevertheless, on Figure 16 we observe that a better approximation for the characteristic function of anySP-MILP and National 1 topology is possible. Indeed, the increasing part of the characteristic function is rather concave than straight. As observed in our later work, presented in section VI.B, as well as in [79], some of the multilayer RG heuristics also have concave characteristic functions.

The analytical explanation of the shape of characteristic functions is much more complex for multilayer RG because the decision to bypass a node on the path chosen for a traffic demand is specific to each demand at every of the node on its path. In the following, we propose an explanation for the two plateaus that are observed for any multilayer RG method.

### 3) Analytical explanation

As for the opaque RG and overlay RG, to study the plateaus we study  $C$  when  $g$  approaches 0 and 1.

When  $g = \varepsilon \rightarrow 0^+$ :

As in the opaque case, when each traffic demand has a very low capacity, to transport all the demands, only a limited number of connections  $C_0$  is needed. It is the number of connections necessary to interconnect all the *communicating nodes* so as to form in one connected graph. We call “communicating nodes”, the subset of the nodes that are sources or destinations of traffic demands. Their quantity is denoted  $N_{COM}$ , ( $N_{COM} \leq N$ ). By analogy to the opaque case when  $g$  is small, for multilayer RG methods constrained to the shortest path,  $C_0 = 2(L - L(0))$ ; when, in addition, density=1,  $L(0) = 0$  and  $C_0 = 2L$ .

In a general case, we can bound  $C_0$ , i.e. provide a higher and a lower bound. Indeed, to interconnect  $N_{COM}$  nodes, at least  $N_{COM} - 1$  optical connections are necessary, i.e.  $C_0 \geq N_{COM} - 1$ .  $N_{COM}$  has a lower bound. Indeed if there are  $M$  pairs of communicating nodes, then

$$M \leq \binom{N_{COM}}{2} = \frac{N_{COM}!}{2!(N_{COM} - 2)!} = \frac{N_{COM}(N_{COM} - 1)}{2}$$

By finding the roots of the polynomial

$$\frac{1}{2}N_{COM}^2 - \frac{1}{2}N_{COM} - M$$

and knowing that  $N$  is strictly positive, one deduces that

$$N_{COM} \geq \frac{1 + \sqrt{1 + 8M}}{2}$$

Since  $C_0 \geq N_{COM} - 1$ ,

$$C_0 \geq \frac{\sqrt{1 + 8M} - 1}{2}$$

As for the upper bound for  $C_0$ , we can be sure that if an optical connection is established in both directions for every link, each node is connected to all the other nodes; therefore,  $2L \geq C_0$ . Also there is no need in deploying more connections than the number of traffic demands. This means that  $M \geq C_0$ . To sum up:

$$\text{MIN}(2L, M) \geq C_0 \geq \frac{\sqrt{1 + 8M} - 1}{2}$$

If we divide the number of connections by  $M$  as it is done when tracing the stair functions we obtain  $C_0/M = y_B$ , and therefore:

$$\text{MIN}(2L/M, 1) \geq y_B \geq \frac{\sqrt{1 + 8M} - 1}{2M}$$

Now we study the value of  $x_B$ . According to the theoretical limit, i.e. the line where  $C/M = g$ , we can state that  $x_B \leq y_B$ .

We know that as the value of  $g$  grows starting from an infinitely small capacity  $\varepsilon$ , the minimum number of optical connections suffices up to a certain value of  $g$ . For this value of  $g$  a new connection needs to be deployed to support all the traffic demands. This value of  $g$  is  $x_B$ . We know that this occurs when the traffic demands fill the optical connection carrying the most traffic demands  $n$  ( $n \in \mathbb{N}^*$ ), therefore  $x_B = 1/n$ .

For the specific case of multilayer RG that routes each demand along its shortest path (e.g. 1SP-MILP) we can be more precise. We know that at most  $i_{max}$  traffic demands can be routed over one link or a sequence of links; therefore,  $n \approx i_{max}$  ( $i_{max}$  defined for opaque RG in IV.B.1).

To sum up:

For any multilayer RG method:

$$\text{MIN}(2L/M, 1) \geq y_B \geq \frac{\sqrt{1 + 8M} - 1}{2M}$$

$$x_B \leq y_B$$

$x_B$  is of the form  $1/n$  with  $n \in \mathbb{N}^*$

For multilayer RG methods constrained to the shortest path:

$$y_B = 2(L - L(0))/M$$

( $L(0) = 0$  for density=1 and  $L(0) \rightarrow L$  when density  $\rightarrow 0$ )

$$y_B \geq x_B \approx 1/i_{max}$$

When  $g \rightarrow 1^-$ :

A multilayer RG is capable of reaching the theoretical limit when  $g=1$ , as we can see for both MILP formulations in Figure 15 and Figure 16. Indeed when each traffic demand has exactly the capacity of the optical connection ( $g=1$ ), one optical connection is allocated to each traffic demand ( $C = M$ ). If we slightly decrease the value of  $g$ , the free capacity that is released in each of the optical connections is not sufficient to transport an additional traffic demand; therefore, one connection is still allocated to each traffic demand and no grooming occurs. This explains the plateau we observe for both MILP formulations in Figure 15 and Figure 16. The A ordinate,  $y_A$  is necessarily 1. The abscissa  $x_A$  of the point A corresponds to the highest value of  $g$  for which  $M$  demands can fit into less than  $M$  optical connections thanks to the grooming capability. When  $g=x_A$ ,  $m$  ( $m \in \mathbb{N}^*$ ) optical connections routed over the same link or a sequence of links can be groomed together to fit into  $m-1$  optical connections, therefore  $x_A = (m-1)/m$ . For any multilayer RG  $m \leq M$ , therefore  $x_A \leq (M-1)/M$ . For multilayer RG routing along the shortest path, we know that at most  $i_{max}$  traffic demands can be routed over one link or a sequence of links; therefore,  $m \leq i_{max}$ , thus  $x_A \leq (i_{max} - 1)/i_{max}$ .

When  $g > 1$ :

Similarly to the characteristic function of opaque RG, when  $g > 1$ , all the optical connections created while  $g \rightarrow 1^-$  are established and are completely filled. The remaining traffic is transported in additional optical connections. The choices of the additional optical connections needed to route the remaining traffic are not influenced by the existence of completely filled connections. The remaining traffic is treated as new traffic demands with smaller capacity; therefore, the pattern composed of three lines is reproduced to the infinity.

To sum up:

$$y_A=1$$

For any multilayer RG method:

$$x_A \text{ is of the form } (m-1)/m \text{ with } m \in \mathbb{N}^* \text{ and } m \leq M, \text{ therefore } x_A \leq (M-1)/M$$

For multilayer RG methods constrained to the shortest path:

$$x_A \leq (i_{max} - 1)/i_{max}$$

In Table 3, we verify these analytical results for National 1 using characteristic functions represented in Figure 15 and Figure 16.

Table3: Validation of the analytical model through the examination of the coordinates of points A and B for National 1 topology. Results for 1SP-MILP density values of 0.6 and 1, anySP-MILP for density value of 0.6

	1SP-MILP density=1	1SP-MILP density=0.6	anySP-MILP density=0.6
$x_A$	0.92	0.67	0.82
$1-1/i_{max}$	0.923	0.917	-----
$x_B$	0.07	0.08	0.05)
$1/i_{max}$	0.077	0.083	-----
$y_B$	0.291	0.447	0.167
$\frac{\sqrt{1+8M}-1}{2M}$	0.130	0.167	0.167
$2L/M$	0.291	0.485	0.485

We verify that all three characteristic functions verify the bounds established in the analytical model for  $x_B$ , and  $y_B$  with a precision of 0.015.

$$\text{MIN}(2L/M, 1) \geq y_B \geq \frac{\sqrt{1+8M}-1}{2M} i_{max}$$

$$x_B \approx 1/i_{max} \leq y_B$$

We also verify that  $x_A$  is of the form  $(m-1)/m$  with  $m \in \mathbb{N}^*$ . Indeed  $0.92 \approx 11/12$ ,  $0.67 \approx 2/3$ , and  $0.82 \approx 5/6$ . Similarly,  $x_B$  is of the form  $1/n$  with  $n \in \mathbb{N}^*$ . Indeed  $0.07 \approx 1/14$  and  $0.058 \approx 1/20$ .

We observe that as predicted for both MILPs  $x_A \leq (M-1)/M$  and for 1SP-MILP  $x_A \leq (i_{max}-1)/i_{max}$ . We also observe that for 1SP-MILP, the coordinates of point B follow the upper bounds. For 1SP-MILP these bounds can thus be used as estimators.

According to analytical explanation, a characteristic function depends on a combination of parameters from the RG method, the topology and the density. To study the influence of the topology and the density we must resort to using heuristics. Indeed for densities exceeding 0.6 or topologies having more nodes than National 1, the solution with MILP is intractable with the computers available to us (see Chapter 3 section IV.B for specifications). As explained in Chapter 1 section II.D, heuristics must be used instead. In the next section, we compare the characteristic function of the heuristic to those of the MILP formulations using National 1 topology.

#### 4) Comparative study of performances of heuristics and MILP formulation using the characteristic function

We propose to study our heuristic allowing the best compromise between performance and computation time. It is described as “V3” in Appendix 2. To validate the efficiency of our heuristic we compare in Figure 17 its stair function to those of 1SP-MILP and anySP-MILP. The hypotheses made here are the same as those used to obtain Figure 16: National 1 topology is studied; the homogeneous traffic matrices have a density of 0.6.

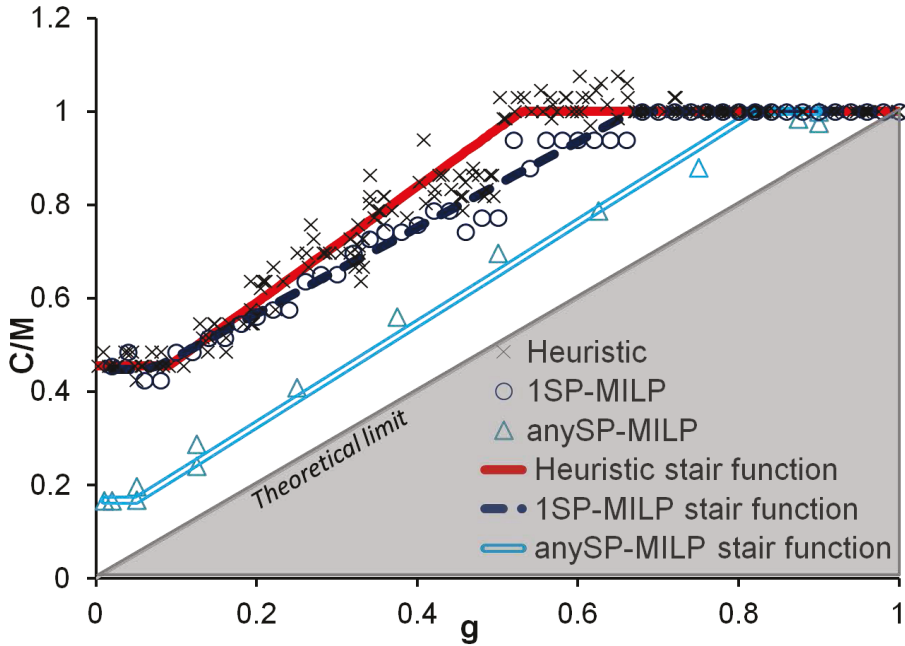


Figure 17: Stair function of our heuristic and 2 multilayer RG MILP formulations for National 1 topology and for density=0.6

We observe that the characteristic function of the heuristic can be approximated with a stair function. For this stair function DELTA is equal to 0.025, which is lower than the 0.035 limit we fixed.

The stair function of the heuristic is always above that of both MILP formulations. Indeed, the heuristic can route and groom traffic demands only along their shortest path, just like 1SP-MILP. Also, for a greater rapidity, the heuristic explores fewer possibilities than 1SP-MILP; this is why the stair function of the heuristic cannot be below that of 1SP-MILP. However for some values of  $g$  (e.g. 0.13, 0.16, 0.33), the number of connections,  $C$ , obtained using the heuristic is lower than that obtained using 1SP-MILP. This can be explained by the differences of the connection matrices. Even though each connection matrix has  $M$  non-zero elements, some connection matrices contain more demand sharing portions of their shortest path; grooming them together allows better sharing of the optical connections.

For small values of  $g$ , the stair functions of the heuristic and of 1SP-MILP coincide. As explained in Appendix 2, the heuristic takes as a basis an opaque RG scheme, and then the optical bypass is made if it brings cost gains. Therefore if the 1SP-MILP solution is close to opaque, the heuristic is likely to find it.

For bigger values of  $g$ , between 0.25 and 0.66, we observe that the heuristic deploys more resources than 1SP-MILP. The maximum distance between two stair functions is 0.14, it occurs for  $g=0.52$ . For  $g$  between 0.5 and 0.7, the heuristic allocates even more

than one optical connection for each optical demand. These differences with the stair function of 1SP-MILP are explained by the fact that the heuristic makes the decision to establish optical connections considering local optimal solution (connection after connection) that do not prove to be global optimal solutions. Such a sequential selection leads to the choice of connections that force (later in the planning process) the algorithm to allocate almost empty connections that would have been avoided if the algorithm had a more global view in the beginning of the RG process.

The maximum distance between the two curves is 0.14 and the mean L1 distance is 0.03. We consider the distance between two stair functions, obtained on National 1 to be sufficiently low to validate our heuristic for the study of multilayer RG for solving more complex planning problems.

For a network with more nodes, the comparison with the MILP formulations is impossible. What we can observe is the distance between the theoretical limit and the stair function of the heuristic. As we mentioned earlier, the stair function is defined by the points A and B, and from their coordinates we can deduce the distance between the stair function and the theoretical limit. Hereinafter, to study this distance we study the evolution of the coordinates of the points A and B.

#### 5) *Characteristic function of a multilayer RG heuristic for large networks*

We now show, on the example of the heuristic, how the characteristic function allows studying the evolution of performances of a multilayer RG algorithm for a growing density and a growing topology (in terms of the number of nodes).

In the following, we study each of the four reference topologies presented in Figure 10. For each of the topologies four densities are explored (0.4, 0.6, 0.8, 1.0). For each of the 16 combinations of topology and density, the multilayer planning is done for random homogeneous traffic matrices (the connection matrix and  $g$  are both random). The resulting graphs are presented in Figure 18 for National 1, Figure 19 for National 2, Figure 20 for Continental 1 and Figure 21 for Continental 2.

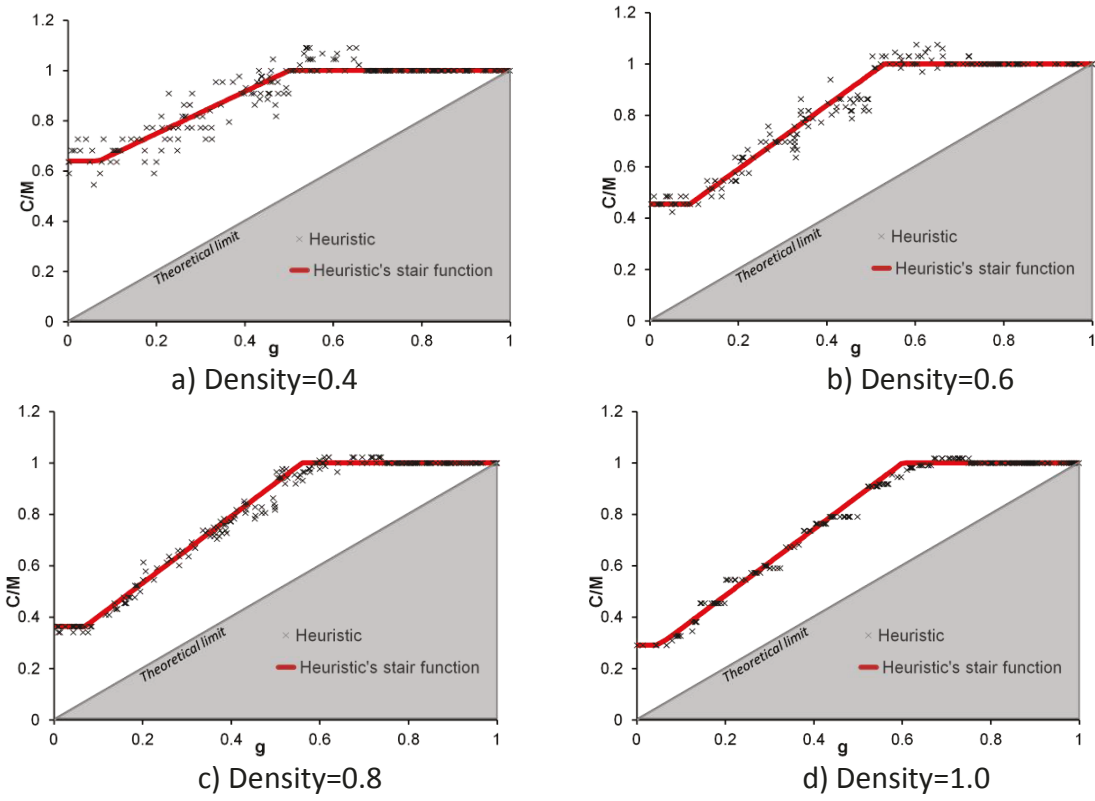


Figure 18: Stair function of our multilayer routing and grooming heuristic for National 1 topology.

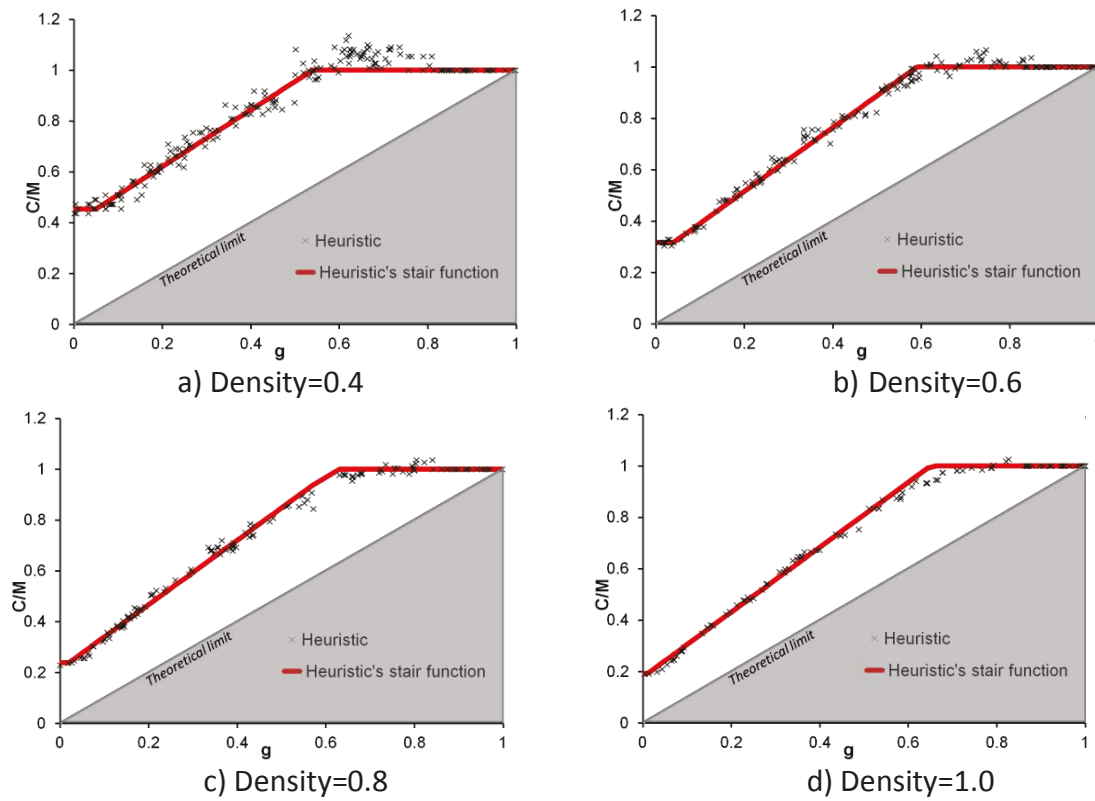


Figure 19: Stair function of our multilayer routing and grooming heuristic for National 2 topology.

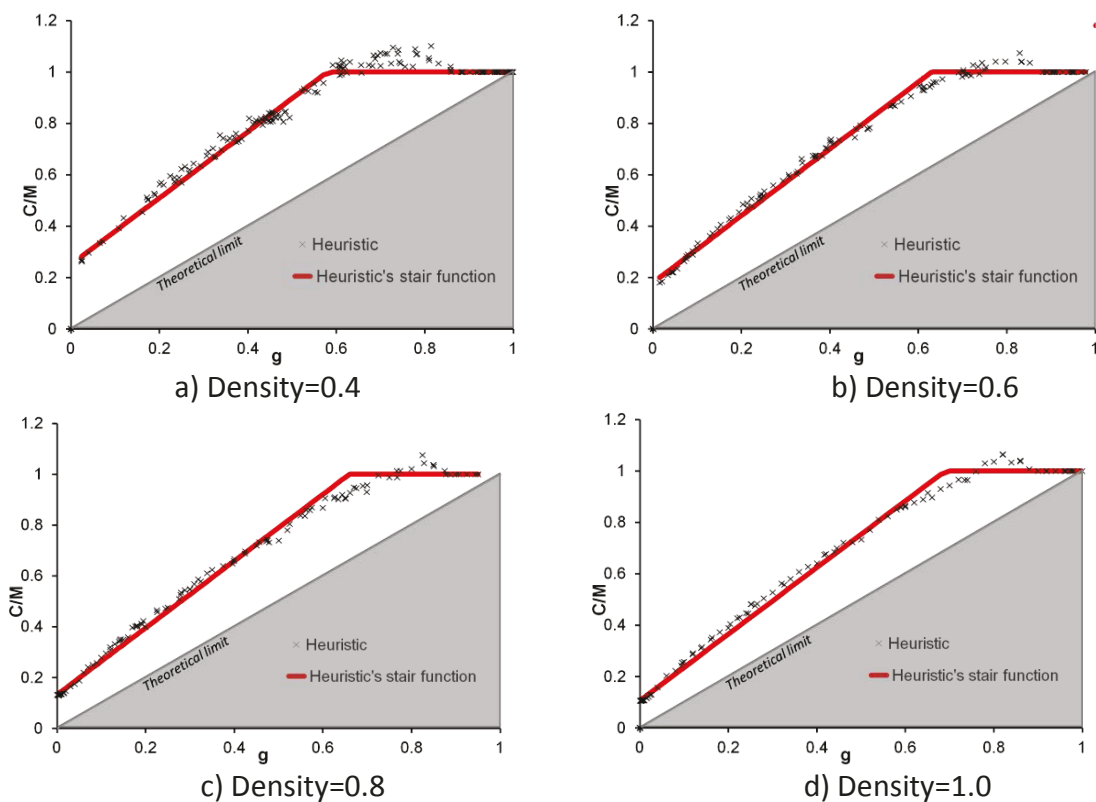


Figure 20: Stair function of our multilayer routing and grooming heuristic for Continental 1 topology.

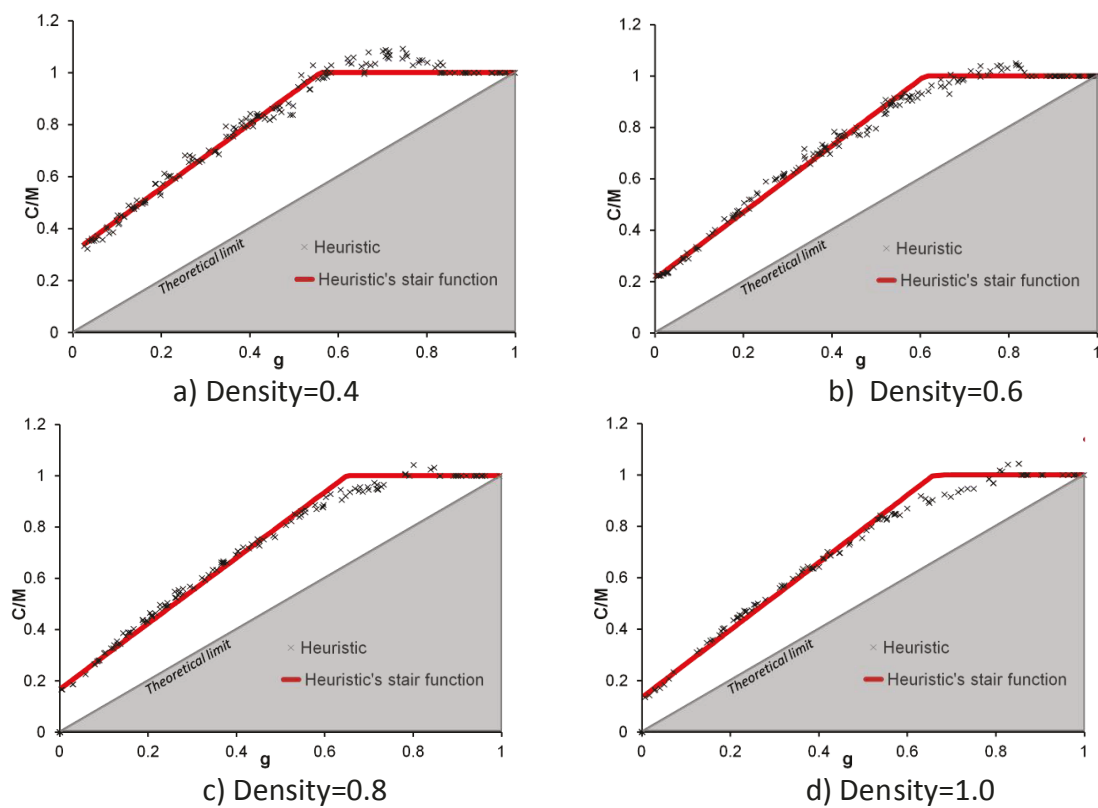


Figure 21: Stair function of our multilayer routing and grooming heuristic for Continental 2 topology.

Since for large networks MILP formulations cannot be solved, the theoretical limit curve ( $C/M=g$ ) and the analytical bounds we found in section IV.C.3) will be used as a reference. For each topology and density, we approximate the characteristic function of our heuristic by a stair function, the distance DELTA quantifies the precision of approximation.

To study further the curves presented in Figure 18, Figure 19, Figure 20, and Figure 21 we extracted the values of DELTA,  $x_A$ ,  $x_B$  and  $y_B$  and plotted them in Figure 22, Figure 23, Figure 24 and Figure 25.

In Figure 22 we present the values of DELTA obtained for each of the 16 curves. We observe that for National 1, National 2, and Continental 1, DELTA decreases with density. As we can see in Figure 18, Figure 19, Figure 20, and Figure 21, for higher values of  $g$  the heuristic allocates more than one connection per demand, i.e. more than overlay network planning would allocate. As explained above this deficiency appears because of the local nature of the algorithm and, as we show in section VI, it can be reduced (once it is identified) by making the algorithm more complex. The resulting “bump” observed for higher granularities increases the value of DELTA. The decrease of DELTA observed in Figure 22 can be explained by the disappearance of the aforementioned “bump” but also the compacting of the cloud of data points. This compacting is due to the fact that as the density of the traffic matrices grows, the correlation between the connection matrices is larger. The same source-destination couples are likely to be present in two different traffic matrices. Therefore, the results of the RG processes are likely to be closer (as mentioned in section 2). The relation between the spreading of the data points and density are studied in detail in Appendix 3. For Continental1 and Continental2 topologies we observe, for high densities, an increase in DELTA. As we see in Figure 21, this is due to the fact that the characteristic function is more and more concave; therefore, a stair function fits worse the data points.

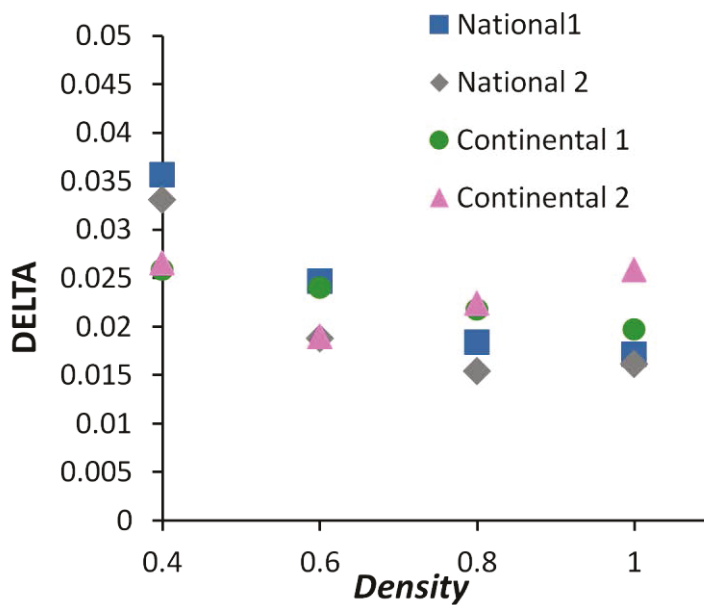


Figure 22: Values of DELTA for 16 stair functions presented in Figure 18 , Figure 19 , Figure 20, and Figure 21.

Finally, we check that for each curve the value of DELTA is beneath the 0.035 threshold established earlier. More precise approximations of the characteristic function can be found in each case, but the stair function fits the data points and can be summarized by

the coordinates of points A and B, which simplifies much the methodology used to study the evolution of the characteristic function with the size of the topology. Therefore we continue to use the stair function approximation to study the behavior of our heuristic for various topologies.

From the graphs shown in Figure 18 , Figure 19 , Figure 20 and Figure 21, we extract the coordinates of points A and B and plot them in the 3 following graphs. By definition,  $y_A$  is equal to 1, so it is not of interest. The values of the three remaining coordinates are plotted in the following figures.

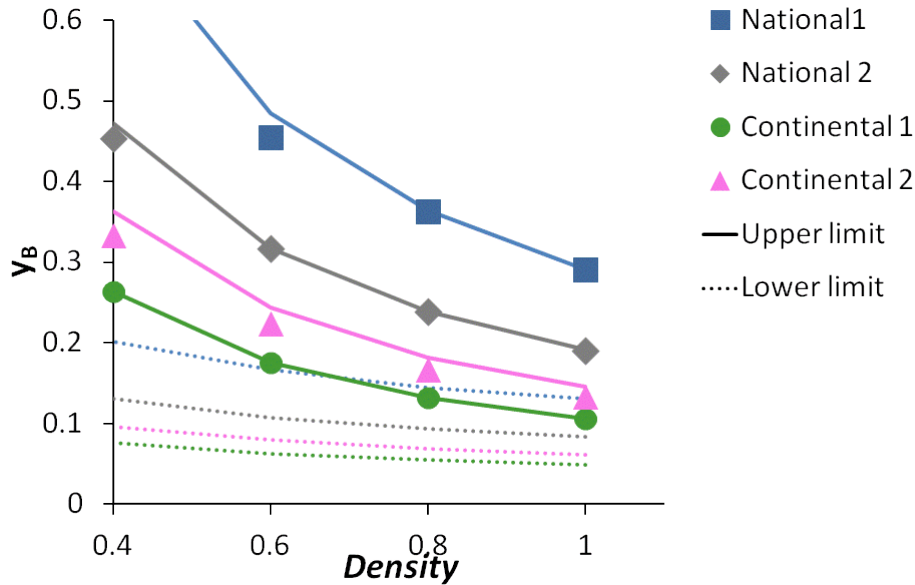


Figure 23: Values of  $y_B$  for the 16 stair functions presented in Figure 18 , Figure 19 , Figure 20 and Figure 21.

In Figure 23 we plot the values of  $y_B$  for 4 values of density and 4 topologies. We also plot, with a continuous line, its upper limit which is shown to be  $2L/M$  and, with a dotted line, its lower limit  $\frac{\sqrt{1+8M}-1}{2M}$ . We observe that the values of  $y_B$  we have obtained are within the theoretical limits.

For our heuristic, the value of  $y_B$  tends to follow the upper limit,  $2L/M$ , especially for high values of the density. We have already seen in IV.C.3) that when routing is constrained to follow the shortest path of each demand,  $y_B = 2(L - L(0))/M$ . Where  $L(0)$  is a number of links not belonging to any of the shortest path between communicating node pairs. As the density grows,  $L(0)$  tends to 0. Indeed, when every node communicates with every other node, each link belongs to the shortest path between its extremities. As we will observe in section VI.B.2), for heuristics that can route on any path,  $y_B$  stays well below the upper limit.

Finally, we observe that as the density and the number of nodes of the topology grow,  $y_B$  decreases.

In Figure 24, we plot the values of  $x_B$  for the 4 values of the density and 4 topologies.

As in the previous graph, the continuous lines correspond to the upper bound and the dashed line, to the lower bound, which here corresponds to  $1/i_{max}$ .  $x_B$  stays within the proposed bounds. The proposed estimate has at a maximum 0.007 L1 distance from the values of  $x_B$  extracted from the stair functions, which is a very good precision.

For all of the studied topologies,  $x_B$  is a decreasing function of density. Indeed, as we have explained in IV.C.3), as the density grows,  $i_{max}$  (the maximum number of demands routed over any link of the topology) grows too.

Finally, we observe that as the density and the number of nodes grows,  $x_B$  decreases.

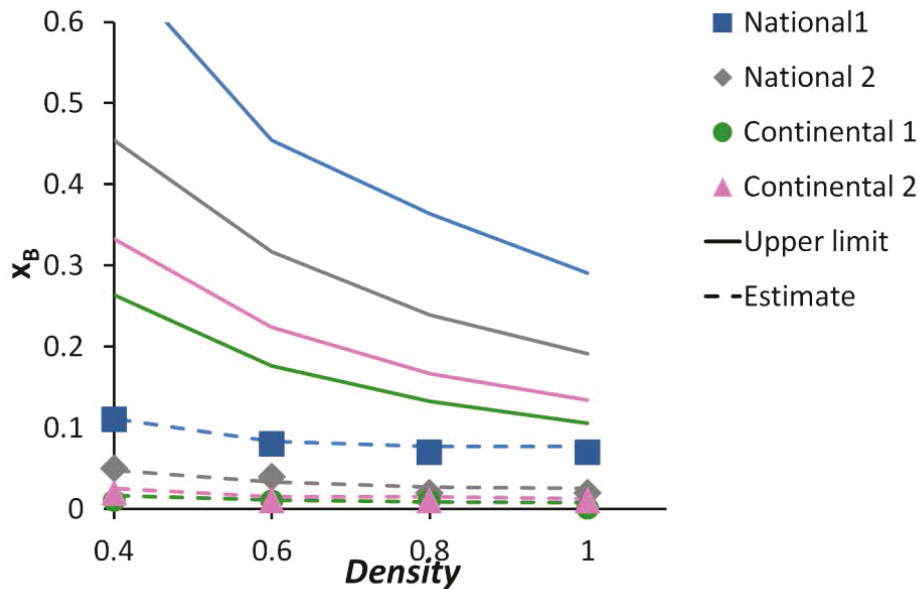


Figure 24: Values of  $x_B$  for the 16 stair functions presented in Figure 18 , Figure 19 , Figure 20 and Figure 21.

In Figure 25, we plot the values of  $x_A$  for the 4 values of the density and 4 topologies.

As previously, the continuous lines correspond to the upper bound that we have shown to be  $(i_{max} - 1)/i_{max}$ . The values of  $x_A$  are well below the upper limit, this limit applies to any type of multilayer RG. As we show in VI.B.2), the heuristics without the “one shortest path” constraint are much closer to the upper bound. As a corollary, we may ask ourselves whether there exists an upper limit for  $x_A$  specific to algorithms with the “one shortest path” constraint.

We observe that  $x_A$  grows with the density and the number of nodes.

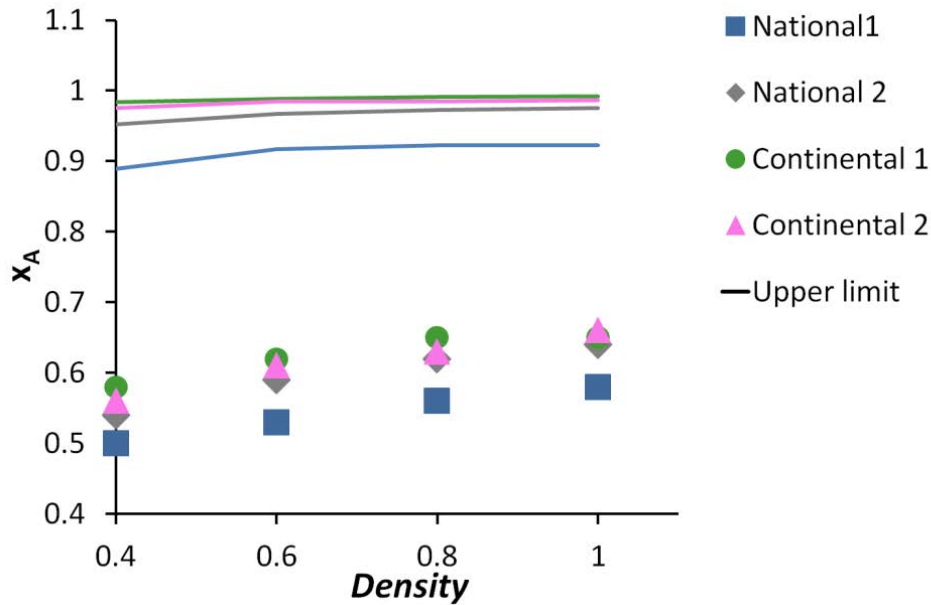


Figure 25: Values of  $x_A$  for the 16 stair functions presented in Figure 18 , Figure 19 , Figure 20 and Figure 21.

In conclusion, after having studied our heuristic for 4 topologies with a growing number of nodes and for 4 values of the density, we observe that as the density grows and the number of nodes in the topology grows, both  $x_B$  and  $y_B$  decrease, i.e. point B gets closer to the origin, and  $x_A$  increases, i.e. point A is getting closer to the point (1;1); the stair function our heuristic gets closer to the theoretical limit  $x=y$ . The characteristic function of the optimal multilayer RG, as achieved by resolving MILP formulations, being necessarily above the theoretical limit, this means that as the density grows and the topology grows our heuristic converges towards the results of MILP formulations. This encourages us to use this heuristic for further studies over large topologies in section V.C and in the next chapter.

We see later in VI.B that different heuristics may be either insensitive to the growth of density and of number of nodes or even diverge. Such a study should be conducted for any heuristic before using it for actual network planning. The stair function is a tool allowing a simple diagnostic of a heuristic over large topologies with a limited number of simulation points.

We have shown that diverse information can be extracted from the characteristic function but the conclusions of such a study are proven only when the traffic matrix is homogeneous. They would be of no interest if they could not be applied to realistic traffic matrices. We now show how the characteristic function can be generalized to other traffic matrices, thus fulfilling the Objective 2 we fixed in the beginning of this chapter.

## V. EXTRAPOLATING A STAIR FUNCTION TO REALISTIC TRAFFIC MATRICES

### A. *Traffic hypotheses*

We suppose that each pair of nodes in the topology exchanges at most one bidirectional aggregated capacity, represented by an element in the traffic matrix called client demand. The traffic matrix is normalized by the transponder capacity for the sake of generality.

In this section, we show how the characteristic function generalizes to traffic matrices whose non-zero elements classified according to their capacity have a compact support and continuous probability distribution function (PDF).

### B. *Explanation and first results*

To generalize the results obtained with homogeneous traffic matrices, we combine the characteristic function with a function extracted from a realistic traffic matrix. To extract this function from the traffic matrix we proceed as follows. We classify all the client traffic demands with respect to their capacity to obtain a probability distribution function (PDF). Hence we convolute the obtained probability PDF with the characteristic function to obtain a precise estimation of the number of optical connections allocated by the RG process.

We can make an analogy between the RG methods and the linear systems treatment. A set of homogeneous traffic matrices with  $g$  going from 0 to 1 are analogous to an impulse input, the characteristic function is analogous to the impulse response function, the PDF of traffic demands is the input function. Thus to obtain an output we have to convolute the input function with the impulse response. (The analogy is not rigorous though because in our case the two functions are not Lebesgue integrable functions.)

We introduce the following notations:

$M$  is a number of non-zero elements of the traffic matrix (by extension of  $M$  defined for homogeneous traffic matrices)

$f_{\underline{g},\alpha}$  is the continuous PDF of the demands of the traffic matrix with respect to their capacity. It is parameterized by an expected value  $\underline{g}$  and the span of the distribution noted  $\alpha$ , it is the halved length of the interval of definition (i.e. the interval where PDF is not equal to zero).

$f_{\alpha}$  is  $f_{\underline{g},\alpha}$  translated so as to have an interval of definition centered at zero:  
 $\forall y \in \mathbb{R}, f_{\alpha}(y) = f_{\underline{g},\alpha}(y - \underline{g})$

$c$  is the characteristic function corresponding to an RG method and a topology

$*$  is the convolution operator

We state that for a given value of  $g$ , the estimation of  $C/M$  is  $c * f_{\alpha}(g)$  :

$$c * f_{\alpha}(g) = \int_{-\infty}^{+\infty} c(y)f_{\alpha}(y - g)dy$$

We note that in the case where  $\alpha=0$ ,  $f_{\alpha}$  and  $f_{\underline{g},\alpha}$  are Dirac delta functions. This means that the traffic matrices having such a distribution are homogeneous traffic matrices hence the estimator returns the characteristic function, i.e.  $c * f_0(g) = c(g)$ .

To give a practical example, in Figure 26 we plot the number of optical connections normalized by  $M$  (symbolized by black crosses), obtained by planning the National 2 topology with our heuristic using traffic matrices with a density of 0.6 whose elements follow a uniform distribution  $u_{\underline{g},\sigma}$  defined by an expected value  $\underline{g}$  and a standard deviation  $\sigma$ . If we denote the span of distribution by  $\alpha$ , we have  $\alpha = \sigma\sqrt{3}$ .

$$u_{\underline{g},\sigma}(x) = \begin{cases} \frac{1}{2\sigma\sqrt{3}}, & \text{for } \underline{g} - \sigma\sqrt{3} < x < \underline{g} + \sigma\sqrt{3} \\ 0, & \text{for } x < \underline{g} - \sigma\sqrt{3}, \text{ for } x > \underline{g} + \sigma\sqrt{3} \end{cases}$$

We remark that for any value of  $\underline{g}$ , if  $u_{\underline{g},\sigma}$  is translated so as to have an interval of definition centered at zero, we obtain  $u_{0,\sigma}$ .

We study in Figure 26, three values of  $\alpha$ , corresponding to three values of  $\sigma$ :  $\alpha=0.1$ ,  $0.3$ ,  $0.55$ . The values of  $\underline{g}$  are between  $\alpha$  and 2. We also plot using a red continuous line, for each  $\alpha$ , the estimator obtained with  $c * u_{0,\sigma}$ , where  $c$  is the characteristic function corresponding to our heuristic and National 2 topology for a density of 0.6 shown in Figure 19b.

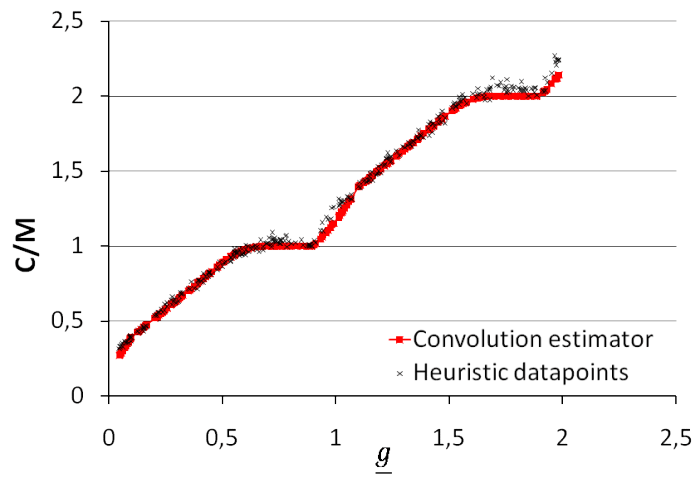
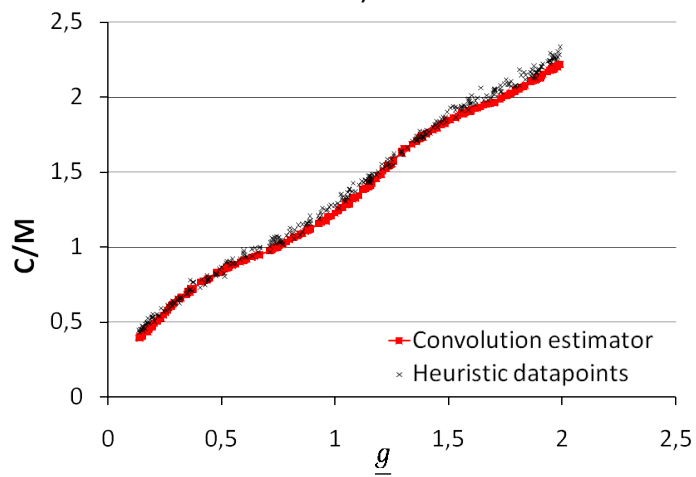
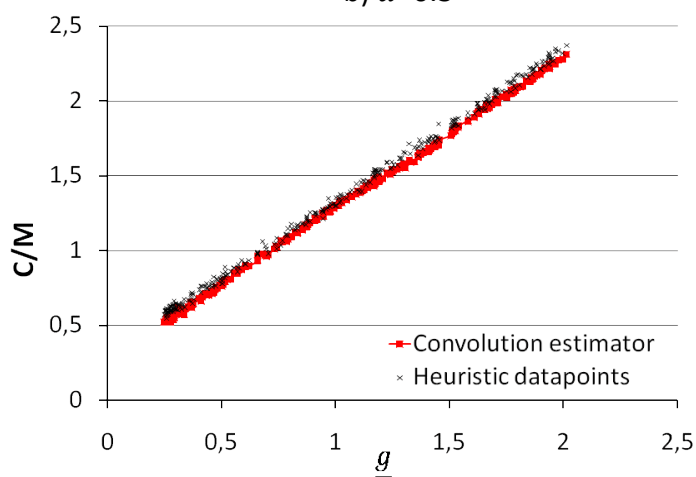
a)  $\alpha=0.1$ b)  $\alpha=0.3$ c)  $\alpha=0.55$ 

Figure 26: Number of optical connections obtained after planning National 2 topology for traffic matrices with uniform distributions.

We observe that as  $\alpha$  (the span of the distribution) grows, the shape of the scatter plot and the estimator are smoothed and eventually become linear. This result is rigorously studied in the general case in D.2).

We also observe that the estimator is very close to the data points obtained by network planning with the heuristic. To evaluate the distance between the estimator and the data points, we use the distance GAMMA. GAMMA is a mean L1-distance between the estimator and the data points. As we did for the stair function, we must fix an upper limit for GAMMA above which we consider the estimator as valid. To do so we must take into account the fact that when traffic matrices are not homogeneous, not only the source and destination of a traffic demand are chosen randomly but also its capacity. This introduces more randomness and therefore the data scatter we obtain after network planning is necessarily larger. We propose therefore an upper limit for GAMMA which is the double of the limit we established for DELTA. The upper limit for GAMMA is thus 0.07. If GAMMA stays under the 0.07 limit we consider that the estimation by convolution is a valid approximation of the RG process

For a),  $\alpha=0.1$  GAMMA=0.031; for b)  $\alpha=0.3$ , GAMMA=0.043; and for c)  $\alpha=0.55$  GAMMA=0.046. As GAMMA between the scatter plot and the estimator is below the 0.07 limit we consider that we are in the domain of validity of the estimator.

In section C, we present the results of a large-scale simulation campaign to determine the domain of validity of the convolution estimator and then we explain in section D how we can exploit the estimator to study analytically the general behavior of algorithms for various PDFs of the traffic demands.

### C. Domain of validity of the estimation by correlation

To explore the domain of validity of the estimator, we conducted a large simulation campaign using our heuristic (V3) presented in Appendix 2 and examined in section IV.C. This heuristic is chosen for its speed of calculation when topologies with a large number of nodes are planned. In this simulation campaign we study four topologies presented in Figure 10. We examine traffic matrices whose PDF is either  $u_{\underline{g},\sigma}$  (defined in section B) or  $\gamma_{\underline{g},\sigma}$ , a Gaussian distribution truncated at  $2\sigma$ :

$$u_{\underline{g},\sigma}(x) = \begin{cases} \frac{1}{2\sigma\sqrt{3}}, & \text{for } \underline{g} - \sigma\sqrt{3} < x < \underline{g} + \sigma\sqrt{3} \\ 0, & \text{for } x < \underline{g} - \sigma\sqrt{3}, \text{ for } x > \underline{g} + \sigma\sqrt{3} \end{cases}$$

$$\gamma_{\underline{g},\sigma}(x) = \begin{cases} \frac{1}{\text{erf}(\sqrt{2})\sigma\sqrt{2\pi}} e^{-\frac{(x-\underline{g})^2}{2\sigma^2}}, & \text{for } \underline{g} - 2\sigma < x < \underline{g} + 2\sigma \\ 0, & \text{for } x < \underline{g} - 2\sigma, \text{ for } x > \underline{g} + 2\sigma \end{cases}$$

We note that for  $\gamma_{\underline{g},\sigma}$  the span  $\alpha$  is equal to  $2\sigma$  whereas for  $u_{\underline{g},\sigma}$  we have shown that  $\alpha = \sigma\sqrt{3}$ .

To study the maximum number of combinations of topologies, traffic distributions and values of  $\sigma$ , we decided to fix the density of the traffic matrices to 0.6, which is the best

compromise between the dispersion of data points and the simulation time (cf. Appendix 3). The characteristic functions corresponding to our heuristic and a density of 0.6 is approximated by a stair function shown in Figure 18b for National1, Figure 19b for National2, Figure 20b for Continental1 and Figure 21b for Continental2 topologies.

For each of the 4 topologies and 2 traffic distributions we studied 8 values of  $\sigma$  {0, 0.06, 0.12, 0.17, 0.22, 0.32, 0.45, 0.55}. For each of these 64 combinations we generated 300 traffic matrices with values of  $\underline{g}$ , the expected value of the normalized capacity of traffic demands, going from  $\alpha$  to 2. We obtained 64 scatter plots similar to those shown in Figure 26. For each plot we computed the curve corresponding to the estimator by convolution with the stair function, as in Figure 26. The distance GAMMA was calculated between the scatter plot and the estimator; their values are presented in Figure 27. As the abscissa, instead of  $\sigma$ , we use the span  $\alpha$ . As we have shown before,  $\alpha = \sigma\sqrt{3}$  for  $u_{g,\sigma}$  and  $\alpha=2\sigma$  for  $\gamma_{g,\sigma}$ .

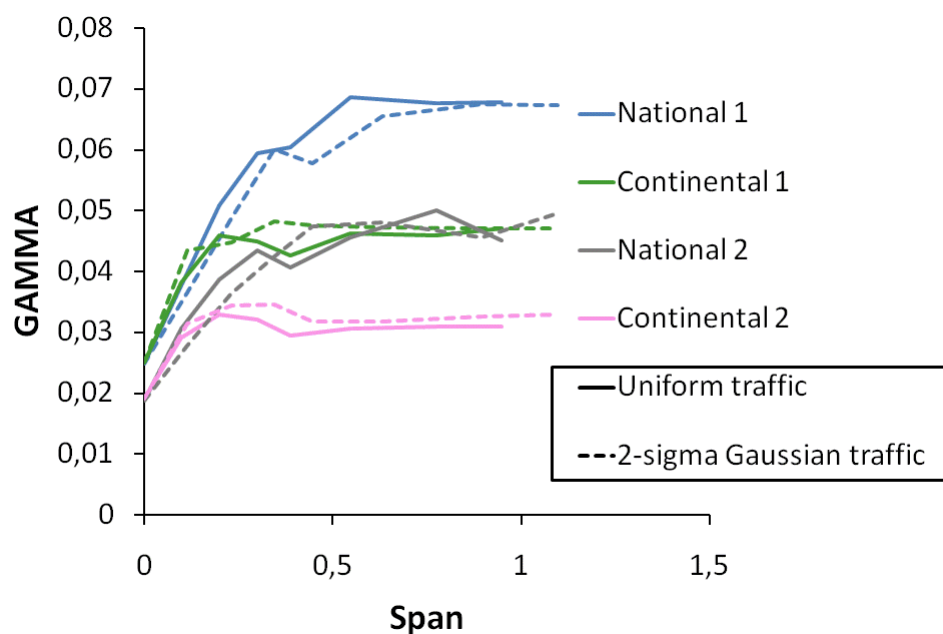


Figure 27: Deviation of the number of optical connections obtained by network planning from that obtained by the convolution estimator. Values obtained for 4 topologies, 2 traffic distributions and 8 values of the span ( $\alpha$ ).

In Figure 27 we observe that for every topology and every traffic law, GAMMA grows with the span of the distribution. This is explained by the fact that as the span grows, there is more diversity among the capacities of the traffic demands yielding more randomness in the traffic and more deviation between the model and the data points. For every topology and every traffic law, GAMMA reaches a plateau when the span of distribution exceeds 0.5. This is due to the fact that when the span of the distribution is equal to 0.5 the distribution of traffic demands stretches out over a whole period of the characteristic function. As we study the case where virtual concatenation is allowed, the integer part of the normalized capacity corresponds to many fully loaded optical connections; the leftover capacity is routed and groomed separately. Thus stretching over more than the period of 1 actually does not bring more diversity to the capacities of the traffic demands.

To obtain the data points plotted in Figure 27, we carried out full network planning in  $300 \times 64 = 19200$  configurations. We studied two very different traffic distribution laws (uniform and 2-Sigma Gaussian) and 4 topologies of different sizes, in every case GAMMA stayed under the 0.07 limit. We deduce that the estimation by convolution is a valid approximation of the RG process for continuous traffic distributions. According our tests on a limited number of real client traffic matrices who had discrete PDFs, the estimation by convolution extends to discrete distributions of traffic demands.

In the cases where a lower deviation from the estimator (GAMMA) is needed, such as the case of topologies with few nodes, mentioned in section IV.C.4), we can propose to use the most precise available interpolation of the characteristic function for the convolution estimator.

## D. Generalization

Now that we validated numerically the estimation by convolution, we explore it analytically to provide more general information.

### 1) Analytical form of estimator for a given type of PDF of traffic demands

If we are interested in one type of PDF of traffic demands, we can calculate analytically the equation of the estimator linking the parameters of PDF to the number of optical connections needed to transport the traffic.

For example, if we are interested in uniform distributions of traffic demands, the main parameters are the expected value and the span. We can rewrite the definition of the uniform law defined earlier as being:

$$u_{\underline{g},\alpha}(x) = \begin{cases} \frac{1}{2\alpha}, & \text{for } \underline{g} - \alpha < x < \underline{g} + \alpha \\ 0, & \text{for } x < \underline{g} - \alpha, \text{ for } x > \underline{g} + \alpha \end{cases}$$

Translated so as to have an interval of definition centered at zero it becomes

$$u_{\alpha}(x) = \begin{cases} \frac{1}{2\alpha}, & \text{for } -\alpha < x < \alpha \\ 0, & \text{for } x < -\alpha, \text{ for } x > \alpha \end{cases}$$

For the sake of simplicity we consider that the characteristic function approximates as a stair function in which case it can be expressed as

$$c(x) = \begin{cases} k + y_B, & x \in [k; k + x_B] \\ \frac{1 - y_B}{x_A - x_B} x + k + 1 - \frac{1 - y_B}{x_A - x_B} (k + x_A), & x \in [k + x_{BA}; k + x_A] \\ k + 1, & x \in [k + x_A; k + 1] \end{cases}$$

where  $k$  is the integer part of  $x$ .

The expression of the estimator is

$$c * u_{\alpha}(y) = \int_{-\infty}^{+\infty} c(x) u_{\alpha}(x - y) dx$$

By definition of  $u_\alpha$  we have:

$$c * u_\alpha(y) = \int_{y-\alpha}^{y+\alpha} c(x)u_\alpha(x-y)dx$$

Let us note  $m = \lfloor y - \alpha \rfloor + 1$  and  $l = \lfloor y + \alpha \rfloor$ .

To calculate the integral, we break it up the interval of integration

$$c * u_\alpha(y) = \int_{y-\alpha}^m c(x)u_\alpha(x-y)dx + \int_m^l c(x)u_\alpha(x-y)dx + \int_l^{y+\alpha} c(x)u_\alpha(x-y)dx$$

The three resulting integrals are called  $I_1, I_{lm}, I_2$ .

$$I_1 = \int_{y-\alpha}^m c(x)u_\alpha(x-y)dx$$

$$I_{lm} = \int_m^l c(x)u_\alpha(x-y)dx$$

$$I_2 = \int_l^{y+\alpha} c(x)u_\alpha(x-y)dx$$

We calculate that

$$I_{lm} = \frac{1}{2\alpha} \int_m^l c(x)dx$$

$$I_{lm} = \frac{1}{4\alpha} (l - m)(1 + l + m - (1 - y_B)(x_A + x_B))$$

For  $I_1$  three cases are possible:

If  $m - 1 \leq y - \alpha < m - 1 + x_B$ :

$$I_1 = \frac{1}{2\alpha} \left[ \int_{y-\alpha}^{m-1+x_B} (m-1+y_B)dx + \int_{m-1+x_B}^{m-1+x_A} \left( \frac{1-y_B}{x_A-x_B} (x-m+1-x_A) + m \right) dx + \int_{m-1+x_A}^m mdx \right]$$

We calculate that

$$I_1 = \frac{1}{2\alpha} \left[ m^2 + m(\alpha - y) + \frac{1}{2} (2 - 2\alpha - x_A - 2m - x_B + 2y)(1 - y_B) \right]$$

If  $m - 1 + x_B \leq y - \alpha < m - 1 + x_A$ :

$$I_1 = \frac{1}{2\alpha} \left[ \int_{y-\alpha}^{m-1+x_A} \left( \frac{1-y_B}{x_A-x_B} (x-m+1-x_A) + m \right) dx + \int_{m-1+x_A}^m mdx \right]$$

We calculate that

$$I_1 = \frac{1}{2\alpha} \left[ m(\alpha + m - y) - \frac{(1-y_B)(-1 + \alpha + x_A + m - y)^2}{2(x_A - x_B)} \right]$$

If  $m - 1 + x_A \leq y - \alpha < m$ :

$$I_1 = \frac{1}{2\alpha} \left[ \int_{y-\alpha}^m mdx \right]$$

We calculate that

$$I_1 = \frac{1}{2\alpha} [m(\alpha + m - y)]$$

For  $I_2$  also three cases are possible:

If  $l \leq y + \alpha < l + x_B$ :

$$I_2 = \frac{1}{2\alpha} \left[ \int_l^{y+\alpha} (l + y_B) dx \right]$$

We calculate that

$$I_2 = \frac{1}{2\alpha} [(l + y_B)(y + \alpha - l)]$$

If  $l \leq y + \alpha < l + x_B$ :

$$I_2 = \frac{1}{2\alpha} \left[ \int_l^{y+\alpha} (l + y_B) dx \right]$$

We calculate that

$$I_2 = \frac{1}{2\alpha} [(l + y_B)(y + \alpha - l)]$$

If  $l + x_B \leq y + \alpha < l + x_A$ :

$$I_2 = \frac{1}{2\alpha} \left[ \int_l^{l+x_B} (l + y_B) dx + \int_{l+x_B}^{y+\alpha} \left( \frac{1 - y_B}{x_A - x_B} (x - l - x_A) + l + 1 \right) dx + \right]$$

We calculate that

$$I_2 = \frac{1}{2\alpha} [(l + y_B)(y + \alpha - l)] + \frac{(1 - y_B)(\alpha - l - x_B + y)^2}{2(x_A - x_B)}$$

If  $l + x_A \leq y + \alpha < l + 1$ :

$$I_2 = \frac{1}{2\alpha} \left[ \int_l^{l+x_B} (l + y_B) dx + \int_{l+x_B}^{l+x_A} \left( \frac{1 - y_B}{x_A - x_B} (x - l - x_A) + l + 1 \right) dx + \int_{l+x_A}^{y+\alpha} (l + 1) dx \right]$$

We calculate that

$$I_2 = \frac{1}{2\alpha} \left[ (l + y_B)(y + \alpha - l) + \frac{(1 - y_B)(\alpha - l - x_B + y)^2}{2(x_A - x_B)} + (l + 1)(y + \alpha - l - x_A) \right]$$

These formulas can be entered into a calculator or a spreadsheet to calculate instantly the estimated number of optical connections as a function of the parameters of the stair function and the PDF of the traffic demands.

Using such a spreadsheet we can find, for example, that as the standard deviation of the uniform distribution grows, the estimator converges toward the linear interpolation of the stair function  $c$  that we call  $d_u$ . The equation of  $d_u$  is

$$d_u(x) = x + \frac{1 + (y_B - 1)(x_A + x_B)}{2}$$

In the following part we check whether this property can be generalized to any characteristic function and any distribution of traffic demands.

## 2) Linearity of the estimator for traffic distributions with high standard deviation

Due to its cyclically additive property, any characteristic function  $c$  can be decomposed into a sum

$$c(x) = d(x) + h(x)$$

where  $d$  is a linear function and  $h$  is a periodical function with a period of 1 and zero average. Using these facts we can deduce a few things about the equation of  $d$ . As  $d$  is linear  $d(x) = ax + b, \forall k \in \mathbb{N}$ , as  $\int_k^{k+1} h(x)dx = 0$ :

$$\int_k^{k+1} d(x)dx = \int_k^{k+1} c(x)dx =$$

$$ak + b + \frac{a}{2} = k + \int_0^1 c(x)dx$$

As  $\int_0^1 c(x)dx$  is independent of  $k$ , we obtain that  $a = 1$  and  $b = \int_0^1 c(x)dx - \frac{1}{2}$ . We have thus determined the equation of the linear interpolation for any characteristic function.

Using the decomposition  $c = d + h$  we consider now  $c * f_\alpha$ . For any  $f_\alpha$  :

$$c * f_\alpha(y) = \int_{-\infty}^{+\infty} c(x)f_\alpha(x-y)dx$$

$$c * f_\alpha(y) - d(y) = \int_{-\infty}^{+\infty} c(x)f_\alpha(x-y)dx - d(y)$$

$$\text{As } d(y) = d(y) \int_{-\infty}^{+\infty} f_\alpha(x-y)dx = \int_{-\infty}^{+\infty} d(y)f_\alpha(x-y)dx$$

$$c * f_\alpha(y) - d(y) = \int_{-\infty}^{+\infty} (d(x) + h(x) - d(y))f_\alpha(x-y)dx$$

As the slope of  $d$  is equal to 1  $d(x) - d(y) = x - y$ , thus

$$c * f_\alpha(y) - d(y) = \int_{-\infty}^{+\infty} (x-y)f_\alpha(x-y)dx + \int_{-\infty}^{+\infty} h(x)f_\alpha(x-y)dx$$

We make a change of variable in the first integral  $w = (x - y)$ .

$$c * f_\alpha(y) - d(y) = \int_{-\infty}^{+\infty} wf_\alpha(w)dw + \int_{-\infty}^{+\infty} h(x)f_\alpha(x-y)dx$$

In the first term, we recognize the expected value of the random variable having the distribution  $f_\alpha$ , we note it  $E[f_\alpha]$ . In the second term, we recognize  $h * f_\alpha(y)$ .

$$c * f_\alpha(y) - d(y) = E[f_\alpha] + h * f_\alpha(y)$$

$\alpha E[f_\alpha]$  is independent of  $y$ , but  $h * f_\alpha(y)$  depends on  $y$  but it is bounded:

$$\left| \int_{-\infty}^{+\infty} h(x)f_\alpha(x-y)dx \right| \leq \max(|h|) \max(f)$$

By definition of a probability density function  $\max(f) = 1$ . To calculate  $\max(h)$  we consider that the characteristic function  $c$  is always under that of the overlay planning as it is the case in the example depicted in Figure 28 a). In Figure 28 b), we plot the  $h$  function corresponding to this function  $c$ . As  $h=c-d$  where  $d$  is a linear function with a linear coefficient of 1,  $h$  is the result of a translation and a rotation by  $45^\circ$  of  $c$ . As we see in Figure 28 b),  $\min(h) = -b/\sqrt{2}$  because  $c$  necessarily passes through the point with coordinates  $(1;1)$ . We also see in Figure 28 b), that because we consider that the characteristic function  $c$  is always under that of the overlay planning, we have  $\max(h) \leq 1/\sqrt{2} - b/\sqrt{2}$ . As we have  $0 < b \leq 0.5$ ,  $1/\sqrt{2} - b/\sqrt{2} \geq b/\sqrt{2}$ , therefore  $\max(|h|) \leq \max(1/\sqrt{2} - b/\sqrt{2}; b/\sqrt{2}) \leq 1/\sqrt{2} - b/\sqrt{2} \leq 1/\sqrt{2}$ .

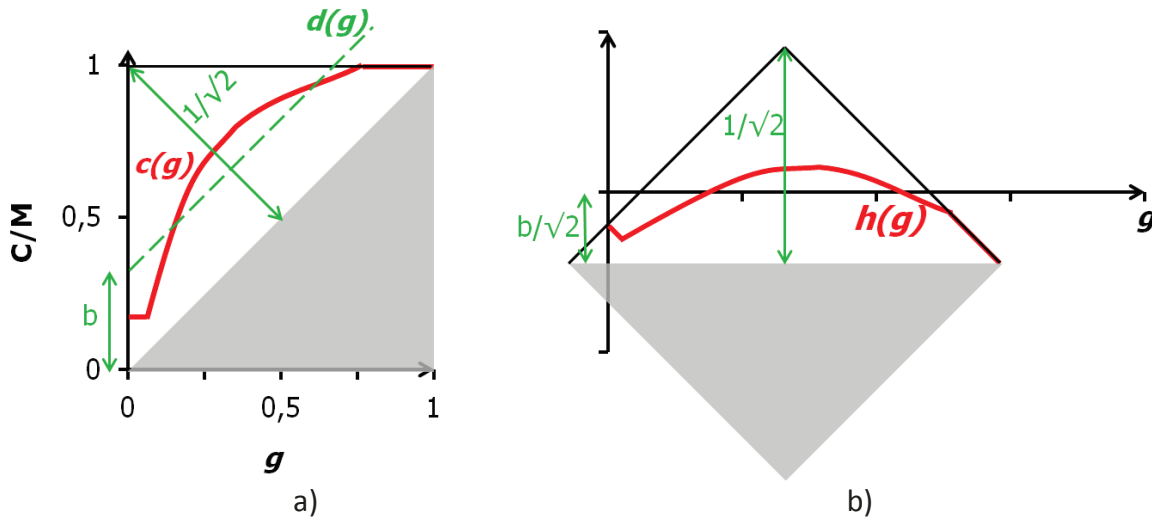


Figure 28: a) Example of a characteristic function.  $c$  is the characteristic function and  $d$  is the linear function obtained by averaging  $c$ . b) Function  $h$  obtained from functions  $c$  and  $d$  from the right-hand figure ( $h=c-d$ ).

Therefore

$$|c * f_{\alpha}(y) - d(y) - E[f_{\alpha}]| \leq \max(|h|) \max(f) \leq 1 \cdot \frac{\sqrt{2}}{2}$$

We have thus shown that for any characteristic function  $c$  below that of the overlay network planning and any continuous distribution of traffic demands  $f_{\alpha}$ , the curve  $c * f_{\alpha}$  as a function  $y$  stays within a limited distance (equal to  $\frac{\sqrt{2}}{2}$ ) from the linear function whose equation is  $d(y) + E[f_{\alpha}] = y + \int_0^1 c(x)dx - \frac{1}{2} + E[f_{\alpha}]$

In practice,  $h * f_{\alpha}(y)$  decreases with  $\alpha$ , because the more  $f_{\alpha}$  is spread, the more  $h * f_{\alpha}$  tends towards the average of  $h$  which is zero. For example for the uniform law

$$h * u_{\alpha}(y) = \int_{-\infty}^{+\infty} h(x)u_{\alpha}(x-y)dx = \frac{1}{2\alpha} \int_{y-\alpha}^{y+\alpha} h(x)dx$$

As  $\forall k \in \mathbb{N}, \int_k^{k+1} h(x)dx = 0$ ,

$$h * u_{\alpha}(y) = \frac{1}{2\alpha} \left[ \int_{y-\alpha}^{\lfloor y-\alpha \rfloor + 1} h(x)(x-y)dx + \int_{\lfloor y+\alpha \rfloor}^{y+\alpha} h(x)(x-y)dx \right]$$

Thus,

$$|h * u_{\alpha}(y)| = \frac{1}{2\alpha} \left| \int_{y-\alpha}^{\lfloor y-\alpha \rfloor + 1} h(x)dx + \int_{\lfloor y+\alpha \rfloor}^{y+\alpha} h(x)dx \right|$$

$$|h * u_{\alpha}(y)| \leq \max(|h|) \frac{1}{2\alpha} = \frac{\sqrt{2}}{8\alpha}$$

Therefore, for the uniform distribution, as  $\alpha$  grows,  $h * u_{\alpha}(y)$  converges to 0 and  $c * u_{\alpha}(y)$  converges towards  $E[u_{\alpha}] + d(y) = d(y) = y + \int_0^1 c(x)dx - \frac{1}{2}$ .

Hence for a continuous distribution of traffic demands, as the standard deviation of the distribution of traffic demands grows, the number of optical connections established by the RG process tends towards a linear dependence of the average traffic demand. We have also shown that the slope of this linear function is equal to 1 while the Y-intercept

equals to  $\int_0^1 c(x)dx - \frac{1}{2} + E[f_\alpha]$  thus bringing out the respective influence of the characteristic function and the distribution of traffic demands.

### *E. Links with existing literature*

As we have mentioned in section II, the linear dependence between the number of established optical connections and the average capacity of the traffic demands has been observed for multilayer planning in the case of traffic distributions having a large standard deviation [12]. Bodamer & al. could not extract from the equations of these curves the parameters linked to the topology, to the planning algorithm, and the statistical distribution of the traffic matrix. We have shown this convergence mathematically and have shown the exact expression for the linear function.

The characteristic function covers a vaster scope of cases than those considered in [12]. It also allows predicting a number of optical connections for wide choice of traffic matrices having diverse PDFs.

In V, we have distinguished and explained the influence of both the characteristic function and the traffic matrix on the number of optical of optical connections. Now we study how the physical topology on the one hand and the RG method on the other interact to shape the characteristic function. In practice, distinguishing the influences of the RG method and the topology can allow benchmarking the RG methods between them and to continuously enhance a given RG algorithm.

## VI. ENHANCING MULTILAYER RG HEURISTICS USING THE STAIR FUNCTION

Most of our work on multilayer RG has been done using our heuristic presented in Appendix 2. By using the characteristic function concept, it has been enhanced. First we present the evolution of our heuristic. Then we present the work on benchmarking and enhancement of two other RG tools.

### *A. Enhancement of our heuristic through the characteristic function*

Throughout the work presented in this thesis we have enhanced our heuristic so that three consecutive versions exist today: V1, V2 and V3. The algorithmic differences between them are presented in Appendix 2. To enhance our heuristic the methodology was to trace its characteristic function for different topologies and values of density. As we have shown in IV.C.4) and IV.C.5), the main gap between the characteristic functions of 1SP-MILPs and of our heuristic appeared for  $g > 0.5$  and decreased when the number of nodes in the topology grew. In Figure 29 we traced the stair functions of two MILP formulations and data points corresponding to the characteristic function of V1, V2 and V3, for National 1 topology and 100 random homogeneous traffic matrices.

#### *1) From V1 to V2*

We see in Figure 29 a), that the gap with 1SP-MILP is very pronounced for V1. Through the characteristic function we learn that a difficulty appears when demands with larger capacities are aggregated and when there are few optical connections overall. After investigation we found that this is because in V1 the “gain” as defined in the algorithm (cf. Appendix 2) of candidate tunnels is proportional to the traffic they carry. For a candidate tunnel whose capacity was greater than the transponder capacity, this causes the establishment of a few fully loaded optical connections and a connection with the remaining traffic, which can be almost empty and is seldom filled afterwards. This brought us to implementation of a possibility to split the capacity of a candidate tunnel whose capacity was greater than the transponder capacity. In V2 these candidate tunnels are split up into a few candidate tunnels whose gains are calculated separately.

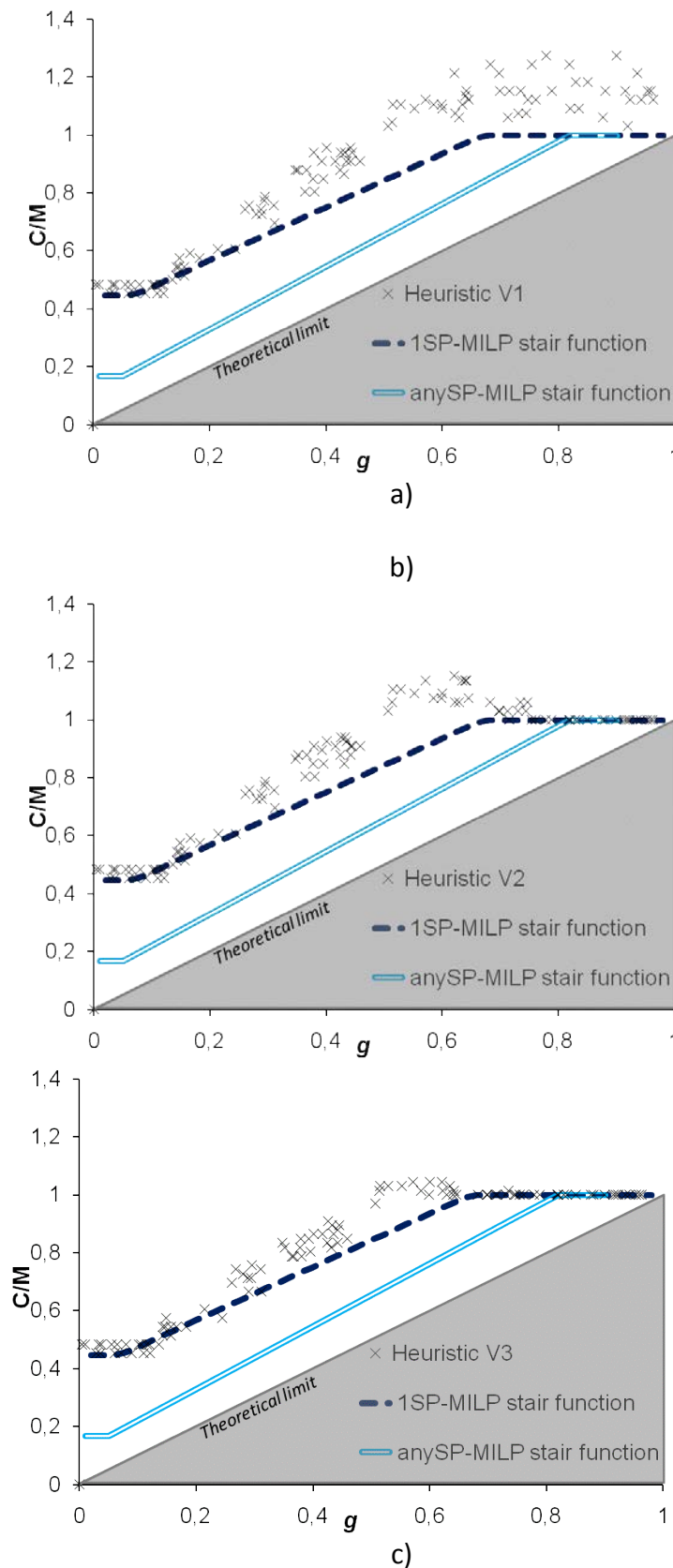


Figure 29: Stair functions of 2 multilayer RG MILP formulations and three versions of our heuristic a) V1, b) V2, and c) V3 for National 1 topology and density=0.6.

An enhancement of performance can be noted in Figure 29b; V2 requires on average (over all  $g$  values) 11% less optical connections.

## 2) From V2 to V3

We were still unsatisfied with the performances of V2, indeed it still frequently established more than one optical connection per demand for  $g > 0.5$ . After investigation we found that it was because, at the beginning of the planning process, V2 established optical connections which, in spite of a high gain, were partly empty, and were not filled later during the planning process. In other words, the heuristic took decision to establish an optical connection locally (one connection after the other) and lacked a global view. This is why we introduced V3, which when electing each optical connection calculates an estimate of the impact of this choice on the final cost. At each step V3 does not choose the candidate connection with the highest gain, but the one whose estimated final cost is the lowest. The estimated final cost is calculated for  $K$  ( $K \in \mathbb{N}$ ) candidate connections having the highest gain. For  $K > 30$  no significant savings in terms of optical connections were observed; we thus fixed  $K$  to 30.

An enhancement of performance can be noted in Figure 29c, V3 requires on average 2% less optical connections (over all the values of  $g$ ).

We have seen how our heuristic's gradual enhancement provided the 12% final saving of the number of optical connections.

## B. Study of two Alcatel-Lucent Bell Labs tools

After enhancing our heuristic we applied the same methodology to 2 multilayer planning tools available in Alcatel-Lucent Bell Labs. We call them Tool A and Tool B. The tool A implements two RG routines combining heuristics and meta-heuristics. Altogether that makes three routines Tool A.1, Tool A.2, Tool B. For each RG routine we have evaluated the efficiency in minimizing the number of optical connections.

Each RG routine has been cleared of all the constraints except of the bidirectionnality of optical connections. This means that once a routine establishes an optical connection, another connection is automatically established between the same nodes in the opposite direction. As heterogeneous traffic matrices are symmetrical, it is not an important constraint. However, small differences can appear. In particular such a constraint may cause the establishment of a slightly larger number of connections, especially for low values of  $g$ .

These RG routines have been studied over a set of three topologies with a growing number of nodes (cf. Table 4). For confidentiality reasons, the exact topologies National 3 and National 4 cannot be revealed.

Table4: The characteristics of the second set of topologies

	National 1	National 3	National 4
<i>Nodes N</i>	11	17	29
<i>Links L</i>	16	26	41

### 1) *Study of Tool A*

In Figure 30, we plot the data points corresponding to the characteristic function of routines Tool A.1 and Tool A.2 obtained with 25 heterogeneous traffic matrices with  $0 < g < 1$  and a density of 0.6. For the National 4 topology, the results could be obtained for less than ten traffic matrices due to problems in the experimental protocol.

In Figure 30a we observe that the characteristic function of Tool A.1 is above that of 1SP-MILP, this means that it is constrained to route each demand over its shortest path, which has been confirmed by the tool's developer. Tool A.2 is an enhancement of Tool A.1, which can route demands on paths other than their shortest path, which we deduce from the fact that its characteristic function is sometimes lower than that of 1SP-MILP.

For all three graphs of Figure 30, Tool A.2 has systematically better or equivalent results comparing to those of Tool A.1. On average, the savings are of 5-10%, which is in line with comparisons conducted with real operator traffic matrices.

In Figure 30 b and c we see that as the number of nodes in the topology grows, the characteristic functions of both RG routines deviate from the theoretical limit, especially for  $g > 0.3$ . This is an undesirable behavior for a RG tool; it is preferable that the characteristic function converge towards the theoretical limit like our heuristic does (cf. section IV.C.5).

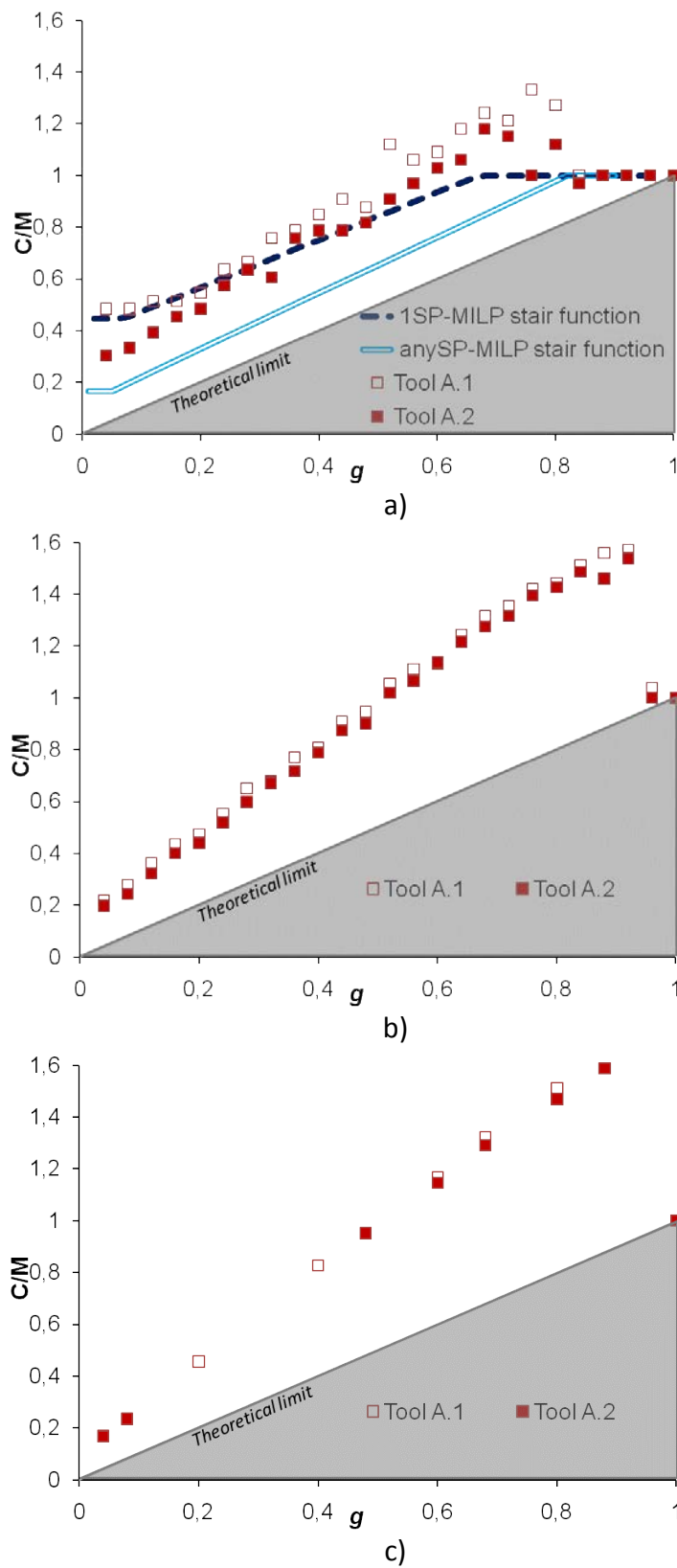


Figure 30: Stair functions of 2 multilayer RG MILP formulations and characteristic functions of Tool A.1 and Tool A.2 for a) National 1 topology, b) National 3 topology, and c) National 4 topology and for density=0.6.

Using the characteristic function we have identified the cases where the performance of Tool A needs to be enhanced: networks with many nodes and traffic matrices with large demands. Using this information we can formulate the hypothesis that Tool A does not behave normally when optical connections composed of several successive links (or hops) need to be established (long optical connections have to be deployed exclusively in topologies with many nodes and where traffic demands are have sufficient capacity to fill connections bypassing a few nodes). To verify this hypothesis we plot in Figure 31 the mean length of optical connections corresponding to the planning results obtained by Tool A.2 and V2 of our heuristic for National 1 and National 4 topologies for heterogeneous traffic matrices with  $0 < g < 1$ .

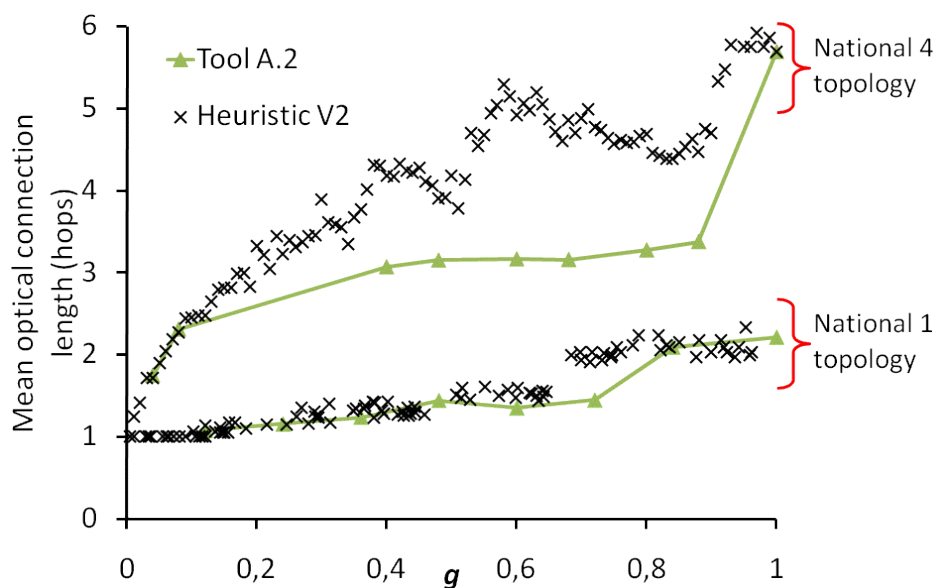


Figure 31: Average length (in hops) of optical connections established by our heuristic V2 and Tool A.2 for National 1 and National 4 topologies. Density=0.6

In Figure 30a we have seen that Tool A has a performance close to our heuristic and to 1SP-MILP on National 1 topology. We note in Figure 31 that for National 1 topology the mean length of optical connections established by Tool A.2 is close to those established by our heuristic. For National 1 topology, the mean length of optical connections does not exceed 2.5 hops.

For National 4 topology, when  $g$  grows our heuristic progressively increases the mean optical length of optical connections up to 5.8, while Tool A.2 creates connections whose average does not exceed 3.5 until  $g=1.0$ . This verifies the hypothesis we formulated earlier and allows developers working on Tool A to enhance the performance of the RG routines for topologies with a large number of nodes. Due to the similarities of their characteristic functions, we extend these conclusions to Tool A.1.

For Tool A, we have compared two routines and obtained results in line with tests on real traffic matrices. Using the characteristic function we determined that the performance of the two routines can be strongly enhanced. By visualizing their characteristic functions we formulated the hypothesis that allowed finding their deficiencies and proposing enhancements.

## 2) Study of Tool B

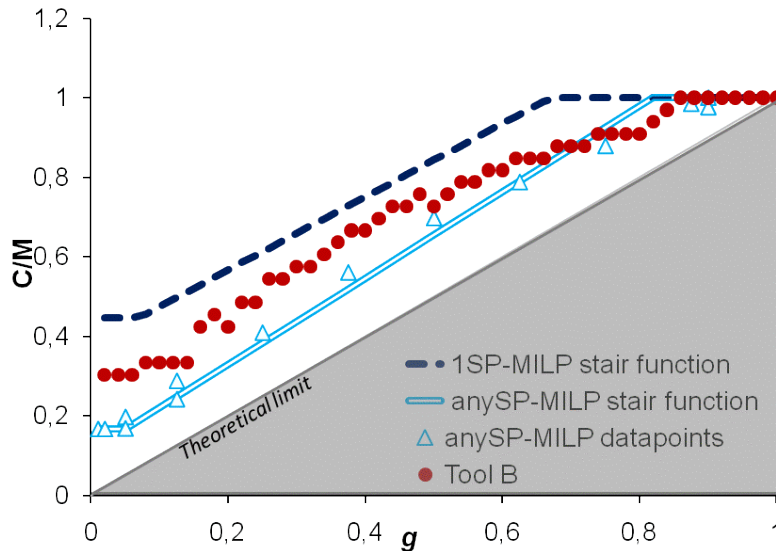


Figure 32: Characteristic function of Tool B and 2 multilayer RG MILP formulations. National 1 topology. Density=0.6

In Figure 32 we plotted the stair functions of two MILP formulation as well as the data points corresponding to the characteristic function of Tool B and anySP-MILP on National 1 topology for traffic matrices with a density of 0.6. We note that the characteristic function of Tool B is well below the stair function of 1SP-MILP. This shows that Tool B is not limited to routing on the shortest path. For  $0.75 < g < 0.85$  the characteristic function of Tool B is even below the stair function of anySP-MILP. As mentioned in section IV.C.2), for anySP-MILP, the stair function is not a very precise interpolation of the characteristic function. Looking at the data points of anySP-MILP, we see that the characteristic function of Tool B is always above that of anySP-MILP.

We note that the characteristic functions of anySP-MILP and Tool B are very close to each other. The mean L1-distance between the two functions is 14%. The difference is larger for  $g < 0.1$ . We hypothesize that it is because of the constraint of bidirectionnality of optical connections of Tool B, but this hypothesis could not be tested. Regardless of the answer, Tool B has the best performance among the tools we have worked with.

Similarly to what we described in section IV.C.5), we study how this characteristic function changes for different topologies and values of density. In Figure 33 we plot the characteristic functions of Tool B for three topologies, for traffic matrix with densities 0.4, 0.6, 0.8, 1.0 and  $0 < g < 1$ . We observe that Tool B characteristic function, like anySP-MILP, is concave and cannot be accurately modeled with a stair function. We also note that for all three topologies the characteristic function changes little with respect to density (with the exception of the case  $g < 0.1$  which has to be studied separately). Moreover, the characteristic function changes little with the topology. To confirm this we superpose in Figure 34 the characteristic functions obtained for the three topologies with homogeneous matrices with a density of 1. We observe that the mean distance between the curves is under 3%. We conclude that the characteristic function of Tool B is remarkably robust to changes of topology and density.

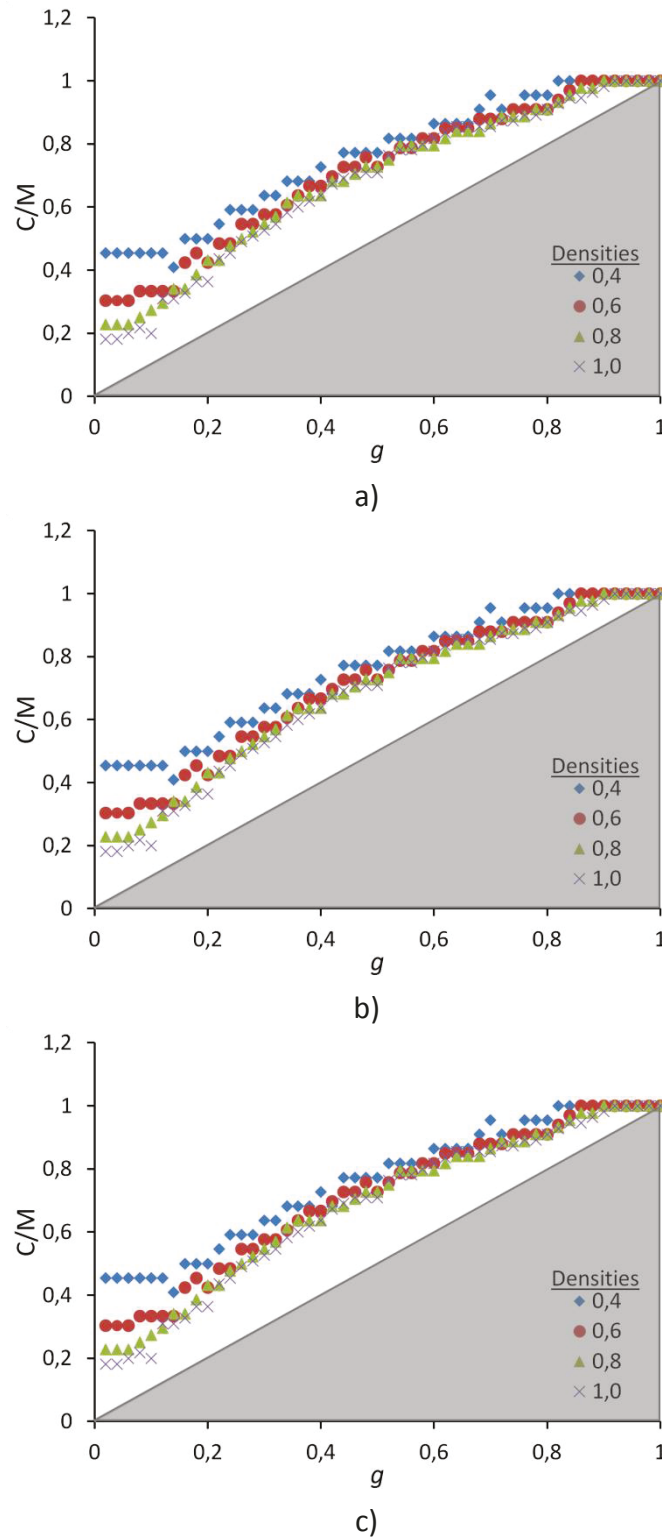


Figure 33: Characteristic function of Tool B for a) National 1 topology, b) National 3 topology, and c) National 4 topology and for density  $\in [0.4; 0.6; 0.8; 1.0]$ .

For topologies larger than National 1 anySP-MILP formulation is intractable, but using the characteristic functions of Tool B we can get some information about it. Indeed the characteristic function of anySP-MILP is necessarily between the theoretical limit ( $g=C/M$  line) and the characteristic function of Tool B. As the characteristic function of Tool B is

stable with the number of nodes and the density of the traffic matrices, we may deduce that the characteristic function of anySP-MILP does not deviate from the theoretical limit when density changes and when the number of nodes in the topology grows.

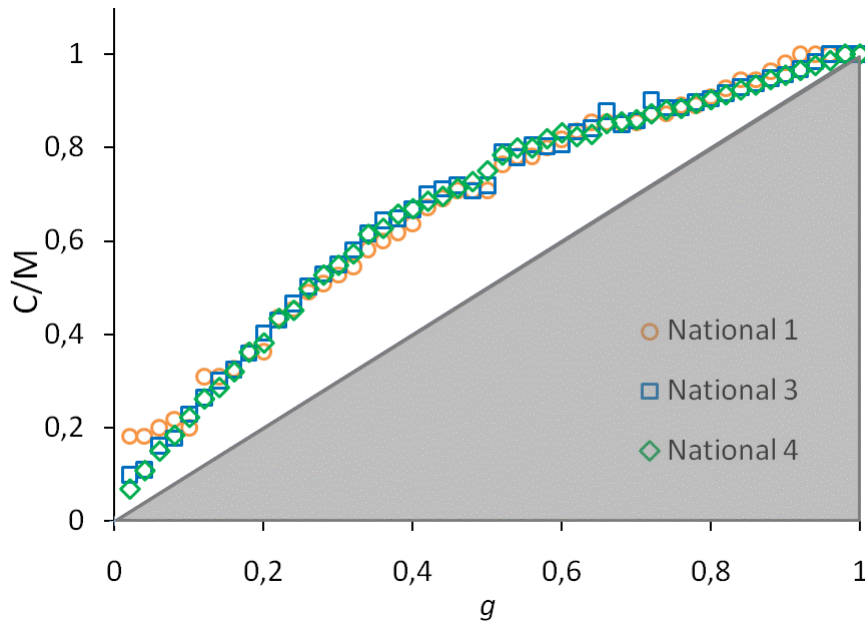


Figure 34: Characteristic function of Tool B for National 1 topology, National 3 topology, and National 4 topology and for density=1.

In section VI we discussed how a methodology allowing visualizing, comparing and enhancing the efficiency of multilayer RG routines is deduced from the characteristic function. The results we have obtained are in line with the tests made on real life traffic matrices and allow evaluating the savings made by enhancing the RG tool.

As for the methodology itself, we have shown the importance of MILP formulations in the evaluation of heuristics. We have shown on three topology examples that the performance of a RG routine may diverge (Tool A), converge (our heuristic) or stay stable (Tool B) as the number of nodes in the topology grows. The absence of a general trend encourages applying the methodology to test every new appearing RG routine.

The methodology we propose can be used to test the enhancements brought to any multilayer tool and can also be used to obtain quick estimators of the results of a multilayer tool.

## VII. CONCLUSION

In this chapter, we introduced the characteristic function of a RG method to address the lack of numerical and analytical models for multilayer network planning. We described how it is obtained for a given RG routine, network topology and density. We explained the shape of its curve and its theoretical bounds for overlay, opaque and multilayer RG. We showed how the characteristic function allows to visualize the gains of using multilayer network planning.

During a large-scale simulation campaign we showed how a characteristic function allows estimating precisely the results of multilayer planning for traffic matrices whose demands have capacities following continuous statistical distributions. Thus the analysis of characteristic functions can be generalized over a large number of traffic matrices.

We showed how the semi-analytical model we propose allows to find general results on multilayer planning that we link to existing literature.

Finally we demonstrated how the performances of a RG algorithm can be assessed by comparing it with the results of MILP formulations and theoretical bounds. We showed the importance of the study for network topologies having a large number of nodes. We studied 4 multilayer RG routines and showed how the characteristic function allows to visualize and assess their performance and in some cases suggest algorithmic enhancements.

# Chapter 3:

## Impact of the optical reach on multilayer planning of IP-over-WDM networks

### I. INTRODUCTION

#### *A. Importance of the optical reach*

In the previous chapter we assessed the accuracy of routing and network grooming mechanisms, essential in multilayer network planning, by the introduction of the “characteristic function”. In the above-mentioned studies the constraints that usually apply to network planning (cf. Chapter 1 section II.B) were ignored. This has been done to ensure the generality of the results as explained in Chapter 2 section III.B.

Among the constraints those that are related to limited switching capacities can be discarded by deploying nodes with higher capacity. For this reason, this constraint will not be taken into account in the following. The one limited to saturation of the optical spectrum in the links intervenes mainly when the network is heavily charged with traffic demands, which means that a network upgrade is imminent. It is the reason why we consider only the last limitation. But as we have seen before in the Introduction, the demand for higher transport capacity is constant. The capacity of optical connections can be increased through the introduction of modulation formats with higher spectral efficiency, but in conformity with the Shannon limit the optical reach decreases with the spectral efficiency [6]. Therefore the optical reach is becoming more and more a limiting constraint in core networks and will impact metropolitan network planning.

Among the constraints on the RG process described in Chapter 1 section II.B, the optical reach limitation appears critical to a network with a WDM transport layer and this constraint will gain importance and apply to the majority of future networks. We have explained in Chapter 1 section II.B that the most limiting constraints should be taken into account to lower the network cost.

## B. *Optical reach constraint in multilayer network planning*

As explained in Chapter 1 section II.D, in multilayer network planning, lower layers share information with upper layers. In this chapter, the optical layer shares its topology, equipment cost, equipment capacity and *optical reach* with the upper layer. Sharing this set of information is important because:

- Topology information allows determining through which node the frames of the client traffic demands will transit in order to know where they can be extracted and groomed with other incoming traffic. This enables sharing optical resources with other client traffic demands.

- Equipment cost and capacity information in both layers allows deciding whether an optical channel must optically bypass a node or if it must be sent to the upper layer to carry out grooming on the frames it carries.

- Optical reach information allows accounting for the regenerator cost during the selection of optical connections thus accounting for the full cost of optical connections longer than the optical reach.

The investigation of the impact of the optical reach on network planning covers the cases where the optical reach is fixed in advance but also those where it is not fixed. Indeed more expensive and/or energy consuming transponders and other WDM devices allow to transmit on longer reaches. It is necessary to know whether these additional expenses allow to decrease the network cost [35]-[38], [80]. So far, this question has been studied in the context of the overlay network model [35]-[38]. We investigated the impact of the optical reach on the networks cost and on the properties of optical connections. On this subject, we had the possibility to collaborate with Giuseppe Rizzelli who had also studied this subject [81]. The results of our collaboration have been reported in [82].

The rest of this chapter is organized as follows. In section II, we introduce an extension of the node architecture and cost model introduced in Chapter 1 section 1.C.3). In section III, we describe our multilayer planning heuristic algorithm and introduce two MILP formulations used to validate it. Numerical simulations of multilayer network planning were carried out with the hypotheses presented in section IV. The results concerning multilayer network planning under optical reach constraint are shown in section V. Finally, conclusions are drawn in section VI.

## II. NETWORK MODEL

### A. Node architecture

For simplicity's sake, all network nodes are assumed to have the same architecture. IP and WDM layers are interconnected through router ports (RPs) and transponders (TSPs). The interconnection allows the insertion/extraction (Add/Drop) of an electrical/optical signal from/to the electrical layer to/from the optical layer. Each transponder is assumed to be connected to only one router port having the same capacity as the transponder. In this chapter, we use a variant of the node architecture presented in Chapter 1 section 1.C.3). Each node has in addition a pool of regenerators. The OXC can switch one of the optical connections towards one of the regenerators available in the node so as to retime, reshape, and reamplify the optical signal without any treatment in the IP router. We consider that each regenerator is composed of two transponders in back-to-back configuration, as shown in Figure 35.

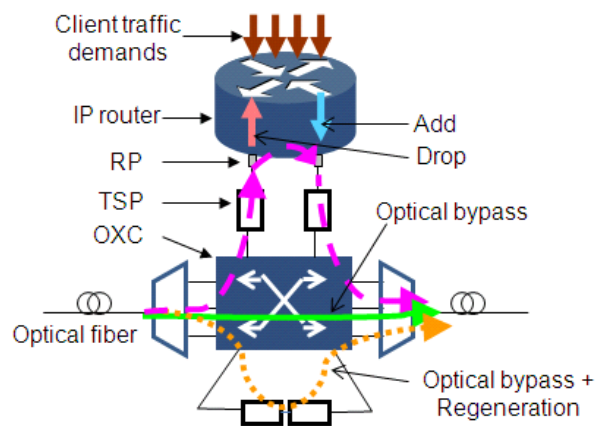


Figure 35: IP-over-WDM node architecture.

An optical connection transiting through a node can:

- Remain at the optical layer and be directly switched to the output port of the OXC. This operation, called optical bypass, is represented in Figure 35 by the continuous green arrow.

- Require a regeneration at the optical layer by the use of a regenerator. This operation is represented by a dotted orange line in Figure 35.

- Be groomed and regenerated by sending the signal to the upper layer where information can be dropped and new information added: this process is called *regrooming*. From the optical layer's point of view, this operation is equivalent to an optical connection Add and Drop. This operation is represented by a dashed purple arrow in Figure 35.

## B. Cost model

To compute the network cost we only take into account devices whose number may vary during network planning process. As wavelength contention and blocking, are not addressed here, we assume having one bidirectional link with a sufficient number of available wavelengths between any two connected nodes. Under these hypotheses the number of devices in the links does not vary; therefore we do not consider the costs related to the equipment in optical links. We also do not address blocking constraints in nodes: the capacities of the OXCs and of the routers are supposed to be sufficient. Therefore the cost of the switching fabric in the optical and the electric part of the node are also considered to be constant whatever the traffic load.

Hence, the *total network cost* is the linear combination of the number of router ports, OXC ports, transponders and regenerators multiplied by their individual cost.

### III. PLANNING METHODS

As mentioned in Chapter 1, to study real size networks, heuristics must be considered due to their lower computational complexity.

In the following, we propose a heuristic-based multilayer planning algorithm. Then, we introduce two MILP formulations used to validate the performances of the heuristic with respect to the optical reach.

#### A. *Heuristic*

Here we introduce the modifications brought to the heuristic V3, described in Appendix 2, to take into account the lengths of optical connections, the reach and the cost of regenerators.

The algorithm is the same as used in Chapter 2, here we have non-zero cost for the regenerators which yields following changes:

- During the calculation of the cost of a candidate connection, if the sum of the length of the links composing the connection is greater than  $N$  times the optical reach, we place regenerators (at least  $N$ ) in intermediate nodes along the optical connection.

- The gain, the estimated total network cost for each candidate connection and the total network cost calculated at the end of the network planning process include the cost of the regenerators necessary to establish each optical connection.

The total network cost is obtained by considering the resources required to set-up all the chosen optical connections (router ports, transponders, and regenerators) and their cost.

#### B. *MILP formulations*

The two MILP formulations are called One-Shortest-Path MILP (1SP-MILP) and any-Shortest-Path MILP (anySP-MILP). The cost of the regeneration is taken into account. They have been written by Giuseppe Rizzelli during his stay in Alcatel-Lucent Bell Labs. The two MILP formulations can be found in Appendix 1.

## IV. SIMULATION HYPOTHESES

### A. Traffic assumptions

We investigate the impact of the optical reach on the cost of an IP-over-WDM network when the client traffic demands vary with respect to the transponder capacity. We assume a fixed capacity for all WDM transponders. Unless specified otherwise, the results presented here, are obtained with homogeneous traffic matrices. Within these assumptions, the interesting parameter is the *traffic granularity*, i.e. the ratio between the client demand capacity and the transponder capacity. We assume traffic granularity never exceeds 1.

Homogeneous matrices have been demonstrated in Chapter 2 to be relevant to the study of network planning tools. The studies performed with these matrices, permit to forecast network planning results obtained with realistic traffic matrices [83]. However, in Chapter 2, network planning is performed without any optical reach constraint, it is the reason why we will validate our final results with realistic matrices in V.B.6).

### B. Implementation of the planning methods

In the heuristic, the parameter  $K$ , indicating the maximum number of candidate optical connections considered at each step (cf. Appendix 2), is set to 30, above which no improvement in the total network cost was observed. To solve MILP formulations we use CPLEX 12.1 software [78]. Both implementations are run using a workstation equipped with 8x2 GHz processors and 16 GB of RAM.

### C. Studied topologies

We consider four different network topologies, called National 1, National 2, Continental 1 and Continental 2 (Figure 10): their main characteristics are summarized in Table 1.

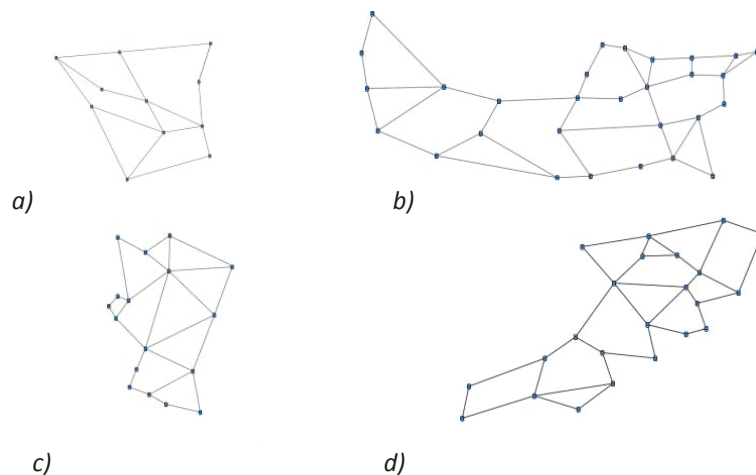


Figure 36: Studied topologies. a) National 1 b) Continental 1 c) National 2 d) Continental 2

Table 5: The characteristics of the studied topologies

	National 1	National 2	Continental 1	Continental 2
<i>Nodes</i>	11	17	29	23
<i>Links</i>	16	26	41	37
<i>Diameter (km)</i>	1760	1000	5240	2900
<i>Max link (km)</i>	820	350	916	683
<i>Mean SP (hops)</i>	2.07	2.85	3.94	3.43
<i>Mean SP (km)</i>	931	410	2246	1068
$\left(\frac{\text{Mean SP (km)}}{\text{Max Link (km)}}\right)$	1.14	1.17	2.45	1.56

The shortest paths (SP) between nodes are obtained using Dijkstra's algorithm [31] using link length in kilometers as the metric. The diameter of the topology is the longest shortest path, in kilometers, between any two nodes of the topology. Mean SP is the mean length of the shortest paths in the topology. It can be calculated in kilometers and in hops (number of links making up a path). Max link is the maximum link length in the topology.

Because of its small size in terms of nodes and links, we use National 1 topology for comparing the heuristic with the MILPs. The remaining topologies are planned only by using the heuristic. Planning them by solving the MILP is impossible within few days or weeks on our machines.

#### D. Cost assumptions

The equipment costs are normalized with respect to the cost of a router port, therefore  $L = 1$  arbitrary units (a.u.). The ratio between regenerator cost and transponder cost is equal to 2, as in this work, a regenerator is implemented by connecting two transponders in back-to-back configuration. We suppose that transponder and regenerator costs are optical-reach-dependent. In practice, only a few values of the couple [optical reach, transponder cost] are available to the network planner but here, for generality's sake, we fit the available [optical reach, transponder cost] couples with  $C$  (in a.u.) as a continuous function of the optical reach (in kilometers), as follows [37]:

$$C = C_0 \times (1 + P\%)^{\log_2(\text{reach}/\text{refReach})} \quad (1)$$

Equation 1 means that the transponder cost increases by  $P\%$  every time the optical reach doubles. The optical reach is normalized by an arbitrary reference distance,  $\text{refReach}$  that we choose to fix to 1000 km as in [37].  $C_0$  is the cost of a transponder normalized by router port cost, a 100 Gb/s transponder is reported to cost half as much as a 100 Gb/s short optical reach router interface, resulting in a normalized cost of a transponder of 0.5 a.u. [22].

$P=0$  means that the optical reach does not impact the transponder cost, which equals to 0.5 a.u. whatever the optical reach. In this case, we expect that the total network cost will decrease with the increase of the optical reach, until no regeneration is required along the optical connection.

$P > 0$  means that the transponder (and regenerator) cost increases with the optical reach. The higher  $P$  is, the faster the cost rises with the optical reach increase. In this case, we expect to find one value of the optical reach which minimizes the total network cost.

## V. SIMULATIONS & RESULTS

### A. *Network planning under optical reach constraint*

As we observed previously (cf. Chapter 2 section IV.C), solving the MILP formulations provides lower-cost solutions than the heuristic, but in a much larger amount of time (the time required for planning on National 1 topology is of the order of milliseconds for the heuristic, tens of minutes for 1SP-MILP, and days for anySP-MILP). Here, the network cost evolution with respect to the optical reach for the three presented planning tools is considered. If the behaviors of the MILP formulations and the heuristic are similar and the gap in terms of cost between the heuristic and 1SP-MILP is acceptable ( $< 10\%$ ), the heuristic is an acceptable tool to draw conclusions on the evolution of the total network cost with respect to the optical reach.

We consider National 1 topology for one given connection matrix with 66 randomly chosen client traffic demands. We choose to do a planning with traffic granularity equal to 0.625 because this is where we expect the most differences between the heuristic and the MILP resolutions according to the figure in Chapter 2 section IV.C.2). We also plan for traffic granularity equal to 0.25, which is more common order of magnitude for traffic demands in real traffic matrices, indeed in OTN standard [84] it is typically the ratio between a client ODU and the transport ODU capacity.  $P$  equal to 25% is chosen as a fixed arbitrary value for the comparison and  $P$  equal to 0 is used to verify that there are no unexpected edge effects. Figure 37 depicts the evolution of the total network cost with respect to the optical reach for the three planning methods. For the granularity of 0.25 the anySP-MILP converges seldom for the studied reaches, so only results of 1SP-MILP are shown. The planning is carried out for different values of the optical reach ranging between 820 km (maximum link length in the network) and 2000 km (greater than the topology's diameter). For each curve, we show the curve minimum having the lowest reach (symbolized by a star).

For short optical reaches, the total network cost decreases with the optical reach due to optical reach constraint relaxation: fewer supplementary opto-electronic conversions are needed as the optical reach increases. For longer optical reaches, when  $P=0$  (Figure 37 a) and c)), equipment cost does not vary with optical reach, therefore when the reach is longer than all candidate optical connections, there are no more variations of the total network cost. When  $P=25$  (Figure 37 b) and d)), the total network cost increases for longer optical reaches. This is due to the fact that, even though equipment quantities do not vary, the transponder cost grows with the optical reach ( $P=25$ ). Therefore even if the set-up optical connections are the same, the total network cost grows. When  $P > 0$ , the minimum of the total network cost corresponds to a trade-off between the decreasing amount of required opto-electronic conversions and their increasing cost due to longer optical reaches.

When the traffic granularity is higher (Figure 37 a) and b)), the network cost is much more impacted by the optical reach than for a lower traffic granularity (Figure 37 c) and d)). It results from the fact that as the traffic granularity grows, less regrooming occurs

and the optical connections are longer (cf. Chapter 2 section VI.B.1). The cost of longer connections is much more impacted by the optical reach: it will be detailed hereafter in section B.3).

Whatever the planning method, MILP or heuristic, the total network cost behaves in the same way with respect to the optical reach. In particular, whatever the traffic granularity and the value of  $P$ , the minimum is achieved for the same optical reach for the heuristic and the MILP formulation we compared it to.

The cost difference between anySP-MILP (asterisks in Figure 37) and 1SP-MILP (crosses in Figure 37) is constant with the optical reach: the average value for all studied optical reaches is 22%. It is consistent with the 18% gap between stair functions of these two planning methods observed in Chapter 2 section IV.C.2) with a 0.625 traffic granularity. The cost difference between the heuristic (diamonds in Figure 37) and 1SP-MILP (crosses in Figure 37), is 7% on average for all the studied reaches, when traffic granularity is equal to 0.625, as noted on Figure 37a) and b). This cost difference averaged over all studied optical reaches is of 4% for a granularity of 0.25 as noted on Figure 37c) and d). The observed cost gap is consistent with the 3% (respectively 2%) difference measured between the stair functions of the two planning methods with 0.625 (respectively 0.25) traffic granularity observed in Chapter 2 section IV.C.2). In conclusion the gap in terms of total network cost stays under the 10% limit for the values of traffic granularity and  $P$  where we expected the largest gap.

As all the validation criteria established at the beginning of this subpart are filled, our heuristic can be considered as an acceptable multilayer planning tool. Moreover, computation time is 100 times shorter than the 1SP-MILP method for the National 1 topology, and even shorter for larger networks, making the heuristic algorithm more suitable for our investigation studies.

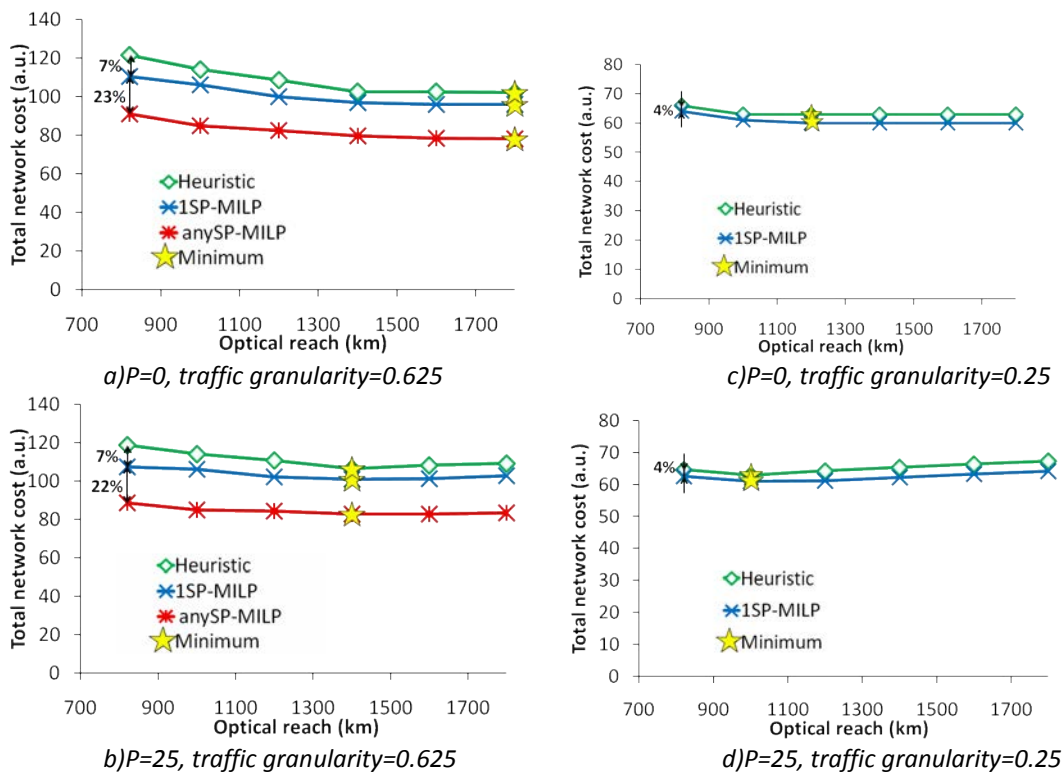


Figure 37: Total network cost obtained by network planning with the heuristic and the resolution of the MILP formulations. National 1 topology (11 nodes). 66 client traffic demands. 2 traffic matrices. 2 values of  $P$ .

## B. *Impact of the traffic granularity on the network planning*

As in the study of the stair function, in Chapter 2, we explore the impact of different values of traffic granularity from (0.125 to 1) for the 4 topologies shown on Figure 10. For each topology, we study optical reach evolution from the longest physical link up to the network diameter (Table 5). For each optical reach value, we plan the network for 10 connection matrices and each traffic granularity value. The presented results are obtained by averaging the total network costs obtained with a set of 10 connection matrices with a density equal to 0.6. The cost evolution with respect to optical reach weakly depends on density; we choose 0.6 because it is a good trade-off between computation time and standard deviation of the total network cost (Appendix 3). We study values of P covering all the range of possible values: from P=0 (transponder cost constant with the reach), to P=100 (transponder cost is multiplied by 2 if the optical reach of the transponder is multiplied by 2). P greater than 100 would have no economical sense, because placing a regenerator would be less expensive than increasing the reach of the transponder. Parameter P has been chosen equal to 50 in this section B. The conclusions would have been the same for any other value of P as shown in Figure 39.

### 1) *Impact of the granularity and the optical reach on the total network cost*

Figure 38 a) shows the mean total network cost averaged over 10 connection matrices as a function of the optical reach. The curves have been obtained for the 8 studied granularities, but only 4 of them are shown for clarity's sake. We observe the same concave evolution of the curves as in Figure 37, but we note also that the total network cost increases with the granularity, for example for Continental 1 the minimum cost for a granularity of 0.125 is 607 a.u. and grows up to 2169 a.u. for granularity equal to 1. The total network cost can be decomposed into the cost of regenerators and the cost of add/drop transponders and router ports, proportional to the number of connections. When the total network cost is minimal, the latter is predominant. The relation between number of optical connections and granularity is explained in Chapter 2. Notably that at a granularity of 1, one optical connection is needed to transport every traffic demand. If the granularity is lower than 1, some demands can be groomed together to share optical connections in order to require less equipment for transportation. In the overlay planning method, there is no possibility to groom together demands having different sources or destinations; at least one optical connection has to be established for each traffic demand whatever the capacity of the demand. It is the reason why for any traffic granularity, the total network cost is equal to the total network cost obtained for granularity equal to 1 (Figure 38). This entails a very high total network cost for overlay network planning as shown in Figure 4 a).

In Figure 38 a), the position of the minimum cost is observed to be greatly dependent on the granularity. The higher cost of regenerators at low optical reaches tends to shift the minimum point to higher optical reaches. This shift can be very important and attains 1550 km for a granularity of 0.125 and 3050 km for a granularity of 1. At this stage, we conclude that network's needs in terms of optical reach can be evaluated only when we have some information on the traffic matrix. Determining the optical reach beforehand entails unnecessary expenses. Thus optical equipment with a given reach should only be chosen after processing the traffic matrix.

To visualize this problem we plot for different granularities the optical reach corresponding to the minimum of the total network cost curve in Figure 38 b). The optical reach corresponding to the minimum is observed to be highly variable with the granularity, for example for Continental 1 there is a 2500 km difference between the optical reach corresponding to the minimum for 0.875 and 0.25 granularity values. That is why we also plotted the lower (pink square symbol) and upper (green triangle symbol) bounds of the 5%-range (range of studied optical reach where total network cost does not exceed 105% of the minimum cost). We note that the lower 5%-range slightly varies with granularity. Sometimes the minimum total network cost is achieved for the shortest of the studied optical reaches. In this case, the lower 5%-range and the reach corresponding to the minimum cost are both set equal to the shortest of the studied reaches. Sometimes lower 5%-range is much lower than the optical reach corresponding to the minimum, e.g. for a granularity of 0.875, meaning that aiming for the minimum cost can lead to choose very high optical reaches while yielding very small gains in terms of total network cost. In addition, aiming for the very high reaches will be more and more difficult as transponder capacities increase; the available optical reaches will be shorter and shorter. To summarize, the lower bound of the 5%-range is much more stable with traffic matrix variations and is much shorter than the reach corresponding to the minimal cost at little expense. Therefore, we will consider in the following, the lower bound of the 5%-range, to be the *required optical reach*.

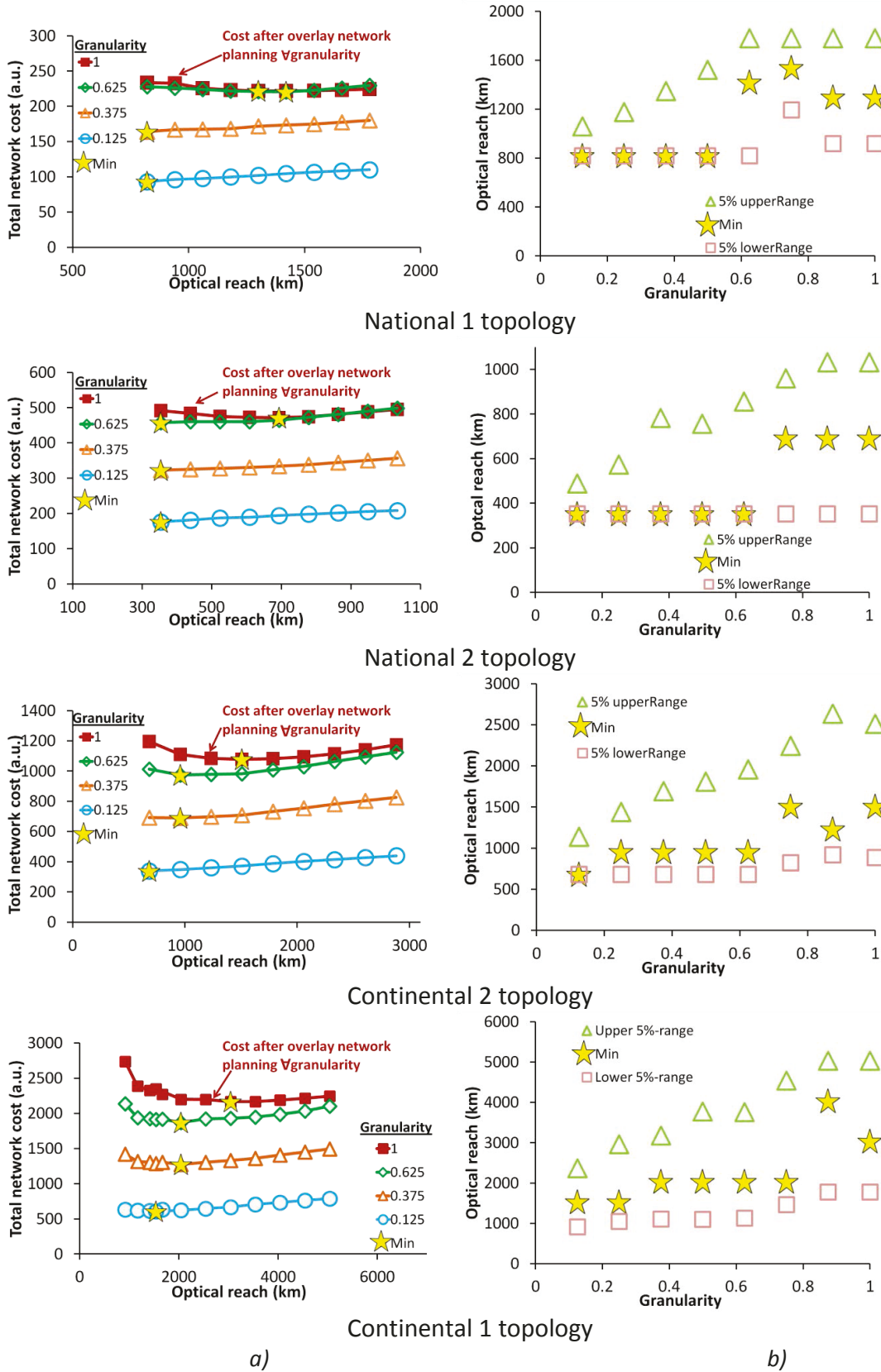


Figure 38: a) Total network cost versus optical reach. b) Optical reach versus traffic granularity: associated 5%-range for the 4 studied topologies, 10 connection matrices, 4 traffic granularities,  $P=50$ .

In the left side graphs we notice that the impact of the optical reach on the total network cost is stronger for some networks. To quantify this observation, the *overcost* is introduced: it is defined as the relative difference between the minimal cost and the cost that has to be paid if the shortest studied reach (which is the longest link of the topology as explained in the beginning of this section V) is chosen. In other terms:

$$\text{overcost} = \frac{\text{cost}(\text{longest link})}{\text{minimal cost}} - 1$$

The higher the overcost is, the more relative gain there is to optimize the optical reach. It is when the overcost is high that the results presented in this chapter have more value. We found that the overcost correlates well with a parameter which is the mean length of the shortest paths in the topology (in km) divided by the longest link of the topology (in km). The value of this parameter for each of the studied topologies is presented in Table 5. In Figure 39, we plot the overcost obtained for homogeneous traffic matrices with a density of 1 and a granularity of 1 as a function of mean shortest path length divided by the longest link. The overcost obtained for this granularity is an upper limit for the overcost for any other granularity. We note that the overcost evolves linearly for P values varying from 0 to 100, for the four topologies and for a density of 1.

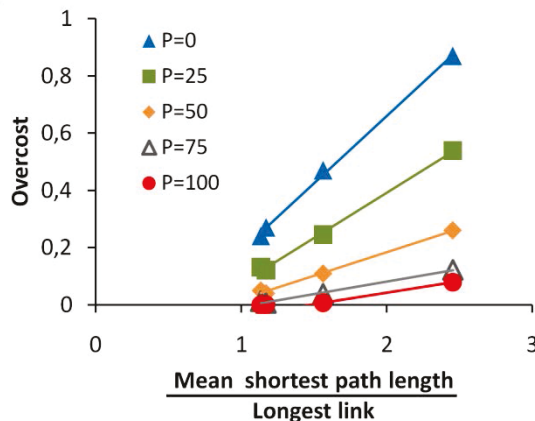


Figure 39: Overcost obtained for traffic matrices with a density of 1, corresponding to the 4 studied topologies and the 5 studied values of P.

The growth of these curves is due to the fact that when the mean shortest path length grows, optical connections are in average longer, more of them are longer than the optical reach (equal to the longest link), and more regenerators are needed to establish the optical connections, resulting in a high overcost.

As we observe in Table 5, the parameter on the abscise grows with the number of nodes in the topology. This means that for networks that will have a greater number of nodes, the overcost will be higher. In these cases, it is important to find the optical reach corresponding to the minimal cost. As we saw in Chapter 1 section I core networks having more and more nodes emerge, so in the future the worst case of the optical reach will be more and more damageable.

Finally, in Figure 38 a), the overcost is shown to decrease as a function of the granularity: for lower optical reaches, as granularity decreases, the total network cost becomes less dependent on the optical reach, because regenerators represent a small proportion of the total network cost.

To understand this, the statistical distribution of the established optical connection is studied in the following. For clarity's sake, Continental 1 topology has been considered in the following as the biggest of the four studied topologies, where optical reach impact on the total network cost is the most acute. Results with other topologies are the same, as demonstrated further in Figure 41.

## 2) Impact of the granularity and the optical reach on the optical connection length

Figure 40 presents the mean optical connection length obtained after network planning with the heuristic. The traffic assumptions are the same that the ones used in section V.B.1) (ten traffic matrices with a density of 0.6 are drawn, for each of them we plan the network for each granularity and each optical reach between longest physical link and the network diameter). Mean optical connection length is observed to grow with the granularity: the mean length value is approximately 1000km for granularity equal to 0.125 and 2200 km for a granularity of 1. This means that when granularity is 1, the majority of optical connections needs one or more regenerators for optical reaches shorter than 2200 km, but their quantity decreases steeply as the optical reach grows. In Figure 38a), for granularity equal to 1, the total network cost curve is very concave because the cost related to the saved regenerators with respect to the reach is higher than the cost increase of optoelectronic device for the chosen value of  $P$  (50). For lower granularities, to minimize the quantity of equipment and to exploit the capacity of deployed resources, the demands are groomed frequently on their paths so as to fill efficiently the optical connections. Therefore most optical connections are shorter than the optical reach and do not need regenerators therefore the total network cost curves are less concave.

In Figure 40, we have also noticed that for granularities lower than 1, mean optical connection length grows with the optical reach. This feature is more pronounced for intermediate granularities (close to 0.5): for a granularity of 0.625, the mean optical connection length varies by 14% between the maximum and the minimum optical reaches.

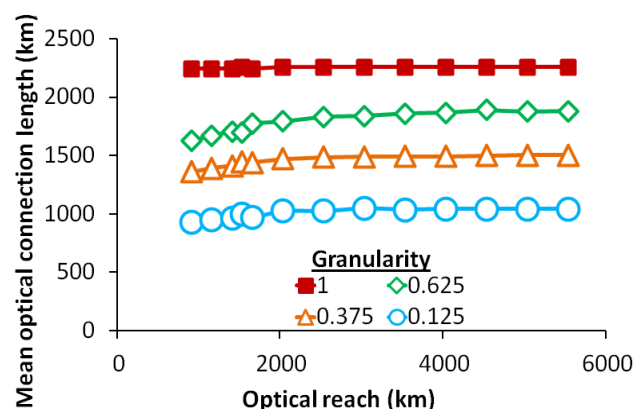


Figure 40: Mean optical connection length obtained for Continental 1 topology, 10 connection matrices, 4 traffic granularities,  $P=50$ .

In Figure 41, we have checked that this behavior is also observed for the other 4 studied topologies, for the granularity value of 0.625. The traffic assumptions are the same that the ones used for tracing Figure 40: for each topology 10 connection matrices with density equal to 0.6 were simulated. The optical reach and the mean optical connection length have been normalized by the diameter of the studied topology (Table

5). We observe that the variation amplitude of the mean optical connection depends on the topology: for National 1 topology, the mean length of optical tunnel varies by 20%, by 14% for Continental 1 and Continental 2 topologies, and only by 9% for National 2 topology. To explain this phenomenon, we analyze, in the next section, the statistical distribution of optical connections with respect to their length.

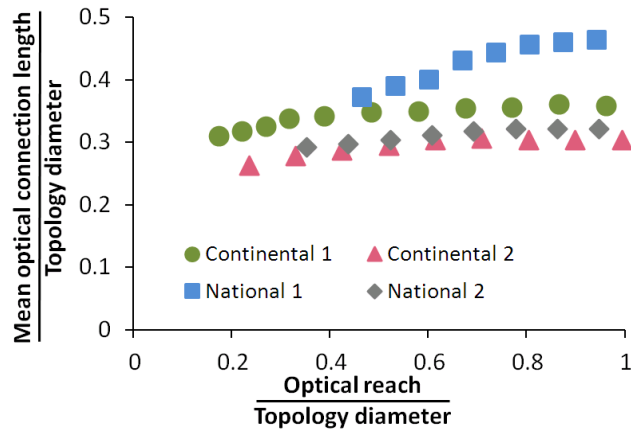


Figure 41: Mean optical connection length obtained for the 4 studied topologies, 10 connection matrices, traffic granularity=0.625,  $P=50$ .

### 3) Impact of the granularity and the optical reach on the distribution of optical connections

Figure 42 shows the distribution of optical connections established during network planning according to their length in kilometers. The traffic assumptions are the same as the ones used for tracing figures from Figure 38 to Figure 41. We have fixed the granularity to 0.625 and optical reach to 2040 km. Figure 42 shows the distribution obtained after network planning with 3 planning methods based on heuristics. The first one is the heuristic proposed in III.A), called *multilayer (ML) w/ physical impairments*, depicted by an empty green line; the second method, represented by a filled green line, is a variant of this heuristic that does not take into account the optical reach limitation (and thus the cost of regeneration) while choosing the optical connections, called *multilayer (ML) w/o physical impairments*; the third method is the overlay planning represented by a dotted red line.

In the insert of Figure 42, we show the distributions of optical connections obtained with ML w/o physical impairments for granularities values equal to 0.125, 0.375, and 1.0.

The distribution of the optical connections established with the overlay method depends neither on the optical reach, nor on the granularity because there is no possibility for regrooming. That is why it corresponds to the distribution of optical connections obtained when the granularity value is 1.0 in the insert of Figure 42. In the overlay method, a pair of transponders is needed for each demand; one regenerator for demands whose path is longer than 2040km and 2 regenerators for the demands whose path is longer than 4080km. This dimensioning method gives for any granularity 488 optical connections and 319 regenerators (as shown in Table 6).

Table 6: Traffic results for granularity=0.625, Continental 1, P=50, optical reach=2040km, averaged over 10 traffic matrices

Granularity	Planning method	Optical connections	Regenerators
0.125	Overlay	488	319
0.125	ML w/o physical impairments	172	20.9
0.125	ML w/ physical impairments	170	15.3
0.375	Overlay	488	319
0.375	ML w/o physical impairments	327	102.9
0.375	ML w/ physical impairments	324.5	88.3
0.625	Overlay	488	319
0.625	ML w/o physical impairments	458.9	229.3
0.625	ML w/ physical impairments	455	178.4

We now examine the number of optical connections and regenerators deployed by ML w/o physical impairments. On Figure 42, as compared to the overlay method, the distribution obtained with ML w/o physical impairments is more concentrated towards the lower lengths and 7% fewer optical connections are required due to the possibility of traffic regrooming (488 optical connections for overlay vs. 459 for the ML w/o physical impairments). The optical connection economy is limited at such a high granularity (0.625), as we see in Table 6, for lower granularities, e.g. 0.125, we can have up to a 65% saving while using ML w/o physical impairments instead of overlay network planning. Indeed 172 optical connections are needed for a granularity of 0.125 (double blue line in the insert) and 327 optical connections for a granularity of 0.375 (double triple orange line in the insert). For a granularity of 1.0 the number of needed connections is, as we explained above, equal to the number of connections obtained by overlay planning.

We also note in Table 6 the number of regenerators deployed by ML w/o physical impairments for each granularity value is lower than that of the overlay method. For example, for a value of 0.625, 229.3 regenerators on average are needed; it is a 39% saving as compared to the overlay planning. This is explained by the distributions of connections in Figure 42. Connections are concentrated toward the lower distances, because when regrooming is done the connections are cut up to allow grooming in intermediate nodes.

We also note that the higher the granularity, the higher the number of regenerators as compared to the number of optical connections. For a granularity of 0.625, regenerators represent up to 42% of the total cost when planning with ML w/o physical impairments. For this granularity saving a proportion of the regenerators will influence most the total network cost. That is why 0.625 granularity value has been chosen to study the gains of ML w/ physical impairments.

Accounting for the optical reach avoids the creation of some of the optical connections longer than the optical reach. That is why in Figure 42 the distribution obtained with ML w/ physical impairments is even more concentrated under the 2040 km length, than ML w/o physical impairments. ML w/ physical impairments establishes sensibly the same number of optical connections as compared to ML w/o physical impairments, but still provides an additional 29% saving in regenerators.

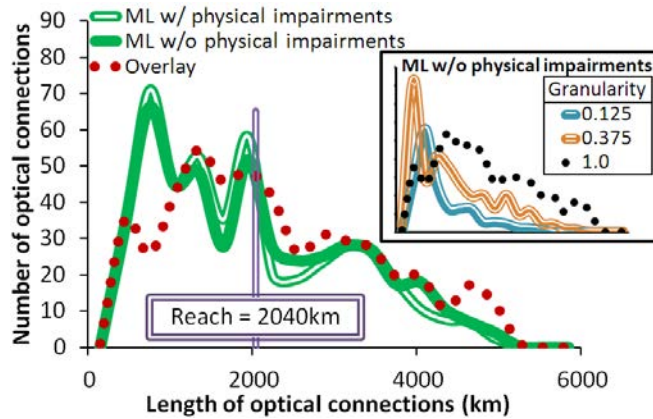


Figure 42: Distribution of the optical connections obtained after network planning of the Continental 1 topology for 10 connection matrices with  $P=50$  and  $\text{granularity}=0.625$

We have seen through the example used above (granularity of 0.625 & Continental 1 topology) that when using ML w/ physical impairments, we can economize regenerators by discouraging the establishment of optical connection longer than the optical reach that would have been established otherwise (as in ML w/o physical impairments). This is possible when there is a non-negligible number of optical connections that would have been established by ML w/o physical impairments that are longer than the reach. This happens for lower optical reaches and high enough granularities (0.625 preferred to 0.125 and 0.375). To avoid the creation of long optical connections, alternative regrooming possibilities are available except for the highest granularities (typically 0.8-1.0), indeed as we saw in Chapter 2 for the highest granularities, the optimal planning is where one optical connection corresponds to each demand, any regrooming is suboptimal. Therefore the economy of regenerators with ML w/ physical impairments occurs for intermediate granularities (around 0.5).

So if we come back to Figure 40 we understand that when using the proposed heuristic (ML w/ physical impairments) the impact of the reach on the mean length of optical connections is more visible for intermediate granularities. This also explains the choice of an intermediate granularity (0.625) for tracing Figure 41, Figure 42 and Figure 43.

The heuristic we use adapts the optical connections to the optical reach in order to minimize the total network cost. Let us now examine these gains in detail.

#### 4) Cost gains of taking into account the optical reach in the planning algorithm

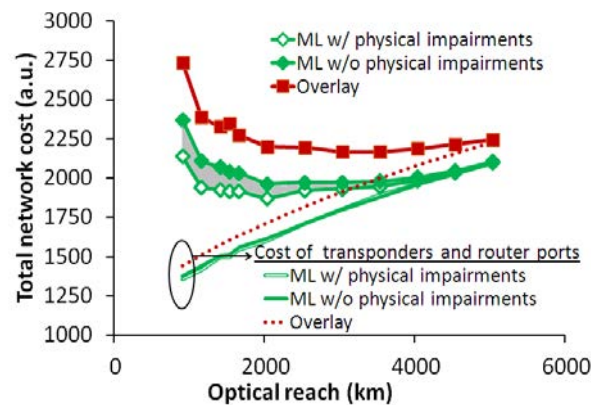


Figure 43: Total network cost as a function of optical reach obtained for 3 planning methods for Continental 1 for 10 connection matrices with  $P=50$  and granularity=0.625

Figure 43 presents the total network cost versus the optical reach obtained with the 3 planning methods previously described. The traffic and network assumptions are the ones used in Figure 42. To explain the cost differences obtained with each planning method, the total network cost and the joint cost of the transponders and router ports (terminal equipment cost) have been studied. The difference between the total network cost and the terminal equipment cost is the cost of the regenerators.

The total network cost obtained by the overlay network planning (red squares) is, as expected, higher than the cost from the two other planning methods. It is due to a greater quantity of terminal equipment (symbolized by the red dotted line) which is, for any reach, 5-7% more than that of the multilayer planning methods (symbolized by the two continuous lines), as well as to a greater number of regenerators (on average 80% more than the ML w/ physical impairments and 38% more than ML w/o physical impairments). As explained previously, it is due to the fact that the overlay planning method cannot regroom traffic demands nor adapt the optical connections to the optical reach.

As to the two multilayer planning methods, the obtained terminal equipment cost is virtually the same (the continuous green lines are almost coincident).

Therefore the difference (the grey zone in Figure 43) in total network cost between ML w/ physical impairments and ML w/o physical impairments comes only from the regenerator costs. The size of this gap depends on the granularity and the optical reach, its maximum is around the required reach. For the required optical reach (1130 km for the considered scenario) ML w/ physical impairments is 8% cheaper than ML w/o physical impairments. These savings are mostly due to a 27% economy in terms of regenerators, the number of router ports and transponders is little influenced by the optical reach. Therefore ML w/ physical impairments may bring substantial gains in the WDM layer and should be used.

Tracing the total network cost with respect to the reach using ML w/ physical impairments, requires planning the network for every possible value of the optical reach which is quite impractical because we want to choose the WDM equipment defining the optical reach before the multilayer planning phase. That is why we present in the following an estimator of the required optical reach with minimal amount of computation.

### 5) Simple estimation of the required optical reach

We have found that even if the total network cost may vary a lot between ML w/ physical impairments and ML w/o physical impairments as shown in V.B.4, the required optical reach found in both cases is very similar. Indeed, in Figure 44 we plot the required optical reach actually obtained using our heuristic versus the traffic granularity, using the same inputs as for Figure 38 b), for the 4 studied topologies (symbolized by filled symbols). We also plot the estimator, which is required optical reach found using ML w/o physical impairments (continuous lines). This is done for  $P=50$  the value used throughout this chapter, as well as for  $P=0$ , a worst-case condition, where the required optical reach varies a lot with the granularity.

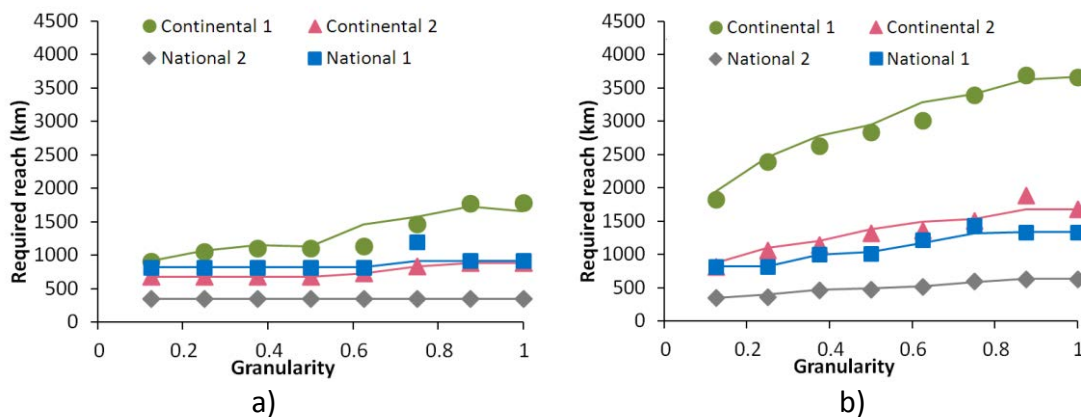


Figure 44: a)  $P=50$  b)  $P=0$ . Optimal optical reach values as a function of the capacity of demands/transponder capacity. Estimation of the optimal optical reach in continuous line obtained for the 4 studied topologies for 10 connection matrices.

We observe that the estimator fits very well the symbols representing the required optical reach. We calculate that for any given topology and for any of the 2 values of  $P$  the L1 distance between the required optical reach and the estimator is on average below 100 km (maximum distance is 300 km).

The advantage of the estimator lies in a relatively easy computation:

- only one multilayer network planning has to be made without taking into account the optical reach constraint (infinite optical reach),
- the obtained optical connections should be classified according to their length,
- to obtain the total network cost for a given optical reach, one pair of transponders is allocated to each optical connection, every optical connection strictly longer than  $Q$  times the optical reach is allocated  $Q$  regenerators,
- the required optical reach obtained with this curve is the estimator of the actual required optical reach obtained through full multilayer network planning.

We have shown using homogeneous traffic matrices the performance of our estimator and the differences in terms of cost between ML w/ physical impairments and ML w/o physical impairments. In the next section, we are validating these results using more realistic and more complex traffic matrices so as to show that these results apply for a wide scope of network planning problems.

### 6) Validation with realistic case study

We consider the Continental 1 topology where all the nodes are to be equipped with 100 Gb/s terminal equipment to route the traffic of four successive traffic forecasts: 4 traffic matrices with a growing total quantity of traffic (called traffic charge) where each bidirectional demand is a multiple of 10 Gb/s. The 10 Gb/s demands were uniformly distributed between the pairs of nodes so as to reach the desired traffic charge. The other inputs were the same as the ones used in Figure 38. The traffic charges are 6.09 Tb/s, 18.27 Tb/s, 30.44 Tb/s, and 48.72 Tb/s. These charges were chosen so as to match the traffic charges corresponding to a homogeneous matrix with a density of 0.6 and granularity values of respectively 0.125, 0.375, 0.625, and 1.0. The obtained total network cost is plotted for different optical reaches provides a concave curve analogous to those we showed Figure 38. On Figure 45, the purple squares correspond to the required optical reach obtained for these curves. The continuous brown line represents the estimation obtained using ML w/o physical impairments.

The mean L2-distance between the required optical reach and the estimator is only 85 km. This confirms that the estimator can be used for realistic traffic matrices before the actual choice of WDM layer equipment and the full multilayer network planning.

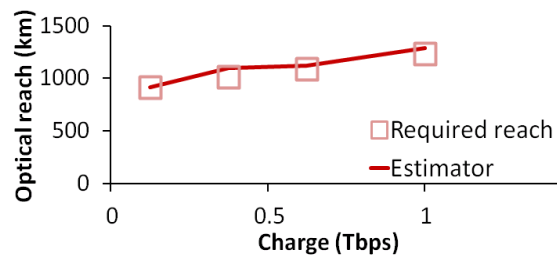


Figure 45: Required optical reach and their estimator obtained for Continental 1 for 4 realistic traffic matrices.  $P=50$

As previously, with homogeneous traffic matrices, the number of optical connections is not influenced by the optical reach, but the number of regenerator is. In Table 7 we note the percentage of regenerators economized at the required optical reach when using of ML w/o physical instead of ML w/o physical impairments. We observe that the proportion of regenerators economized by taking the physical constraints into account is non-negligible. This is all the more interesting knowing that this requires no technological changes, only a modification of the network planning tool.

Table 7: Percentage of regenerators saved by ML w/ physical impairments as compared to ML w/o physical impairments at the required optical reach, for four traffic matrices each with a different charge. Continental 1 topology,  $P=50$ .

Charge (Tb/s)	6.09	18.27	30.44	48.72
% of economized regenerators	15%	19%	17%	13%

In conclusion, both versions of a heuristic are useful. To estimate the required optical reach a version of the heuristic not taking into account physical impairments is sufficient. This allows computing only one virtual topology and then place regenerators by classifying established optical connections according to their reach, thus values of the total network cost with respect to the reach can be easily calculated. Once the required optical reach is determined, a more computationally intensive version of the heuristic, taking into account the physical impairments can be used so as to choose the virtual topology minimizing the number of regenerators while leaving the number of transponders unchanged.

## VI. CONCLUSION

We have used a heuristic algorithm for multilayer planning of IP-over-WDM networks accounting for the cost of equipment in IP and WDM layers, physical topology and optical reach constraint. We assessed the performance of our algorithm by comparing it with two MILP formulations. We have shown that planning a network with a multilayer tool entails an economy of resources as compared to the legacy overlay method (up to 4-5 times total cost reduction for smallest traffic granularities). We have further demonstrated that taking into account the optical reach in the multilayer network planning algorithm can economize up to 30% of regenerators without changing the quantity of terminal equipment.

We have observed that the total network cost presents a minimum for a certain optical reach. We have introduced the parameter called overcost representing the interest of choosing this reach as opposed to aiming for the longest link of the topology. In the cases we studied the overcost could be as high as 90%. Using the overcost, we have shown that is more profitable to optimize the reach for networks having a lot of nodes and high traffic loads.

We noted that the optical reach corresponding to the minimal cost depends strongly on the total traffic capacity. It is also extremely sensitive to small variations in the traffic matrix. The shortest optical reach for which the cost is within 5% of the minimum cost appears to be a far more reliable and predictable required optical reach.

We have shown how the establishment of optical connections and the required reach are dependent on the traffic capacity. Therefore the choice of the optical equipment defining the optical reach should not be finalized before the network planning process so as to avoid unnecessary expenses.

Finally, we have proposed a new method which allows estimating with good precision the value of the required optical reach before multilayer network planning. This estimator requires minimal computation and a forecast of the traffic matrix. This method permits to choose the optical equipment that minimizes the total network cost, before network planning.



---

# Conclusion and Perspectives

## I. CONCLUSION

We have shown that the Routing and Grooming (RG) process is essential to the multilayer network planning. Today the majority of network planning tools are multilayer and we believe the future tools for network planning and administration will be multilayer too. Multilayer RG algorithms have been extensively presented in the literature during the past decade but we found no numerical or theoretical studies that allowed in depth understanding of the RG process. Indeed only empirical results are available in the literature. That is why we have researched a numerical model of the RG mechanism. We found that for each RG routine a “characteristic function” can be obtained.

We have explained how to trace the “characteristic function” for a RG routine. We have shown how characteristic functions can vary with the size of the topology. We have also used it to study the advantages of multilayer planning over overlay and opaque network planning.

The main advantage of the characteristic function is that it enables to extrapolate a precise estimate of the number of optical connections for simple traffic matrices. This has been proven in a large scale simulation campaign on the example of traffic matrices whose demands have capacities following continuous statistical distributions.

The characteristic function also allows visualizing the performance of different RG algorithms. This introduces a common scale on which all algorithms can be evaluated. But it also enables to determine how many transponders can be saved by enhancing the algorithm, and even to suggest the nature of the modifications. This has been demonstrated through the analysis of five multilayer planning routines. This usage of the characteristic function is promising for industrial applications.

And finally our work on the homogeneous traffic matrices has given us a framework where the theoretical limits of network planning and asymptotic behaviors were studied. The numerical model we provided was used as a basis for another team’s work on a theoretical model of multilayer network ([79] and a journal publication under review).

In network planning tools, the results have to comply with certain constraints. The constraints are due to technical limitations of the available devices or to physical limitations. Among all the constraints, the optical reach is a physical constraint whose importance is bound to grow in the coming years. Also we see no way of mitigating it. In the short-term we expect the optical reach of optical systems to decrease, which will increase the number of regenerators. In the same time, the networks are becoming mix line rate or elastic. In these networks the relation between the cost, the capacity and the optical reach is essential during network planning. Understanding this relation is critical to create efficient multilayer planning tools for these networks.

In the second part of the manuscript we have shown how taking into account the optical reach during the RG process allows to save a non negligible part of regenerators. We have also explained in which cases the savings are significant.

When the optical reach is taken into account we have explained how it influences the total network cost. In cases where a choice between different models of configurations of WDM devices is to be made we demonstrated that this choice can significantly impact the network cost. We have determined in which cases the impact is at its highest and for these cases proposed a methodology to simplify the choice.

Finally we have shown and explained why the optical reach impacted the statistical distribution of the lengths of optical connections.

## II. PERSPECTIVES

Even though certain game-changing technologies such as optical packet switching or multicast-to-multicast networks can change completely the network planning paradigm, it seem that today's circuit switched network still have a future.

The gains of multilayer network planning are sufficiently to keep it the main paradigm. When optical networks become dynamic it will be necessary to allocate transport capacity fast, while processing information from two (or more) layers. This will be very challenging. It will require finding a balance between efficiency and computation time. In this sense the characteristic function can be used to compare these faster and more primitive heuristics.

The characteristic function has shown very interesting potential, but we have studied it in the case of a simple node architecture. It can be extended to more complex node architectures such as the node architecture with muxponders where the ratio between router port capacity and transponder capacity as well as ratio between their costs would be two additional parameters. With the increasing processing power of the machines, we expect even more parameters to be included into the planning process.

But the most important study is the one that could use the results of the two parts of this manuscript and study network planning for mixed line rate and elastic networks. In these cases the number of parameters that the network planning algorithms have to consider explodes and the overall complexity of the problem is multiplied. It is therefore much more difficult to create a good planning algorithm and evaluate intuitively its efficiency. That is why we believe that the extensions of the characteristic function to these cases would be most fruitful.

# Appendixes

## I. APPENDIX 1: MILP FORMULATION

Here we present the MILP formulations called One-Shortest-Path MILP (1SP-MILP) and any-Shortest-Path MILP (anySP-MILP). They are two formulations of the RG problem capable to take into account the optical reach and the cost of the regeneration. AnySP-MILP can route and groom client traffic demands in any node of the topology, whereas 1SP-MILP is constrained to route and groom demands only in nodes belonging to the shortest path of the client traffic demand.

These MILP formulations are based on the Connectivity Graph (CG) [33]. Given a physical graph of the network  $G(N,A)$ , where  $N$  is the set of nodes and  $A$  the set of undirected physical links, the CG is  $G'(N,A')$ :  $A'$  is the set of logical links connecting two nodes  $(i,j) \in N$  such as the shortest path on  $G(N,A)$  between nodes  $i$  and  $j$  is shorter than the optical reach. Thus, if a logical link exists between two nodes  $i$  and  $j$ , it means that they can be connected without any regeneration.

Data:

$G(N,A)$  : physical graph of the network

$G'(N,A')$  : connectivity graph

$R$  : set of client traffic demands

$s_r$  : source node of a client traffic demand  $r \in R$

$t_r$  : destination node of a client traffic demand  $r \in R$

$d_r$  : capacity in Gb/s of a client traffic demand  $r \in R$

$N_r$  : subset of nodes at which regrooming is allowed for each client traffic demand  $r \in R$

$H_p$  : set of physical links crossed by the shortest physical route  $p$  associated to the logical link  $(i,j) \in A'$

$B$  : data-rate of each router port

$S$  : data-rate of each transponder

$C$  : cost of a single bidirectional transponder

$L$  : cost of a single bidirectional router port

$\alpha$  : ratio between regenerator cost and transponder cost

Variables:

$J_{ijr}$  : IP traffic flow in Gb/s between node pair  $(i,j)$  for a given demand  $r \in R$ , real  $\geq 0$

$X_{ij}$  : number of optical connections set up between node pair  $(i,j)$ , integer  $\geq 0$

$Y_{ijmn}$  : number of optical connections between node pair  $(i,j)$  routed on the logical link  $(m,n) \in A'$ , integer  $\geq 0$

$R_n$ : number of bidirectional regenerators at node  $n \in N$ , integer  $\geq 0$

$U_n$ : number of bidirectional router ports at node  $n \in N$ , integer  $\geq 0$

$T_n$ : number of bidirectional transponders at node  $n \in N$ , integer  $\geq 0$

## A. Objective function

The formulation minimizes the total network cost while routing all client traffic demands. The total network cost is:

$$\alpha \sum_n R_n C + \sum_n T_n C + \sum_n U_n L \quad (1)$$

## B. Constraints

-Solenoidality of IP flow:

a) For 1SP-MILP. For each demand  $r$ , we apply the constraint only to  $i \in N_r$ , then the index of summation is restricted to  $j \in N_r$ .

$$\sum_{j \in N_r} J_{ijr} - \sum_{j \in N_r} J_{jir} = \begin{cases} d_r & \text{if } i = s_r \\ -d_r & \text{if } i = t_r \\ 0 & \text{otherwise} \end{cases} \quad (2a)$$

$$\forall r \in R, i \in N_r$$

b) For anySP-MILP.

$$\sum_j J_{ijr} - \sum_j J_{jir} = \begin{cases} d_r & \text{if } i = s_r \\ -d_r & \text{if } i = t_r \\ 0 & \text{otherwise} \end{cases} \quad (2b)$$

$$\forall r \in R, i \in N$$

-Traffic Grooming:

$$S \cdot X_{ij} \geq \sum_r J_{ijr} \quad \forall i, j \in N \quad (3)$$

-Solenoidality of CG flows:

$$\sum_{n|(m,n) \in A'} Y_{ijmn} - \sum_{n|(n,m) \in A'} Y_{ijnm} = \begin{cases} X_{ij} & \text{if } m = i \\ -X_{ij} & \text{if } m = j \\ 0 & \text{otherwise} \end{cases} \quad (4)$$

$$\forall i, j, n \in N$$

-Regeneration:

$$\sum_{i,j} \left[ \sum_{m \in N \setminus \{(m,n) \in A' \wedge n \neq j\}} Y_{ijmn} \right] = R_n \quad \forall n \in N \quad (5)$$

-Number of router ports per node

$$\sum_r \sum_j J_{ijr} / B \leq U_i \quad \forall i \in N \quad (6)$$

-Number of transponders per node

$$T_i = \sum_j X_{ij} \quad \forall i \in N \quad (7)$$

The objective function minimizes the total cost of the network by accounting for transponders, router ports and regenerators and their cost (Equation 1). The solenoidality constraint (Equation 2) guarantees the spatial continuity of the IP flow ensuring that each client traffic demand is satisfied. The total input IP flow minus the total output IP flow must be zero in transit nodes and equals to the total offered traffic with appropriate sign in the source and destination nodes. In the case of 1SP-MILP, the transit nodes belong to the shortest path connecting the source and destination nodes (i.e.  $N_r$ ). Equation 3 enables grooming at IP layer: the total electronic traffic between two IP routers ( $i, j$ ) must be accommodated in one or more optical connections each having a maximum capacity  $S$ . Such optical connections have to be routed on the physical layer while accounting for physical impairments (i.e., maximum transparent optical reach). Since we do not address capacity constraints and wavelength contention, we can route each optical connection  $X_{ij}$  by only enforcing the solenoidality constraint on the CG related to a given maximum transparent optical reach (Equation 4). In this case, at each intermediate node on the CG, a regenerator has to be placed (Equation 5). Equation 6 counts the number of used router ports as the overall IP traffic flow divided by the port data-rate. Finally, the number of transponders per node is given by the total amount of optical connections set up over that node (Equation 7).

## II. APPENDIX 2: HEURISTIC FORMULATION

Here we present the heuristic we have developed and that served as a starting point for most of our work. The first versions of this algorithm have been implemented by Pierre Peloso, Magalie Prunaire and Martin Vigoureux of the Alcatel-Lucent Bell Labs.

Here we present the three consecutive versions of the algorithm denoted V1, V2, and V3. If not mentioned otherwise the heuristic refers to V3 of the algorithm. In V3 the value  $K$  is set to 30, value above which no enhancement of performances was observed. (The difference between the 3 versions appears during the choice of candidate connections.) The gradual enhancement of this heuristic is presented in Chapter 2 of the manuscript.

To each client traffic demand, we associate the shortest path in terms of distance (based on Dijkstra algorithm). Regrooming can occur only in nodes belonging to the shortest path connecting the source and destination nodes of the demand.

We define a candidate optical connection as a potential connection in the optical layer linking two nodes. The candidate optical connections taken into consideration by the heuristic are: the shortest paths associated to every pair of nodes exchanging client traffic demands and all their possible partition sets. A shortest path's partition is the finite sequence of consecutive links composing it. A partition set considers all the possible partitions related to the considered path. A representation of the partition set of the path between  $i$  and  $k$  is presented in Figure 35. We suppose that in the studied topology the shortest path between  $i$  and  $k$ , in terms of distance, is the path passing through the nodes  $j$  and  $l$ . Therefore the candidate optical connections corresponding to the client traffic demand between the nodes  $i$  and  $k$  are the connections represented by the 6 black arrows.

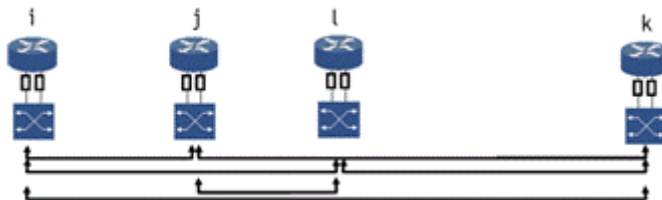


Figure 46: Example of candidate optical connections corresponding to a traffic demand between  $i$  and  $k$  in an IP-over-WDM network.

Then we compute the amount of total client traffic that is transported in each candidate connection and the cost associated to it. The cost of a candidate connection is calculated from the number of router ports, transponders and regenerators needed to set it up, multiplied by their individual costs. We define as “reference cost” of a candidate connection, the cost required to transport the same traffic in an opaque way, i.e. regrooming is performed at every intermediate node. Then we define the relative gain of a candidate optical connection as the difference between its cost and its reference cost, normalized by its reference cost.

In version V1: the gain is calculated simultaneously for all the candidate connections having same source and destination

In versions V2 and V3: the gain is calculated separately for the candidate connections having same source and destination.

All the candidate connections are then sorted according to their relative gain following a decreasing order.

In versions V1 and V2: the candidate connection having the highest gain is accepted.

In version V3: the first K candidates with the highest relative gain are selected. To each of these candidate connections, we associate an “estimated total network cost”. (Such estimation is obtained by firstly selecting one candidate connection and then sequentially choosing the candidate connections having the highest relative gain. The cost corresponding to this set of optical connections is the *estimated total network cost* relative to the selected candidate connection.) The chosen candidate connection is the one providing the lowest estimated cost.

Once a candidate connection is chosen, it is removed from the list of candidate connections with the associated served traffic. Then the set of candidate connections and their relative gains are recalculated considering the remaining traffic, and the procedure iterates until no traffic remains.

The total network cost is obtained by considering the resources required to set-up all the chosen optical connections and their cost.

### III. APPENDIX 3 : IMPACT OF THE DENSITY

As we have noted in Chapter 2 section IV.C.2), a lower density of the traffic matrix leads to lower computation times. In our work we conduct large simulation campaigns for topologies having tens of nodes, so we want to decrease the computation time as much as possible. But we cannot use very small densities. Indeed in Chapter 2 section V.C.2), we also note that the lower the density, the higher the standard deviation of the network cost obtained for different traffic matrices. Thus a value of density corresponds to a compromise between computation time and standard deviation of the obtained data points.

In our work we want to fix a value of density that we can use in our simulations with our heuristic (cf. Appendix 2) and the four topologies (National 1, National 2, Continental 1 and Continental 2).

For this purpose we study our heuristic in twenty situations: four topologies and for five values of density. In each of the twenty situations we examine eight values for the traffic granularity and nine values of the optical reach. In each situation we have therefore seventy two study cases. In each study case we generate ten connection matrices and carry out the network planning for each of them. The ten obtained network costs are averaged and the standard deviation is also calculated. The averaged standard deviation for each situation is shown in Figure 47b. In Figure 47a we plot the calculation time needed to carry out one network planning.

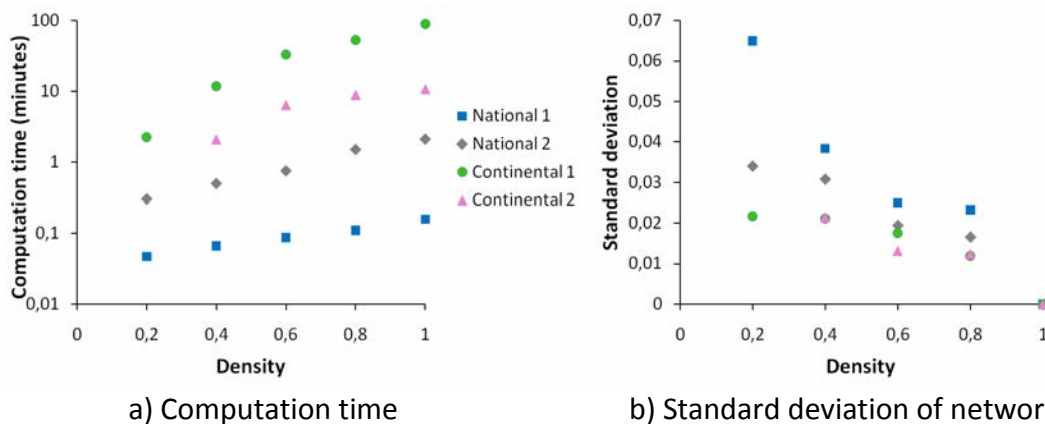


Figure 47: Standard deviation and computation time for our heuristic for the four studied topologies and five values of density

Computation time is represented in log scale. We observe that it increases almost exponentially with density reaching approximately 100 minutes per data point for Continental 1 topology and a density of 1. Standard deviation is, as expected a decreasing function of density, but we note that the curve presents plateaus. When density is equal to 1, standard deviation is equal to zero, indeed for this value of density there is only one connection matrix possible, therefore there is no variation of network cost from one network planning to the other.

As we see in Figure 47 a and b, the compromise between computation time and standard deviation will be a compromise between the computation time for Continental 1 topology and the standard deviation for National 1 topology. We cannot accept calculation times of 100 minutes per data point, therefore density=1 is out of the question but a density of 0.8 offers a low standard deviation (0.022) for National 1

topology, and as we gain computation time and do not increase much the standard deviation by choosing a density of 0.6, that is the value we fix for our studies.

When density is set to the value chosen above (0.6), the standard deviation of the required optical reach is under 6% of the average required optical reach. This density corresponds therefore to an acceptable standard deviation of the required optical reach.

We emphasize that the value of 0.6 corresponds to a compromise specific to our heuristic and studied topologies and has value only for studies based on our heuristic.

## Bibliography

- [1] P. Winzer, "Challenges and evolution of optical transport networks," in *Optical Communication (ECOC), 2010 36th European Conference and Exhibition on*, September 2010, pp. 1–3.
- [2] P. Leisching and M. Pickavet, "Energy footprint of ICT: Forecasts and network solutions," in *OFC/NFOEC'09, Workshop on Energy Footprint of ICT: Forecast and Network Solutions*, San Diego, CA, March 2009.
- [3] W. Vereecken, W. Van Heddeghem, B. Puype, D. Colle, M. Pickavet, and P. Demeester, "Optical networks: How much power do they consume and how can we optimize this?" in *European Conference and Exhibition on Optical Communication (ECOC)*, September 2010, pp. 1–4.
- [4] E. Bonetto, L. Chiaraviglio, F. Idzikowski, and E. Le Rouzic, "Algorithms for the multi-period power-aware logical topology design with reconfiguration costs," *Optical Communications and Networking, IEEE/OSA Journal of*, vol. 5, no. 5, pp. 394–410, May 2013.
- [5] E. Bertin, N. Crespi, and M. L'Hostis, "A few myths about telco and OTT models," in *Intelligence in Next Generation Networks (ICIN), 2011 15th International Conference on*, October 2011, pp. 6–10.
- [6] P. Winzer, "Energy-efficient optical transport capacity scaling through spatial multiplexing," *Photonics Technology Letters, IEEE*, vol. 23, no. 13, pp. 851–853, July 2011.
- [7] S. K. Korotky, "Traffic trends: Drivers and measures of cost-effective and energy-efficient technologies and architectures for backbone optical networks," in *Optical Fiber Communication Conference*. Optical Society of America (OSA), 2012, p. OM2G.1.
- [8] S. Woodward, W. Zhang, B. Bathula, G. Choudhury, R. Sinha, M. Feuer, J. Strand, and A. Chiu, "Asymmetric optical connections for improved network efficiency," *Optical Communications and Networking, IEEE/OSA Journal of*, vol. 5, no. 11, pp. 1195–1201, November 2013.
- [9] D. M. Marom, D. Neilson, D. Greywall, C.-S. Pai, N. Basavanhally, V. Aksyuk, D. Lopez, F. Pardo, M.-E. Simon, Y. Low, P. Kolodner, and C. Bolle, "Wavelength-selective 1xK switches using free-space optics and MEMS micromirrors: theory, design, and implementation," *Lightwave Technology, Journal of*, vol. 23, no. 4, pp. 1620–1630, April 2005.
- [10] S. Mechels, L. Muller, G. Morley, and D. Tillett, "1D MEMS-based wavelength switching subsystem," *Communications Magazine, IEEE*, vol. 41, no. 3, pp. 88–94, March 2003.
- [11] B. Rajagopalan, J. Luciani, and D. Awduche, "IP over optical networks: a framework," IETF RFC 3717, 2004.
- [12] S. Bodamer, J. Spath, and C. Glingener, "An efficient method to estimate transponder count in multi-layer transport networks," in *Global Telecommunications Conference (GLOBECOM)*. IEEE, vol. 3, 2004, pp. 1780–1785.
- [13] M. Fukutoku, T. Ohara, A. Kadohata, A. Hirano, T. Kawai, T. Komukai, M. Suzuki, S. Aisawa, T. Takahashi, M. Tomizawa, O. Ishida, and S. Matsuoka, "Optimized multi-layer optical network using in-service ODU/wavelength path re-grooming," in *Optical Fiber*

*Communication Conference and Exposition (OFC/NFOEC), 2011 and the National Fiber Optic Engineers Conference*, March 2011, pp. 1–3.

[14] S. Yang and F. Kuipers, “Energy-aware path selection for scheduled lightpaths in IP-over-WDM networks,” in *Symposium on Communications and Vehicular Technology in the Benelux (SCVT)*, IEEE, November 2011, pp. 1–6.

[15] N. Sengezer and E. Karasan, “Multi-layer virtual topology design in optical networks under physical layer impairments and multi-hour traffic demand,” *Journal of Optical Communications and Networking, IEEE/OSA*, vol. 4, no. 2, pp. 78–91, February 2012.

[16] J. Baliga, R. Ayre, K. Hinton, W. Sorin, and R. Tucker, “Energy consumption in optical IP networks,” *Lightwave Technology, Journal of*, vol. 27, no. 13, pp. 2391–2403, July 2009.

[17] G. J. Eilenberger, S. Bunse, L. Dembeck, U. Gebhard, F. Ilchmann, W. Lautenschlaeger, and J. Milbrandt, “Energy-efficient transport for the future internet,” *Bell Labs Technical Journal*, vol. 15, no. 2, pp. 147–167, September 2010.

[18] D. Kilper, G. Atkinson, S. Korotky, S. Goyal, P. Vetter, D. Suvakovic, and O. Blume, “Power trends in communication networks,” *Selected Topics in Quantum Electronics, IEEE Journal of*, vol. 17, no. 2, pp. 275–284, March 2011.

[19] E. Palkopoulou, D. Schupke, and T. Bauschert, “Energy efficiency and CAPEX minimization for backbone network planning: Is there a tradeoff?” in *International Symposium on Advanced Networks and Telecommunication Systems (ANTS)*, IEEE, December 2009, pp. 1–3.

[20] R. Huelsermann, M. Gunkel, C. Meusburger, and D. A. Schupke, “Cost modeling and evaluation of capital expenditures in optical multilayer networks,” *Journal of Optical Networking*, vol. 7, no. 9, pp. 814–833, September 2008.

[21] “Juniper T640 core router PIC guide.” [Online]. Available: <http://www.juniper.net>

[22] F. Rambach, B. Konrad, L. Dembeck, U. Gebhard, M. Gunkel, M. Quagliotti, L. Serra, and V. López, “A multilayer cost model for metro/core networks,” *Journal of Optical Communications and Networking, IEEE/OSA*, vol. 5, no. 3, pp. 210–225, March 2013.

[23] G. Rizzelli, A. Morea, M. Tornatore, and O. Rival, “Energy efficient traffic-aware design of on-off multi-layer translucent optical networks,” *Computer Networks*, vol. 56, no. 10, pp. 2443–2455, 2012, green communication networks.

[24] *ITU-T recommendation G.694.1*, ITU-T Std., Rev. (02/12). [Online]. Available: <http://www.itu.int/rec/T-REC-G.694.1>

[25] M. Sivakumar and K. Sivalingam, “Limited grooming architectures and groomer-port placement in optical WDM mesh networks,” in *Broadband Communications, Networks and Systems, 2006. BROADNETS 2006. 3rd International Conference on*, October 2006, pp. 1–10.

[26] G. P. Agrawal, *Nonlinear Fiber Optics*, (4th edition), Ed. Academic Press, San Diego, USA, 2006.

[27] A. Morea, N. Brogard, F. Leplingard, J.-C. Antona, T. Zami, B. Lavigne, and D. Bayart, “QoT function and A routing: an optimized combination for connection search in translucent networks,” *Journal of Optical Networking*, vol. 7, no. 1, pp. 42–61, January 2008.

[28] W. Zhang, J. Tang, K. Nygard, and C. Wang, “REPARE: Regenerator placement and routing establishment in translucent networks,” in *Global Telecommunications Conference (GLOBECOM)*, IEEE, December 2009, pp. 1–7.

- [29] X. Dong, T. El-Gorashi, and J. Elmirghani, "Green IP over WDM networks with data centers," *Journal of Lightwave Technology*, vol. 29, no. 12, pp. 1861–1880, June 2011.
- [30] C. Lee and J.-K. Rhee, "Traffic grooming for IP-over-WDM networks: Energy and delay perspectives," *Optical Communications and Networking, IEEE/OSA Journal of*, vol. 6, no. 2, pp. 96–103, February 2014.
- [31] E. W. Dijkstra, "A note on two problems in connexion with graphs," *Numerische Mathematik*, vol. 1, pp. 269–271, 1959.
- [32] O. Gerstel, R. Ramaswami, and G. Sasaki, "Cost effective traffic grooming in WDM rings," in *INFOCOM '98. Seventeenth Annual Joint Conference of the IEEE Computer and Communications Societies. Proceedings. IEEE*, vol. 1, March 1998, pp. 69–77 vol.1.
- [33] G. Rizzelli, F. Musumeci, M. Tornatore, G. Maier, and A. Pattavina, "Wavelength-aware translucent network design," in *Optical Fiber Communication Conference and Exposition and the National Fiber Optic Engineers Conference (OFC/NFOEC)*, March 2011, pp. 1–3.
- [34] J. Strand, A. Chiu, and R. Tkach, "Issues for routing in the optical layer," *Communications Magazine, IEEE*, vol. 39, no. 2, pp. 81–87, February 2001.
- [35] A. Morea, H. Nakajima, L. Chacon, E. Le Rouzic, B. Decocq, and J.-P. Sebillie, "Impact of the reach of WDM systems and traffic volume on the network resources and cost of translucent optical transport networks," in *International Conference on Transparent Optical Networks*, vol. 1, July 2004, pp. 65–68.
- [36] A. Morea and J. Poirrier, "A critical analysis of the possible cost savings of translucent networks," in *International Workshop on the Design of Reliable Communication Networks (DRCN), IEEE*, October 2005, p. 7.
- [37] J. Simmons, "On determining the optimal optical reach for a long-haul network," *Journal of Optical Networking, IEEE*, vol. 23, no. 3, pp. 1039–1048, March 2005.
- [38] —, "Network design in realistic "all-optical" backbone networks," *Communications Magazine, IEEE*, vol. 44, no. 11, pp. 88–94, November 2006.
- [39] M. Tornatore, G. Maier, and A. Pattavina, "WDM network optimization by ILP based on source formulation," in *Annual Joint Conference of the IEEE Computer and Communications Societies (INFOCOM). IEEE*, vol. 3, June 2002, pp. 1813–1821.
- [40] A. Chiu and E. Modiano, "Traffic grooming algorithms for reducing electronic multiplexing costs in WDM ring networks," *Lightwave Technology, Journal of*, vol. 18, no. 1, pp. 2–12, January 2000.
- [41] K. Zhu and B. Mukherjee, "Traffic grooming in an optical WDM mesh network," in *Communications, 2001. ICC 2001. IEEE International Conference on*, vol. 3, 2001, pp. 721–725 vol.3.
- [42] S. Huang, R. Dutta, and G. Rouskas, "Traffic grooming in path, star, and tree networks: complexity, bounds, and algorithms," *Selected Areas in Communications, IEEE Journal on*, vol. 24, no. 4, pp. –82, 2006.
- [43] J. Wang, W. Cho, V. Rao Vemuri, and B. Mukherjee, "Improved approaches for cost-effective traffic grooming in WDM ring networks: ILP formulations and single-hop and multihop connections," *Lightwave Technology, Journal of*, vol. 19, no. 11, pp. 1645–1653, November 2001.
- [44] C. Xin, B. Wang, X. Cao, and J. Li, "A heuristic logical topology design algorithm for multi-hop dynamic traffic grooming in WDM optical networks," in *Global Telecommunications Conference, 2005. GLOBECOM '05. IEEE*, vol. 4, December 2005.
- [45] S. AjayKumar and S. Ghosh, "Traffic grooming in optical WDM mesh networks," in *Industrial and Information Systems, 2008. ICIIS 2008. IEEE Region 10 and the Third international Conference on*, December 2008, pp. 1–6.

- [46] I. Katib and D. Medhi, "Optimizing node capacity in multilayer networks," *Communications Letters, IEEE*, vol. 15, no. 5, pp. 581–583, May 2011.
- [47] A. Patel, P. Ji, J. Jue, and T. Wang, "Traffic grooming in flexible optical WDM (FWDM) networks," in *OptoElectronics and Communications Conference (OECC)*, July 2011, pp. 405–406.
- [48] M. Ruiz, O. Pedrola, L. Velasco, D. Careglio, J. Fernandez-Palacios, and G. Junyent, "Survivable IP/MPLS-Over-WSN multilayer network optimization," *Journal of Optical Communications and Networking, IEEE/OSA*, vol. 3, no. 8, pp. 629–640, August 2011.
- [49] S. Zhang, D. Shen, and C.-K. Chan, "Energy efficient time-aware traffic grooming in wavelength routing networks," in *Global Telecommunications Conference (GLOBECOM 2010)*, 2010 IEEE, December 2010, pp. 1–5.
- [50] G. Rizzelli, A. Morea, and M. Tornatore, "An analysis of daily power consumption under different on-off IP-over-WDM translucent design approaches," in *Optical Fiber Communication Conference and Exposition and the National Fiber Optic Engineers Conference (OFC/NFOEC), 2013*, March 2013, pp. 1–3.
- [51] A. Ahmad, A. Bianco, E. Bonetto, L. Chiaraviglio, and F. Idzikowski, "Energy-aware design of multilayer core networks," *Optical Communications and Networking, IEEE/OSA Journal of*, vol. 5, no. 10, pp. A127–A143, October 2013.
- [52] M. Xia, M. Tornatore, Y. Zhang, P. Chowdhury, C. Martel, and B. Mukherjee, "Greening the optical backbone network: A traffic engineering approach," in *International Conference on Communications (ICC)*, IEEE, May 2010, pp. 1–5.
- [53] S. Subramani and K. Sivalingam, "Reservation based wavelength assignment for sparse groomed optical WDM mesh networks," in *International Conference on Broadband Networks. BroadNets 2005*, vol. 1, October 2005, pp. 175–183.
- [54] J. Zhao, S. Subramaniam, M. Brandt-Pearce, and null, "QoT-aware grooming, routing, and wavelength assignment (GRWA) for Mixed-Line-Rate translucent optical networks," in *Communications in China (ICCC), 2012 1st IEEE International Conference on*, August 2012, pp. 270–275.
- [55] P. Chowdhury, M. Tornatore, A. Nag, E. Ip, T. Wang, and B. Mukherjee, "On the design of energy-efficient mixed-line-rate (MLR) optical networks," *Lightwave Technology, Journal of*, vol. 30, no. 1, pp. 130–139, January 2012.
- [56] K. Christodoulopoulos, K. Manousakis, and E. Varvarigos, "Reach adapting algorithms for mixed line rate WDM transport networks," *Lightwave Technology, Journal of*, vol. 29, no. 21, pp. 3350–3363, November 2011.
- [57] S. Korotky, "Network global expectation model: a statistical formalism for quickly quantifying network needs and costs," *Lightwave Technology, Journal of*, vol. 22, no. 3, pp. 703–722, March 2004.
- [58] A. Patel, C. Gao, J. Jue, X. Wang, Q. Zhang, P. Palacharla, and T. Naito, "Traffic grooming and regenerator placement in impairment-aware optical WDM networks," in *Conference on Optical Network Design and Modeling (ONDM)*, February 2010, pp. 1–6.
- [59] E. Yetginer and G. Rouskas, "Power efficient traffic grooming in optical WDM networks," in *Global Telecommunications Conference (GLOBECOM)*. IEEE, December 2009, pp. 1–6.
- [60] G. Shen and R. Tucker, "Sparse traffic grooming in translucent optical networks," *Journal of Optical Networking*, vol. 27, no. 20, pp. 4471–4479, October 2009.
- [61] M. Z. Feng, K. Hinton, R. Ayre, and R. S. Tucker, "Reducing NGN energy consumption with IP/SDH/WDM," in *International Conference on Energy-Efficient Computing and Networking*, ser. e-Energy '10. ACM, 2010, pp. 187–190.

[62] M. Bertolini, O. Rocher, A. Bisson, P. Pecci, and G. Bellotti, "Benefits of OTN switching introduction in 100Gb/s optical transport networks," in *In proceedings of National Fiber Optic Engineers Conference(NFOEC)*. Optical Society of America, 2012, p. NM2F.2.

[63] K.-i. Sato and H. Hasegawa, "Optical networking technologies that will create future bandwidth-abundant networks [invited]," *Journal of Optical Communications and Networking, IEEE/OSA*, vol. 1, no. 2, pp. A81 –A93, July 2009.

[64] I. Yagyu, H. Hasegawa, and K.-i. Sato, "An efficient hierarchical optical path network design algorithm based on a traffic demand expression in a cartesian product space," in *European Conference on Optical Communications (ECOC)*, September 2006, pp. 1 –2.

[65] S. Thiagarajan, M. Frankel, and D. Boertjes, "Spectrum efficient super-channels in dynamic flexible grid networks - a blocking analysis," in *Optical Fiber Communication Conference and Exposition and the National Fiber Optic Engineers Conference (OFC/NFOEC)*, March 2011, pp. 1 –3.

[66] T. Zami, "What is the benefit of elastic superchannel for WDM network?" in *Optical Communication (ECOC 2013), 39th European Conference and Exhibition on*, September 2013, pp. 1–3.

[67] —, "Co-optimizing allocation of Nyquist superchannels and physical impairments aware placement of regenerators in elastic WDM networks," *Lightwave Technology, Journal of*, vol. PP, no. 99, pp. 1–1, 2014.

[68] R. Gemelli, A. Paparella, G. Bellotti, and G. Parladori, "Reducing emissions of core networks: A comparative analysis," in *Conference on Optical Network Design and Modeling (ONDM)*, February 2010, pp. 1 –6.

[69] Q. Zhang, Q. She, X. Wang, P. Palacharla, and M. Sekiya, "Traffic grooming in metro networks with mixed line rates," in *OptoElectronics and Communications Conference (OECC)*, July 2011, pp. 407 –408.

[70] Y. Zhang, P. Chowdhury, M. Tornatore, and B. Mukherjee, "Energy efficiency in telecom optical networks," *Communications Surveys Tutorials, IEEE*, vol. 12, no. 4, pp. 441 –458, 2010.

[71] F. Idzikowski, S. Orłowski, C. Raack, H. Woesner, and A. Wolisz, "Saving energy in IP-over-WDM networks by switching off line cards in low-demand scenarios," in *Conference on Optical Network Design and Modeling (ONDM)*, February 2010, pp. 1 –6.

[72] M. Z. Feng, K. Hinton, R. Ayre, and R. S. Tucker, "Energy consumption in intelligent optical networks," *Networks*, pp. 978–981, 2010.

[73] B. Puype, W. Vereecken, D. Colle, M. Pickavet, and P. Demeester, "Power reduction techniques in multilayer traffic engineering," in *International Conference on Transparent Optical Networks. ICTON '09.*, July 2009, pp. 1 –4.

[74] S. Huang and R. Dutta, "Dynamic traffic grooming: the changing role of traffic grooming," *Communications Surveys Tutorials, IEEE*, vol. 9, no. 1, pp. 32 –50, 2007.

[75] Y. Lui, G. Shen, and W. Shao, "Design for energy-efficient IP over WDM networks with joint lightpath bypass and router-card sleeping strategies," *Optical Communications and Networking, IEEE/OSA Journal of*, vol. 5, no. 11, pp. 1122–1138, November 2013.

[76] A. Chiu, G. Choudhury, M. Feuer, J. Strand, and S. Woodward, "Integrated restoration for next-generation IP-over-optical networks," *Journal of Lightwave Technology*, vol. 29, no. 6, pp. 916 –924, March 2011.

[77] I. de Miguel, R. Duran, T. Jimenez, N. Fernandez, J. Aguado, R. Lorenzo, A. Caballero, I. Tafur Monroy, Y. Ye, A. Tymecki, I. Tomkos, M. Angelou, D. Klondis, A. Francescon, D. Siracusa, and E. Salvadori, "Cognitive dynamic optical networks

[invited],” *Optical Communications and Networking, IEEE/OSA Journal of*, vol. 5, no. 10, pp. A107–A118, October 2013.

[78] IBM ILOG CPLEX 12.1. [Online]. Available: <http://www-01.ibm.com/software/integration/optimization/cplex/>.

[79] S. Korotky, J. Simsarian, and G. Atkinson, “Network global expectation model of optimized routing and grooming in multi-layer service transport (to be published),” in *Optical Communication (ECOC 2014), 40th European Conference and Exhibition on*, September 2014.

[80] G. Rizzelli, A. Morea, C. Dorize, O. Rival, and M. Tornatore, “On the energy impact of transmission reach for 100G IP-over-WDM translucent optical networks,” in *Optical Communications (ECOC), 2012 38th European Conference and Exhibition on*, September 2012, pp. 1–3.

[81] G. Rizzelli, A. Morea, M. Tornatore, and A. Pattavina, “Reach-related energy consumption in IP-over-WDM 100G translucent networks,” *Lightwave Technology, Journal of*, vol. 31, no. 11, pp. 1828–1834, June 2013.

[82] M. Nikolayev, A. Morea, G. Rizzelli, P. Peloso, C. Lepers, J.-C. Antona, and G. Charlet, “Impact of the optical reach on multilayer planning of IP-over-WDM networks (under review),” *Optical Switching and Networking*, 2014.

[83] M. Nikolayev, A. Morea, Y. Pointurier, and J.-C. Antona, “An efficient model for the multilayer network planning of IP-over-WDM networks,” in *Optical Communication (ECOC 2013), 39th European Conference and Exhibition on*, September 2013, pp. 1–3.

[84] *ITU-T recommendation G.709*, ITU-T Std., Rev. (02/12). [Online]. Available: <http://www.itu.int/rec/T-REC-G.709>



# Summary in French / Résumé en français

## Contribution à l'amélioration de l'efficacité des réseaux IP sur WDM en évaluant et en dépassant les limites du dimensionnement multicouche

### I. INTRODUCTION

Pendant la dernière décennie, la consommation énergétique des réseaux de télécommunications a connu une augmentation de 60% par an et les réseaux consomment aujourd'hui 2 à 4% de l'électricité mondiale. Cette croissance exponentielle continue actuellement : les principaux moteurs de cette croissance sont les services de vidéo 3D et de vidéo très haute définition. La délocalisation du stockage et du traitement des données vers des serveurs distants contribue également à cette dynamique de croissance. Cette augmentation de la consommation associée à celle des coûts des équipements doit être maîtrisée le plus possible.

Le travail de thèse s'est focalisé sur l'étude de cette problématique dans les réseaux métropolitains et dorsaux. Ces réseaux sont actuellement composés de deux couches fonctionnelles : l'une électronique que nous appelons couche IP, qui permet d'analyser et de router les trames constituant le trafic et l'autre que nous appelons couche WDM, qui assure le transport des flux de trames entre deux nœuds au travers de connections au sein de la fibre optique. Sauf cas exceptionnels les nœuds de ce réseau sont donc constitués d'un routeur IP et un nœud optique.

Les architectures de nœud ont beaucoup évolué ces dernières années. L'architecture des nœuds actuels est détaillée dans la Figure 5.

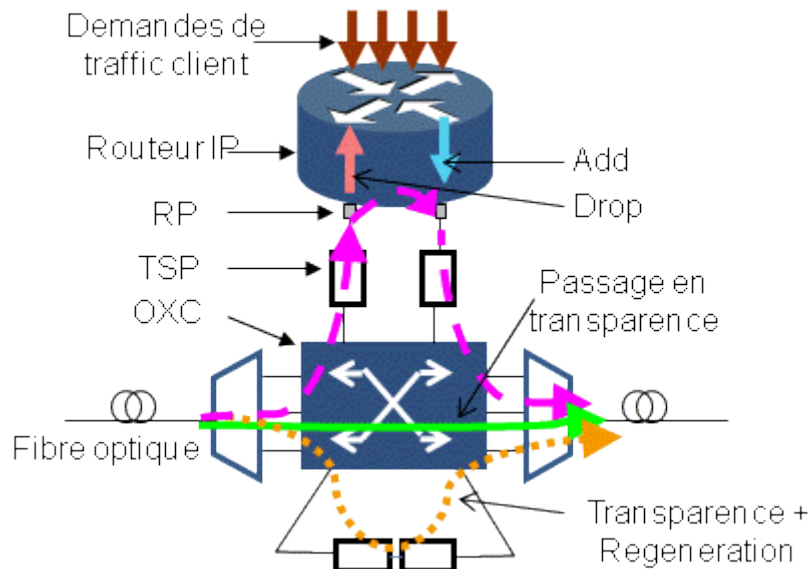


Figure 48: Operations possible dans un nœud hybride IP-over-WDM. OXC= commutateur optique, TSP=transpondeur, RP=port de routeur..

Le nœud est constitué d'un routeur IP qui reçoit les demandes de trafic client, les traite, les « multiplexe » dans le domaine temporel, les agrège ensemble pour mieux remplir les connections optiques puis les envoie dans la couche optique. Les données arrivent sur un port de routeur (RP) qui est connecté à un transpondeur (TSP). Les transpondeurs sont des dispositifs optoélectroniques qui émettent et reçoivent les connections optiques.

La partie optique du nœud est le commutateur optique qui permet de commuter les connections optiques : elles peuvent être émises et envoyées par/vers les transpondeurs ou passer en transparence.

En résumé, une connexion optique arrivant dans un nœud peut :

- être commutée vers une autre fibre connectée au nœud et passer en transparence sans aucun traitement électronique dans le nœud (flèche verte continue).
- être commutée vers un transpondeur, y être transformée en signal électronique (flèche rose avec tirets). Les trames transportés par la connexion optique peuvent alors être traitées. Celles dont le nœud est le nœud destination, sortent du réseau (flèche « Drop »), et les autres sont rassemblées avec d'autres trames, dont les trames entrantes à ce nœud (flèche « Add »), pour être mises dans d'autres connections optiques.

Les opérations d'agrégation et de ré-agrégation constituent la fonction de « grooming », la définition des chemins des connections optiques dans la couche WDM est la fonction de routage : ces deux fonctions sont corrélées et constituent le problème de « routage et grooming » (RG). Lorsque, pour résoudre ce problème, on prend en compte les coûts et les contraintes des deux couches simultanément afin d'obtenir une solution plus optimale ; on parle d'approche multicouche.

Ces problèmes sont résolus lors du dimensionnement des réseaux de cœur avant leur déploiement. Ce processus de dimensionnement est aujourd'hui automatisé grâce à des

outils de dimensionnement. Le problème RG ne peut pas être résolu en un temps polynomial.

La résolution du problème RG par des formulations mathématiques exactes (Mixed Integer Linear Programming en anglais) ne permet d'obtenir des résultats que pour les réseaux de moins de 20 nœuds en un temps « raisonnable ». Pour cette raison, la plupart des outils de dimensionnement implémentent des méthodes approchées, dites méthodes heuristiques.

Le mécanisme RG est au centre des heuristiques de dimensionnement actuelles et se trouvera certainement au cœur des algorithmes de dimensionnement des futurs réseaux dynamiques et/ou réseaux élastiques.

## II. FONCTION CARACTERISTIQUE

Une étude bibliographique ne nous a pas permis de trouver une étude détaillée du mécanisme RG, comme cela existe dans le cas du dimensionnement de la couche optique seule. Les études qui visaient à mieux comprendre les résultats du RG, contenaient plutôt des observations empiriques.

Nous avons donc créé un modèle semi-analytique de ce mécanisme. Nous nous sommes fixés trois objectifs.

Le modèle doit permettre de:

Objectif 1: comparer toutes les méthodes RG sur une échelle commune en prenant en compte la cause des écarts entre les solutions qu'elles fournissent.

Objectif 2: introduire un scénario représentatif tel que les résultats obtenus dans ce scénario puissent être extrapolés à des matrices de trafic génériques.

Objectif 3: estimer et borner les coûts obtenus par une heuristique étant données une topologie et une matrice de trafic simple.

Nous avons introduit une « fonction caractéristique » qui remplit ces trois objectifs.

Pour tracer la fonction caractéristique d'une méthode RG, il faut générer des matrices de trafic « homogènes », où il y a au maximum une demande de trafic client entre deux nœuds du réseau et où toutes les demandes ont une capacité égale.

Le rapport entre la capacité des demandes de trafic client et la capacité des transpondeurs de la couche optique, est appelé «granularité du trafic». En effectuant le dimensionnement avec ces matrices de trafic client, une topologie et la méthode RG étudiée, nous obtenons pour chaque matrice de trafic un nombre de connections optiques déployées pour le transport des demandes.

En résumé, la fonction caractéristique est la fonction reliant la granularité au nombre de connections (normalisé par le nombre de demandes dans la matrice de trafic).

Nous avons ensuite comparé les fonctions caractéristiques de différentes méthodes de dimensionnement multicouches avec celles des méthodes de dimensionnement plus primitives (overlay et opaque). Nous avons établi les bornes théoriques de la fonction caractéristique.

Ensuite, nous avons étudié comment la fonction caractéristique d'une méthode RG dépend de la topologie. Cela nous a permis de mieux comprendre le processus RG en général.

Par la suite, nous avons montré que les résultats obtenus avec les matrices homogènes s'extrapolent à d'autres matrices de trafic client. En effet, en effectuant une convolution entre la fonction escalier et la distribution statistique des capacités des demandes de trafic, nous avons obtenu une estimation précise du nombre de connections optiques que l'algorithme RG établirait pour cette matrice de trafic.

Ceci a été démontré dans une campagne de simulations étendue pour les matrices dont la distribution des capacités de demandes suit des lois continues.

Enfin, nous avons comparé les fonctions caractéristiques de deux formulations MILP et de cinq heuristiques, dont quatre ont un code qui nous est inconnu. Nous avons montré que nous pouvons découvrir des informations sur le fonctionnement d'outils inconnus, que nous pouvons comparer leurs performances pour chacun d'entre eux et étudier la façon dont leur comportement change avec le nombre de nœuds dans la topologie. Pour chaque outil, nous avons évalué l'économie de connections optique qui peut être obtenue et avons distingué les cas où les gains à réaliser sont les plus importants, ce qui permet d'avoir des indications sur les modifications algorithmiques à réaliser. Les performances des 5 heuristiques ont ensuite été comparées pour déterminer la meilleure des heuristiques. En conclusion, nous avons montré que la fonction caractéristique remplit bien les trois objectifs fixés ci-dessus.

Ces travaux permettent d'améliorer les outils de dimensionnement. De plus, la fonction caractéristique est un modèle numérique qui permet une meilleure compréhension du dimensionnement multicouche et nos résultats ont été utilisés dans l'élaboration d'un modèle théorique par une autre équipe (publication en cours de soumission).

Ces résultats sont utiles pour les outils actuellement en cours de développement ; ils le seront d'autant plus lorsque les réseaux deviendront dynamiques car les outils de dimensionnement mais aussi les outils de gestion des réseaux seront multicouches. Ces derniers devront provisionner les connections optiques en temps réel et effectuer des ré-optimisations périodiques.

### III. IMPACT DE LA PORTEE OPTIQUE SUR LE DIMENSIONNEMENT DE RESEAUX IP-SUR-WDM

Dans les outils de dimensionnement opérationnel, le processus RG est soumis à des contraintes physiques et techniques imposées par les différents éléments du réseau. Parmi ces contraintes, la limitation en portée optique est la plus importante. En effet elle ne peut être palliée par aucune modification technique, car il s'agit d'une limitation physique. De plus, conformément à la limite de Shannon, la portée optique diminuera encore dans un futur proche avec l'augmentation des capacités dans la couche optique. Or si la limitation en portée optique est ignorée des régénérateurs devront être déployés quand une connections sera établie pour en assurer la faisabilité physique, ce qui augmente considérablement le coût du réseau.

Dans la deuxième partie de nos travaux, nous avons démontré qu'il est nécessaire d'intégrer cette contrainte lors du processus RG multicouche. Ainsi, nous avons montré que cela permet d'économiser un nombre non-négligeable de régénérateurs. Nous nous sommes ensuite intéressés à l'impact de la portée optique sur le coût total du réseau ; nous avons étudié le cas où il existe plusieurs choix d'équipements optiques offrant différentes portées optiques pour différents coûts. Il s'avère que ce choix peut impacter considérablement le coût total du réseau et ne peut être fait que lorsque la matrice de trafic est connue.

Enfin, nous avons étudié comment la portée optique influence la distribution statistique des longueurs des connections optiques. Nous avons déterminé les scénarios de trafic où cette portée influence le plus les résultats du dimensionnement.

### IV. CONCLUSION

En conclusion, ce travail de thèse nous a permis de mieux comprendre les mécanismes de dimensionnement multicouche qui ont fait leur apparition ces dix dernières années. Aujourd'hui, la plupart des outils de dimensionnement réseau sont multicouches et demain, les outils de gestion et de dimensionnement des nouvelles architectures de réseau le seront aussi. Nous avons étudié le processus RG qui est au cœur des algorithmes multicouche.

Pour la première fois à notre connaissance, nous en avons fourni un modèle numérique sous forme de « fonction caractéristique ». Cette modélisation permet de prévoir les résultats d'un algorithme RG, de diagnostiquer et d'améliorer ses performances. Ce modèle numérique nous a également permis d'étudier les limites théoriques et les comportements limites du processus RG. Ce travail a été utilisé par un autre groupe de recherche pour bâtir un modèle théorique et trouver des applications industrielles.

Enfin, nous avons travaillé sur l'impact de la portée optique sur le dimensionnement multicouche. Ces recherches ont permis de montrer les économies réalisées sur le nombre de régénérateurs en intégrant la portée dans le processus RG. Nous avons également pu formuler des recommandations sur le choix des équipements optiques pour adapter leur portée aux besoins de la matrice de trafic IP. Ces travaux peuvent

servir de point de départ pour la compréhension des outils multicouches pour les réseaux du futur de capacité hétérogène sur la couche optique et/ou réseaux élastiques.